

ERDC/CERL TR-02-12

Construction Engineering
Research Laboratory



US Army Corps
of Engineers®
Engineer Research and
Development Center

Alternative Shear Panel Configurations for Light Wood Construction

Development, Seismic Performance, and Design Guidance

James Wilcoski, Chad Fischer, Tim Allison, and Kelly Jo Malach

April 2002



Foreword

This study was conducted for Building Science Corporation (BSC), Westford, MA, under a Technical Assistance Agreement with the U.S. Army Research and Development Center, Construction Engineering Research Laboratory (CERL). The work was funded through the U.S. Department of Energy (DoE) Building America Program and administered under CERL Reimbursable Work Unit GQ9, “Testing of Wood Shear Wall Assemblies.” Under the Building America Program, BSC has organized the Building Science Consortium, under which this study was conducted. The BSC technical monitors were Joseph Lstiburek and Betsy Pettit, and the DoE technical monitor was George James, Program Manager, Office of Building Systems.

The work was performed by the Materials and Structures Branch (CF-M) of the Facilities Division (CF), Construction Engineering Research Laboratory (CERL). The CERL Principal Investigator was James Wilcoski. The technical editor was Gordon L. Cohen, Information Technology Laboratory – Champaign. Martin J. Savoie is Chief, CEERD-CF-M, and L. Michael Golish is Chief, CEERD-CF. Dr. Paul A. Howdyshell, CEERD-CV-ZT, is Technical Director of the Facility Acquisition and Revitalization business area, and Dr. Alan W. Moore is the Director of CERL.

CERL is an element of the U.S. Army Engineer Research and Development Center (ERDC), U.S. Army Corps of Engineers. The Commander and Executive Director of the ERDC is COL John W. Morris, EN, and the Director is Dr. James R. Houston.

DISCLAIMER: The contents of this report are not to be used for advertising, publication, or promotional purposes. Citation of trade names does not constitute an official endorsement or approval of the use of such commercial products. All product names and trademarks cited are the property of their respective owners. The findings of this report are not to be construed as an official Department of the Army position unless so designated by other authorized documents.

DESTROY THIS REPORT WHEN IT IS NO LONGER NEEDED. DO NOT RETURN IT TO THE ORIGINATOR.

Contents

Foreword	2
List of Figures and Tables.....	5
1 Introduction.....	9
Background	9
Objectives	10
Approach.....	10
Scope	11
Units of Weight and Measure.....	12
2 Test Panel Configurations.....	13
P3-1 Configuration	15
Common Features of the P3-2, P3-3, P3-4, and P3-5 Panel Configurations.....	16
P3-2 Configuration	17
P3-3 Configuration	19
P3-4 Configuration	19
P3-5 Configuration	20
P3-3M Medium Configuration	20
P3-6 Configuration	21
P3-7 Configuration	21
PSP-Std Configuration	22
3 Predicted Response of Shear Panels.....	23
Wood Shear Panel Model	24
Diagonal Strap Shear Panel Model.....	34
4 Test Configuration and Procedures	35
Test Apparatus	35
Test Procedure	35
Instrumentation	38
5 Test Results and Observations	40
Test Documentation Based on City of Los Angeles (LA) Guidance	42
Test Documentation Based on FEMA 273 Guidance	44
Calculated Allowable Design Capacity.....	45
P3-1 Test Results	46
P3-2 Test Results	49
P3-3, P3-4, and P3-5 Monotonic Test Results.....	52
P3-3M Test Results	55
P3-6 Test Results	59

P3-7 Test Results	62
PSP-Std Phase I Test Results	65
6 Recommended Allowable Shear Capacities	69
7 Summary	75
References	77
Figures	79
Appendix A: Predicted Allowable Strength Design Capacities	124
Appendix B: Cyclic Test Protocols for Phase I Wood Shear Panels	129
Acronyms	133
CERL Distribution	135

List of Figures and Tables

Figures

1. P3-1 diagonal strap shear panel.....	80
2. P3-2 OSB shear panel.....	80
3. P3-3 OSB shear panel.....	81
4. P3-4 OSB shear panel.....	81
5. P3-5 OSB shear panel.....	82
6. P3-3M medium-strength OSB shear panel.....	82
7. P3-6 OSB shear panel.....	83
8. P3-7 OSB shear panel.....	83
9. P3 OSB shear panel details.....	84
10. P3 OSB shear panel fastener details.....	84
11. P3-2 OSB shear panel corner details.....	85
12. P3-3 OSB shear panel corner details.....	85
13. P3-5 OSB shear panel corner details.....	86
14. P3-3M OSB shear panel corner details.....	86
15. PSP-Std plywood shear panel tested in Phase I.....	87
16. Wood shear panel showing forces applied to the panel and nails.....	88
17. Graphical illustration of connection yield modes.....	89
18. Predicted lateral yield and ultimate capacities for the Phase III shear panels.....	89
19. Overall view of test frame for testing shear panels at CERL.....	90
20. Monotonic load history with 0.5 inches per minute stroke rate.....	91
21. CUREE loading history with $\Delta = 2$ in., 0.1 Hz initial cyclic rate and 0.05 Hz later rate.....	91
22. Schematic drawing showing sensor locations on wood shear panels.....	92
23. Lateral force (TSF) vs deflection for the P3-1 monotonic panel.....	92
24. Crushing of bottom plate due to tensioning of steel strap.....	93
25. Nails attaching steel strap to top plate yielded and pulled out.....	93
26. Lateral force (TSF) vs deflection hysteretic behavior of the P3-1 CUREE1 panel.....	94
27. P3-1 CUREE1 panel strap failure showing straps still attached at the bottom and middle.....	94

28. Lateral force (TSF) vs deflection hysteretic behavior of the P3-1 CUREE2 panel.	95
29. Damage in bottom plate due to tensioning of steel strap.	95
30. Damage in top plate at location of steel strap connection (P002987).	96
31. Damage state after completion of P3-1 CUREE2 test (7-7).	96
32. Lateral force (TSF) vs deflection for the P3-2 monotonic panel.	97
33. Gap at bottom of panel (right side) due to nail yielding.	97
34. OSB pulling out of inset and crushing of hem-fir bottom plate.	98
35. Longitudinal split in top plate due to bending.	98
36. Block shear pullout of OSB from TP35 nailing plate.	99
37. Lateral force (TSF) vs deflection hysteretic behavior of the P3-2 CUREE1 Panel.	99
38. Gap in inset panel due to nails yielding in OSB to panel connection.	100
39. OSB pulling out of frame in lower right corner.	100
40. Top plate splitting above the right side of the OSB.	101
41. Lateral force (TSF) vs deflection hysteretic behavior of the P3-2 CUREE2 panel.	101
42. Lateral force (TSF) vs deflection for the P3-3 monotonic panel.	102
43. Crushing of top-right corner of OSB in the P3-3 mono panel.	102
44. OSB outside the 2x6 frame and nail pullout along right vertical edge of panel.	103
45. Lateral force (TSF) vs deflection for the P3-4 monotonic panel.	103
46. Crushing and buckling of lower left corner of OSB in the P3-4 mono test.	104
47. Damage to OSB and inset panel bottom plate at right corner of P3-4 mono panel.	104
48. Torsion and bending in top plate.	105
49. Inset panel detached from 2x6 frame.	105
50. Lateral force (TSF) vs deflection for the P3-5 monotonic panel.	106
51. Top plate bending and nail yielding along OSB left edge.	106
52. Splitting and bending failure of P3-5 mono top plate.	107
53. Lateral force (TSF) vs deflection for P3-3M monotonic panel.	107
54. Overall view of damaged P3-3M mono test panel.	108
55. Bottom of P3-3M mono panel showing the OSB pulled away from frame.	108
56. Interior face of P3-3M mono panel showing threaded rods.	109
57. Load cell force vs lateral deflection in the P3-3M mono test.	109
58. Stress vs strain plot for the north threaded rod.	110
59. Lateral force (TSF) vs deflection hysteretic behavior of P3-3M CUREE1 panel.	110
60. Nail yielding and OSB crushing in P3-3M CUREE1 test.	111
61. Stud to interior of the threaded rod cavity split in P3-3M CUREE1 test.	111

62. Threaded rod tension measured by north and south load cells in P3-3M CUREE1 test.....	112
63. Stress vs strain plot for north threaded rod in P3-3M CUREE1 test.....	112
64. Lateral force (TSF) vs deflection hysteretic behavior of P3-3M CUREE2 panel	113
65. Threaded rod tension measured by north and south load cells in P3-3M CUREE2 test.....	113
66. Stress vs strain plot for the north threaded rod in the P3-3M CUREE2 test.....	114
67. Back face corner of P3-3M panel showing stud cavity and threaded rod.....	114
68. Lateral force (TSF) vs deflection for P3-6 monotonic panel.	115
69. Stud lifting off of bottom plate in P3-6 monotonic test.....	115
70. Shear failure of hurricane tie and nail yielding.....	116
71. Lateral force (TSF) vs deflection hysteretic behavior of P3-6 CUREE1 panel.	116
72. Nails pulled through bottom right corner of the OSB of P3-6 CUREE1 panel.....	117
73. Bending failure (cracking) of the top plate above the right edge stud.	117
74. Lateral force (TSF) vs deflection hysteretic behavior of P3-6 CUREE2 panel.	118
75. Interior face of P3-6 CUREE2 panel showing OSB nail and H4 tie nail failure.	118
76. Bending failure of the 2x4 top plate on P3-6 CUREE2 panel.	119
77. Lateral force (TSF) vs deflection for P3-7 monotonic panel.	119
78. Overall view of damaged P3-7 mono panel at the end of test.....	120
79. Lateral force (TSF) vs deflection hysteretic behavior of P3-7 CUREE2 panel.	121
80. Failure of H4 ties, OSB, bottom plate, and nail connections of P3-7 CUREE2 panel.	121
81. Lateral force (TSF) vs deflection hysteretic behavior of PSP-Std SPD1 panel.	122
82. Bottom left corner of the PSP-Std-SPD1 panel showing plywood to bottom plate nail connection failure and stud lifting.....	122
83. Lateral force (TSF) vs deflection hysteretic behavior of the PSP-Std MS1 panel.	123
84. Bottom of the PSP-Std-MS1 panel showing plywood to stud nail connection failure.	123
B-1. Sequential Phase Displacement time history	131
B-2. Modified SAC-2 time history	132

Tables

1. Nail details for shear Panels P3-1 through P3-7.....	15
2. Connection calculated capacities.....	27
3. Wood shear panel connections.....	27
4. Predicted panel lateral yield capacity, P_y	33
5. Predicted panel lateral ultimate capacity, P_u	33
6. CUREE load history cycles.....	37

7. Wood shear panel instrumentation.	39
8. Summary of panels tested.	41
9. Maximum measured moisture content for each test panel.	42
10. Calculated panel allowable strength design capacities.	46
11. Performance of P3-1 shear panels.	48
12. Performance of P3-2 shear panels.	51
13. Performance of P3-3, P3-4 and P3-5 Monotonic Shear Panels.	52
14. Performance of P3-3M shear panels.	56
15. Performance of P3-6 shear panels.	60
16. Performance of P3-7 shear panels.	64
17. Performance of PSP-Std shear panels.	67
18. Summary of baseline panel ultimate capacities.	71
19. Wood shear panel recommended design values.	73
B-1. Sequential Displacement Protocol.	130
B-2. Modified SAC Cyclic Test Protocol.	132

1 Introduction

Background

This study addresses light wood-frame construction, which is used in most single- and multi-family structures today. Most modern wood frame buildings incorporate shear walls or structural panels to provide primary lateral-load resistance. Conventional wood shear panels are typically made of plywood fastened to a light wood frame. They generally perform well in earthquakes if constructed according to industry guidance. However, a problem with these shear panels is that sheet insulation cannot easily be installed over them. Consequently, shear-reinforced portions of many wood frame buildings are constructed with no thermal insulation; siding is instead applied directly to the shear wall sheathing. This practice establishes a thermal bridge between the building's interior and exterior, wasting considerable amounts of energy.

The U.S. Department of Energy (DoE) tasked Building Science Corporation (BSC) of Westford, MA, to develop advanced framing concepts that eliminate the thermal bridging problem while providing the lateral load resistance required in standard light wood frame construction. BSC's basic alternative concept was a wood-based shear panel that can be inset between studs in conventional wood frame construction. This inset positioning places the shear panel flush with the external surfaces of the wall studs, thus presenting no obstacle to the attachment of sheet insulation. Such panels could be used anywhere desired in a stud wall without interrupting the building's insulation envelope or creating a thermal bridge.

A number of alternative inset shear panel designs were developed and fabricated using standard dimensional framing lumber and a pressure-treated wood product called oriented strand board (OSB). Standard off-the-shelf fasteners, nailing plates, and framing brackets were used to assemble prototypes of each alternative design. An essential feature of these alternative designs was the use of threaded steel post-tensioning tie rods to provide resistance to overturning forces.

Although the alternative shear panels are made of common materials and are easy to fabricate, no performance data or construction guidance are available for such designs. In order to test performance of these shear panels, BSC entered into a

Technical Assistance Agreement with the U.S. Army Engineer Research and Development Center, Construction Engineering Research Laboratory (ERDC/CERL), Champaign, IL. The agreement was established to provide BSC access to an Army Corps of Engineers experimental shear wall test facility with capabilities not available elsewhere in the United States. ERDC/CERL provided seismic engineering expertise and experience developing earthquake-resistant construction designs.

Objectives

The purpose of this work was to define the capacity of various experimental wood shear panel configurations under simulated seismic load by cyclic testing. The specific objectives of the study were to:

1. Define the lateral-load-carrying behavior of shear panels subjected to cyclic loading representative of earthquakes. This behavior is defined by hysteretic load/deflection envelopes that show the ability of the panels to continue resisting load through significant degradation (i.e., system ductility).
2. In conjunction with BSC, develop alternative inset shear panel configurations that perform as well as or better than industry-accepted panels with plywood sheathing. Acceptability of performance is measured not in terms of lateral-load-resisting strength alone, but also largely in terms of achieved system ductility.
3. Evaluate the ability of a single-element 2x6 top plate to resist the applied loads under simulated seismic loading of the panels. The top plates in an inset panel may be subjected to significant bending and shear forces, but if a single-element top plate can perform well in place of a double plate, then construction costs can be reduced.
4. Recommend design capacities for those shear panels that provide adequate ductile behavior.

Approach

The alternative designs are 2x4 stud panels inset into a 2x6 frame. Common materials and hardware were used to assemble the panels. Specifically, the experimental specimens were fabricated using half-inch sheathing (mostly OSB, but in one case plywood), Simpson Strong-Tie nailing plates and seismic ties, 5/8 in. diameter threaded rods of mild steel, and common nails. The shear panels were constructed by nailing the 2x4 prefabricated panels into a 2x6 wall frame. The alternative panel designs, designated in this study as P3-2, P3-3, P3-4, and P3-5, were tested using

uniform procedures in order to compare their performance with an industry-accepted plywood configuration (designated in this study as P3-6).

At least one specimen of each inset shear panel configuration (P3-2, P3-3, P3-4, and P3-5) was fabricated as described in Chapter 2, and pretest predictions were developed for each configuration to better understand the mechanics and failure mechanisms (Chapter 3). These predictions were intended to help refine test panel designs, interpret test results, develop design recommendations, and contribute to future panel testing and evaluation programs.

Each experimental panel was first tested monotonically to gain an initial understanding of its behavior. Next, the P3-2 and P3-3M configurations (the latter being a slight modification of P3-3) were tested cyclically according to the test procedures described in Chapter 4. Three specimens of the industry-standard plywood panel configuration (i.e., P3-6) were tested monotonically and cyclically to establish a performance baseline, and test results from an earlier related study (i.e., Phase I) were also used to help establish the baseline.

In addition, to take advantage of the experimental setup for this work, two fundamentally different alternative configurations were also tested: (1) P3-1, a panel utilizing only steel straps as the lateral-force-resisting system, and (2) P3-7, a 24 in. wide inset panel. Both of these configurations, also described in Chapter 2, were tested monotonically and cyclically according to the same test procedure and loading protocols used for the other panels.

Finally, recommended design capacities were developed based on the test results, comparisons with the baseline panel performance, and published 2000 International Building Code (IBC) allowable strength design capacities.

Scope

This report documents the third phase of a three-part study exploring advanced framing approaches to enhance shear and seismic resistance. Results from the first two studies fed directly into the current test series, and relevant results from those studies are presented here to help establish a baseline for evaluating the performance of the latest shear panel alternative configurations.

The shear panels tested here were assumed to be well anchored at their bottom plates. The top plates also were assumed to be well anchored, but were conservatively installed in the test frame in order to allow top plate bending as a possible

failure mode. A small 2x4 block was used in the setup to limit out-of-plane displacement. Actual shear panels installed in the field must be anchored to a floor diaphragm or footing below, and to the floor diaphragm or roof joists above in order to ensure that the panels are not loaded out of plane and that the top and bottom plates are held horizontal. The calculated capacities of the shear panels neglect the bearing strength contribution of the inset OSB, and therefore the calculations underestimate actual panel capacities.

Although the testing protocols simulate seismic loads, the test results presented herein can also be used to assess the capacity of these panels under wind loading.

Units of Weight and Measure

U.S. standard units of measure are used throughout this report. A table of conversion factors for Standard International (SI) units is provided below.

SI conversion factors		
1 in.	=	2.54 cm
1 ft	=	0.305 m
1 in ²	=	6.452 cm ²
1 lb (force)	=	4.448 N
1 kip (force)	=	4.448 kN
1 psi	=	6.89 kPa
1 ksi	=	6.89 MPa
1 lb-in	=	0.113 N-m
1 lb/ft	=	14.59 N/m
1 lb/in	=	0.1751 KN/m

2 Test Panel Configurations

Figure 1 through Figure 14 show the details of the eight Phase III shear panel configurations tested at CERL. Figure 15 shows the PSP-Std panel that was tested in the Phase I project, the test results from which help to establish the performance baseline for the Phase III panels. The sheathed test panels (all but P3-1 with diagonal metal straps) were no greater than 4 ft wide and used a single OSB sheet. This approach conservatively removed the strengthening effect that would result if wider specimens were tested. An 8 ft wide specimen made up of two OSB sheets would be expected to have more than twice the capacity of a 4 ft wide panel. This is because 4 ft wide panels apply net vertical forces to both edge studs, and these vertical loads must be resisted either by an overall vertical load applied to the panel or holddown anchors that affix the studs against the top or bottom plates. Without this vertical resistance at the edge studs, the nails along the OSB sheet edge provide no resistance to the overturning effects of lateral load, and thus contribute nothing to the lateral capacity of the panel. However, with an 8 ft wide panel, the nails along the center stud between the two OSB sheets do provide overturning resistance without vertical load. When the 8 ft wide panel racks laterally in one direction, the nails from one sheet apply an upward force to the center stud while the nails from the adjoining sheet apply a similar downward force. These forces cancel each other out so that overturning resistance is created at any seam between panels, even with no vertical load. Therefore, to be conservative in experimental design, all sheathed panels tested in this study were no more than 4 ft wide to remove the strengthening effects that would be provided by center studs in 8 ft wide specimens. Also, because the purpose of this study was primarily to define the relative capacity of alternative OSB shear panel configurations compared to the baseline configuration (i.e., the industry-accepted plywood panel), the width of the panels was not critical to the validity of the comparison as long as the experimental and baseline panels were all 4 ft wide.

All Phase III panels are anchored to the test fixture at both their tops and bottoms using 5/8 in. A325 high-strength bolts. The baseline panels (P3-6 and PSP-Std from Phase I) had a double 2x4 top plate while all other Phase III panels had a single 2x6

spruce-pine-fir (SPF^{*}) top plate. The single top plate may have significantly reduced panel strength and ductility. This was a particular concern for the inset panel configurations (P3-2, P3-3, P3-4, P3-5, P3-3M, and P-3-7), where bearing load from the inset panel could fail the top plate in bending or shear. In real construction, roof trusses or floor joists would rest on top of the top plate directly above the studs, which removes gravity-induced bending load on the top plates. However, when panels are loaded laterally, the inset panels will bear against the bottom surface of the top plate and load it in bending. The purpose of the threaded rods is to provide hold-down resistance for the studs at both sides of the panels. These rods hold the studs against the top and bottom plate in bearing, which is essential to the overturning resistance provided by the bearing of the inset panels in the corners and nails along the panel sides. The rods must be post-tensioned so they can provide bearing pressure at the studs without any lateral deformation. Without post-tensioning the panels could rack laterally with little resistance until the top plate begins to crush under the rod bearing plate and the threaded rod elongates. The panels would have to rack enough to develop the lateral resistance of the panel. Therefore, the threaded rods in the panels tested earlier were post-tensioned to 8000 lb; in the panels tested later the post-tensioning was 6000 lb. During panel lateral deformation, the load in the rods increases. In addition, the bearing plate of the threaded rod pushes down on the top plate while the inset panel pushes up from a few inches away, creating a force couple leading to potentially large bending stresses, particularly when the threaded rod is to the outside of the panel and a larger distance (larger couple moment arm) from the bearing surface of the inset panel.

Therefore, the ability of the single top plate to resist the bending and shear forces was evaluated in all Phase III panels using the top plate connection configuration shown at the top of Figures 1 through 8, and detailed in Figures 9 and 10. Lateral loads are applied to the test panels only at the extreme ends of the 2x6 top plates, as shown in the detail in Figure 10. In this configuration, the top test fixture does not unintentionally increase the bending capacity of the top plate. The top plate must also carry the entire lateral load axially along its length, as it may also be possible for this plate to fail in a combination of buckling and bending when it is significantly bent vertically. In reality the trusses and blocking (if it exists between trusses) will increase bending resistance, but this test configuration conservatively ignores that effect. The top plate is protected to a degree by seismic ties (Simpson Strong-Tie H4) shown in the panel drawings, and these ties are an integral part of

* ASTM D 1165, vol 04.10 (2000).

the panel design for each configuration. Finally, a wood block is placed between the center of the top plate and test fixture (as shown in Figures 1 through 6, plus the details in Figure 9) to restrain out-of-plane movement of the top plate and prevent it from buckling out of plane. In real-world construction the out-of-plane restraint would be provided by roof trusses or floor joists where they rest on the top plate above the studs. This block in the test setup was designed to be very flexible in-plane so it would not pick up load, and was located at the panel center where there should be no vertical motion in the top plate. The top plate will bend up at one edge while bending down at the other as the panel is displaced laterally, so there should be no net vertical motion at the center. However, for the P3-6 and P3-7 panels shown in Figures 7 and 8, the block was removed because it could interfere with the bending of the top plate, and the plate was much less likely to move out-of-plane because it was shorter and not loaded as heavily in the lateral direction.

Two nail guns were used to install nails in all the Phase III test panels. The 6d nails were coil nails installed with a Stanley-Bostitch N80 coil nailer, and the 8d, 10d, and 16d nails were stick nails installed with the Stanley-Bostitch N95162 common nailer (see Table 1). The following sections provide details on shear panels that are unique to each panel.

Table 1. Nail details for shear Panels P3-1 through P3-7.

Nail Symbol	Stanley Bostitch Item Number	Nail Description (length, diameter and surface)	Nailing Details
6d	C6P99D	2 in. x 0.099 in. smooth	Coil nails used in the Stanley-Bostitch N80 coil nailer
8d	RH-058D131EP	2.5 in. x 0.131 in. smooth	Roundhead plastic collated stick nails used in the Stanley-Bostitch N95162 common nailer
10d	RH-510D148EP	3 in. x 0.148 in. smooth	
16d	RH-516D162EP	3.5 in. x 0.162 in. smooth	

P3-1 Configuration

Figure 1 illustrates the details for the P3-1 shear panel. This panel comprises 2x6 spruce pine fir (SPF) studs spaced at 24 in. on center (o.c.). Connected to the frame are two 54-mil (0.054 in. thick or 16 gage) by 1.25 in. wide diagonal straps of ASTM* A653 Grade 33 steel attached in an “X” configuration. These straps are attached to the top and bottom plates just 4 in. to the outside of the center of the studs

* The standards organization ASTM International, formerly the American Society for Testing and Materials.

in an attempt to optimize this simple panel configuration. These locations were selected close to the studs to minimize the bending forces on the top and bottom plate while still keeping the angles between the straps and the horizontal members at 59.6 degrees, slightly less than the maximum desired angle of 60 degrees.* The straps are bent over and nailed to both the top and bottom plates, with three nails driven into the top and bottom surfaces of these plates and one into the edges of the plates. The straps are also nailed to the studs, where the straps pass over near the top and bottom plate connections. This connection with the stud also carries a reasonable load because the connections are near the top and bottom plates, so the studs can carry lateral load in weak-axis bending to these plates. Simpson Strong-Tie H6 seismic ties are used to connect the studs near the top of the panel connections to the top plate. These replace the Simpson Strong-Tie H4 seismic ties used at all the other connections between the studs and top and bottom plates. In real-world construction, Simpson-Strong-Tie H2 ties would be used to connect the studs to the roof trusses or floor joists, thereby clamping the studs to the top plate. Since trusses and joists were not part of the test panel design, however, H6 ties were used to fasten the studs and top plates together, providing similar strength and stiffness as the H2 ties. The H4 ties are used at the bottom of all the studs, as they would in real-world construction. However, H4 ties are also used at the top of the studs for those studs away from the panel edges because they do not carry significant vertical load and will have little effect on panel performance. 8d nails were used to connect the steel straps to the wood frame in the locations shown in Figure 1.

Common Features of the P3-2, P3-3, P3-4, and P3-5 Panel Configurations

The P3-2, P3-3, P3-4, and P3-5 shear panels are all very similar to each other (see Figures 2 through 5). Each panel has 2x6 SPF studs at 24 in. o.c., a single SPF top plate, a single hem-fir[†] bottom plate, and Simpson Strong-Tie H4 seismic ties at the bottoms of all studs and tops of studs not located at the panel edges. All specimens use H6 seismic ties between the studs at the edge of the panels and top plate. These model the strength and stiffness that H2 ties would provide in real-world construction when the panels are constrained by floor and ceiling elements, as explained previously for the P3-1 panel. Each of these specimens has a ½ in. thick

* The 60-degree maximum angle was used because this is the maximum used for wood let-in braces in shear panels (2000 *International Building Code* [IBC], sec 2308.9.3, "Bracing.")

† ASTM D 1165, vol 04.10 (2000).

APA^{*}-approved OSB sheet nailed to a 2x4 frame with 8d nails to create an inset panel. The nails are spaced 4 in. o.c. around the panel perimeter and 8 in. o.c. to the center stud and horizontal blocking. Each inset panel is configured so it can be assembled in a shop. The overall dimensions are 46.5 in. x 94 in., so the panels can be inserted in the field into the standard opening inside a 2x6 stud wall frame with studs 24 in. o.c., where the center 2x6 stud is left out. The inset panel is installed so that the OSB is flush with the 2x6 frame. The 2x6 top plate is then nailed to the inset panel 2x4 top plate with 16d nails oriented vertically at 6 in. o.c. The 2x6 studs along the sides of the inset panel are nailed to the inset panel 2x4 studs with 10d nails at 8 in. o.c.

One important detail of all the inset panels is that the 2x4 frame is configured so the vertical 2x4 studs bear against the horizontal 2x4 top and bottom plates. Then when the threaded rods are post-tensioned, they not only clamp the 2x6 studs against the top and bottom plates, but also clamp the 2x4 inset panel studs against the inset panel top and bottom 2x4 plates. This prevents the inset panel top and bottom plates from pulling away from the 2x6 top and bottom plates and forces the panel lateral deformation to be primarily accommodated by ductile failure of the 8d nail connections between the OSB and inset frame.

P3-2 Configuration

The members of the 2x4 frame for the inset panel were oriented out-of-plane, as shown in the plan view at the bottom of Figure 2. The inset panel has a center stud, so the overall depth of the inset panel at the center and around the perimeter is 4 in. ($\frac{1}{2}$ in. OSB plus $3\frac{1}{2}$ in. framing). The 2x6 frame is $5\frac{1}{2}$ in. deep, so an in-plane 2x4 stud with a thickness of $1\frac{1}{2}$ in. is nailed to the inside surface of the inset frame, making this stud flush with the inside surface of the 2x6 frame center stud. The in-plane stud provides a flush surface so drywall can be nailed to it at 24 in. centers.

The right side of Figure 11 shows an elevation view detail of the top left corner of the P3-2 panel. This drawing shows that a Simpson Strong-Tie TP35 nailing plate is used to connect the top corners of the inset panel to the 2x6 frame. These plates increase the shear capacity of the panel along the surface between the inset panel top plate and overall panel top plate. Figure 2 also shows that vertical 16d nails 6

* APA: American Plywood Association.

in. o.c. connect the inset panel top plate to the overall panel top plate. The vertical nails increase shear capacity but have little influence on overturning resistance. The nailing plates also increase the overturning resistance by carrying tensile loads when racking in one direction and keeping the OSB from moving out of the frame when racking the other direction. Figure 11 shows the particular holes where 8d nails are installed in this connection.

The P3-2 panel had a mild steel (AISI* C-1008 – C-1012†) 5/8 in. diameter threaded rod placed outside the 2x6 edge studs. These rods were centered only 1-½ in. from the center of the studs, which is ¾ in. from the stud outside surface. This spacing was as close as possible to the stud so as to minimize the bending load applied to the top plate. Another 2x6 stud was added, 2-½ in. o.c. outside of each threaded rod, as shown in the bottom of Figure 2 and the details in Figure 11. This extra stud was installed to minimize the bending and shear load on the top plate. The 2-½ in. cavity created between the end stud and the extra stud accommodates the threaded rod. The extra stud was braced against buckling at its mid-height by adding a 12 in. tall block between it and the edge stud, as shown in Figure 2. The threaded rod was then centered ¾ in. from the edge stud and 1-¾ in. from the extra stud surface so that the majority of the post-tension load in the threaded rod would be applied to clamping the edge stud and the panel. These rods were connected to another short rod near the base of the panel through a coupling nut. The short rods represent anchor bolts that would be installed in the field, where the anchor bolts would be coupled to the threaded rods. Holes are drilled through the top and bottom plate so the overall wall panel can be stood up over the anchor bolts. The threaded rod is cut so the top will be about 1 in. above the top plate when installed. One end of the threaded rod is fed through the hole in the top plate and other end is connected to the anchor bolt with the coupling nut. A USP‡ BP583 (3 in. x 3 in. x ¼ in.) plate washer and nut are attached to the threaded rod above the top plate and the nut is tightened using a torque wrench to apply a post-tensioning force — 8000 lb for the earlier monotonic test and 6000 lb for the cyclic tests. The post-tension force crushed the 2x6 top plate below the USP BP583 by indenting it 3/16 in. This crushing perpendicular to the grain increases wood density and increases its resistance to bearing load. Similar crushing is expected and desired in the field construction.

* AISI: American Iron and Steel Institute.

† McMaster-Carr Supply Company, Chicago, IL, 2002. Strength properties are comparable to Grade 2 and ASTM A307 low-strength steel.

‡ United Steel Products Company, Montgomery, MN 56069.

The threaded rods of each test panel were instrumented with a load cell to measure the post-tension prior to testing and variation in load during testing. The rods were also instrumented with a displacement sensor that would be used with the load cell data to determine if the threaded rods yield during testing.

P3-3 Configuration

Figure 3 and Figure 12 show the details of the P3-3 shear panel. This panel is almost identical to P3-2, the only difference being that the threaded rod is placed inside the panel. Also, since the threaded rods were placed inside the panel perimeter, the additional stud to prevent a bending failure is also placed inside the panel. This extra stud is a 2x4 built into the inset panel. Installing the extra stud to the inset panel makes construction in the field simpler. This configuration also provides an additional nailing surface to attach the OSB. The overturning resistance and ductility of this panel are increased by nailing the OSB to the extra stud with 8d nails 8 in. o.c. The threaded rods are moved 4-½ in. to the panel interior, centering it ¾ in. inside the inset panel edge stud. Similar to the P3-2 panel, a 2-½ in. cavity is available for the threaded rod, as shown in Figure 12, but in the P3-3, holes for the threaded rod need to be drilled in the top and bottom plates of the inset panel frame in addition to the 2x6 frame. This placement of the threaded rod has the advantage of placing the clamping force of the threaded rod more directly over where the inset panel applies a bearing force to the bottom side of the top plate when the test panel racks laterally. However, the disadvantage of this panel is that, because the threaded rods are closer to the panel interior, they have a smaller moment arm and will need to carry a greater tensile force to provide the same overturning resistance as the rods in the P3-2 configuration. This panel was only tested monotonically with a threaded rod post-tension force of 8000 lb.

P3-4 Configuration

Figure 4 and Figure 11 show the details of the P3-4 shear panel. This panel is very similar to the P3-2 panel except that the inset panel 2x4 framing members are oriented in-plane, as seen in the plan view on the bottom of Figure 4. The overall depth of the inset panel is then 2 in. (½ in. OSB plus 1-½ in. framing). After this inset panel is nailed into the overall frame (5-½ in. thick), an out-of-plane 2x4 stud with a depth of 3-½ in. is nailed to the inside surface at the center inset panel stud to make this surface flush with the rest of the frame. One additional difference between P3-4 and P3-2 panel is that the 2x4 bottom plate of the P3-4 inset panel is not bolted to the test frame by the interior anchor bolts. This difference can be seen by

comparing the plan views of the panels at the bottoms of Figures 2 and 4. The bolts cannot practically be installed through the narrow deep edge of the P3-4 bottom plate. Therefore it is possible that this inset frame could pull out from the 2x6 frame along with the OSB during later stages of testing.

Figure 4 shows TP35 nailing plates installed at both the top and bottom corners of this panel. The nailing plates are added to the bottom because the inset panel bottom plate is not bolted with the interior anchor bolts. These nailing plates then provide a direct load path between the inset panel and overall panel bottom plate for both overturning and shear forces. On these panels the nailing plates restrict the OSB from moving out of the 2x6 frame at both the top and bottom of the panel, thereby increasing panel ductility.

The threaded rods are placed at exactly the same location as P3-2 panel, inside the 2-½ in. cavity between the 2x6 edge stud and the extra stud to the outside. The detail shown in Figure 11 is actually for the P3-2 because the details around the threaded rod are identical to the P3-2 panel.

P3-5 Configuration

The P3-5 panel is similar to the P3-4 panel in that the inset panel frame is oriented in the plane of the panel and TP35 nailing plates are placed at both the top and bottom of the panel. However, in the P3-5, the threaded rods are placed inside the inset panel area similar to the P3-3 panel. Figure 5 and Figure 13 show the details of this panel. The plan view at the bottom of Figure 5 shows an additional 2x4 stud to prevent a bending failure of the top plate, placed inside the threaded rods and against the inset panel after the panel is installed in the overall frame. This configuration provides an additional nailing surface to attach the OSB. This additional stud was nailed to the inset panel by nailing through the entire 2 in. thick inset panel (½ in. OSB and 1-½ in. frame) with 10d nails. The 10d nails are only 3 in. long so that they penetrate only 1 in. into the studs. Nevertheless, this additional nailing does provide some overturning strengthening compared to the P3-4 panel. The extra stud at the panel center was nailed to the inset panel in a similar manner to provide a flush surface for nailing drywall on the inside face.

P3-3M Medium Configuration

The P3-3 panel provided the best performance of the P3-2, P3-3, P3-4, and P3-5 panels, so this design was subsequently optimized based on observations of the be-

havior of the earlier panels. The P 3-3 panel had the tie rods placed to the panel interior and the 2x4 inset frame member oriented out-of-plane with respect to the panel. Three improved variations on the P3-3 panel were designed: (1) a light panel with no nailing plates at the top corners and increased nail spacing; (2) a medium panel very similar to P3-3; and (3) a heavy panel with nailing plates at both the top and bottom corners and nail spacing reduced. Only the P3-3 medium (P3-3M) shear panel was tested, and the details are displayed in Figure 6 and Figure 14. This panel optimized the P3-3 design to improve ductile performance, slightly improve strength, and make construction more practical. The threaded rods were moved $\frac{1}{2}$ in. toward the panel center, and the interior 2x4 studs moved 1 in. toward the center to create a 1 in. wider cavity (increased to $3\frac{1}{2}$ in.) for easier field installation. The nail pattern to the interior studs was reduced from 8 in. o.c. to 4 in. o.c. to improve strength and ductility by improving the capacity to redistribute forces to these nails after the nails at the exterior studs had yielded. Also, the threaded rods appeared to have yielded even before testing, so the post-tension force was reduced from 8000 lb to 6000 lb. The reduced post-tension force was sufficient to crush the 2x6 top plate in a beneficial way below the plate washer.

P3-6 Configuration

Figure 7 shows the details of the P3-6 shear panel. This configuration, used as a performance baseline in these studies, is an industry-accepted design using $\frac{1}{2}$ in. OSB sheet and 2x4 SPF studs spaced 16 in. o.c. The top plate consisted of two SPF 2x4s and the bottom plate was a single hem-fir 2x4. The studs were attached to the top and bottom plates with two 16d nails and Simpson Strong-Tie H4 seismic ties. H6 seismic ties were used in place of the H4 ties at the top of the panel edge studs as shown in Figure 7. The $\frac{1}{2}$ in. OSB was attached to the frame with 8d nails spaced at 4 in. o.c. along the top and bottom plates and edge studs.

P3-7 Configuration

Figure 8 shows the details of the P3-7 shear panel, a narrow inset panel without threaded post-tensioning rods. This panel has a 94 in. tall by $22\frac{1}{2}$ in. wide inset panel that is installed into a standard opening of a 2x6 frame with studs spaced 24 in. o.c. The inset panel consists of $\frac{1}{2}$ in. OSB nailed to 2x4 SPF inset panel studs and top and bottom plates. The overall frame has 2x6 SPF studs, a single-member SPF 2x6 top plate, and a single hem-fir bottom plate. Similar to the other panels, H4 seismic ties are installed at the bottom of all studs and tops of studs that are not

at the edge of the panels. At the top of the studs at the panel edge, H6 ties are installed for the reasons explained for the P3-1 panel.

PSP-Std Configuration

In an earlier related study (see Chapter 1) several other shear panel configurations were evaluated. From that study, the PSP-Std panel provides baseline data that help to quantify design guidance for the Phase III (i.e., P3) panels. Figure 15 shows the details of the PSP-Std shear panel, which is constructed of a ½ in. 5-ply Douglas Fir Structural Grade I plywood sheet and 2x4 studs spaced 16 in. o.c. The top plate is a double 2x4, the bottom plate is a single 2x4, and all plates and studs are Douglas Fir Grade II. The top and bottom plates were bolted directly to the test fixture as shown in Figure 15. No seismic ties or holddown anchors were used at either the tops or bottoms of the studs.

3 Predicted Response of Shear Panels

Effective seismic resistance requires that shear panels yield, while continuing to provide load resistance through several times the yield deflection of the panels. This ability to sustain loads through significant degradation is called *panel system ductility* and is defined as the ultimate deflection, δ_u , divided by the yield deflection, δ_y^* . The panel system is made up of several components of structural elements and connections. Ductile system performance requires that individual components fail in a ductile (rather than brittle) manner. Brittle failure is the sudden loss of load resistance soon after yielding of the component. Ductile panel system behavior can be achieved if all component failures allowed are detailed to fail in a ductile manner. Modes of failure for which brittle behavior cannot practically be eliminated must be strong enough relative to ductile modes such that brittle failures never occur. Each individual component may have multiple modes of failure, both brittle and ductile. Either strengthening brittle components or detailing them to behave in a ductile manner can prevent brittle modes of failure.

Pretest predictions lead to minor changes in panel details to prevent possible brittle failures. The cyclic tests conducted here define the system behavior of shear wall panels. In general, cyclic tests provide loading representative of an earthquake, which will cause a more rapid degradation of the panels than monotonic loading (loading in one direction until ultimate failure). Acceptable panel performance must provide significant system ductility under the cyclic loading conditions.

Prior to testing, pretest predictions of lateral capacity of each test panel were developed based on established design guidance. The pretest predictions were computed to guide failure observations, improve understanding of test results, and guide development of design recommendations. These predictions defined an array of failure modes, some of which may not have been seen in tests. However, those not seen were useful nevertheless in providing guidance to avoid brittle failure modes.

* Ductility is in fact more complex than this, but this simplified definition is useful for the current discussion.

Wood Shear Panel Model

A model was developed in the Phase I study to represent the behavior of shear panels with plywood nailed to the framing exterior (including PSP-Std and P3-6). This same model was used for the OSB inset panel configurations (i.e., P3-2, P3-3, P3-4, P3-5, P3-3M, and P3-7). Figure 16 is a schematic diagram of the panel model showing the variables used to calculate capacity. The model capacity was limited and defined by the nail connections between the frame and the plywood perimeter. The OSB inset panels developed in this study were expected to have greater strength than conventional plywood panels, but this extra strength is not accounted for in the model. The additional strength of the OSB inset panels arises from the bearing forces applied between the edge of the inset panel and the 2x6 frame. Tests revealed that the bearing surfaces did little to increase the yield capacity of the panels, but they did significantly increase the panel ultimate capacity or over-strength (capacity beyond yield). Tests also revealed that the modes of failure were correctly predicted by the model. Furthermore, the tests revealed that inset panel configuration also can increase panel ductility compared to the standard plywood configuration. Therefore, the model developed here is applicable but conservative for predicting the behavior of inset panel configurations.

Design capacity was based on established guidance from the National Design Specification (NDS) for Wood Construction.* Connection capacities were defined based on equations presented in Section 12.3.1, “Wood-to-Wood Connections.” Figure 17 illustrates each of the connection yield modes upon which the following equations are based. Each equation is based on single shear wood-to-wood connections. For each OSB or plywood panel connection, a nail is driven through the OSB into the perimeter members of the panel with the nail axis perpendicular to the wood fibers. The depth of the nail in these plates or studs is greater than the minimum penetration required by NDS (section 12.3.4). The nominal nail lateral design capacity, Z , based on OSB failure (Mode I_s), is calculated as follows (NSD, Eq 12.3.1):

$$\text{Mode I}_s \quad Z = \frac{Dt_s F_{es}}{K_D} \quad [\text{Eq 1}]$$

where,

* *National Design Specification (NDS) for Wood Construction*, ANSI/AF&PA NDS-1997, 1997 Edition, American Forest and Paper Association.

D = nail diameter, in.

t_s = thickness of the side member (OSB for Phase III shear panels), in.

F_{es} = dowel bearing strength of side member (OSB) from NDS Table 12A, psi.

$K_D = 2.2$ for $D \leq 0.17$ in.

$K_D = 1.0 D + 0.5$ for $0.17 \text{ in.} < D \leq 0.25$ in.

$K_D = 3.0$ for $D \geq 0.25$ in.

The nominal nail lateral design capacity, Z , based on single-point nail bending and nail rotation in the frame members (Mode III_m), is calculated as follows (NDS, Eq 12.3-2):

$$\text{Mode III}_m \quad Z = \frac{k_1 D p F_{em}}{K_D (1 + 2R_e)} \quad [\text{Eq 2}]$$

where,

$$k_1 = -1 + \sqrt{2(1 + R_e) + \frac{2F_{yb}(1 + 2R_e)D^2}{3F_{em}p^2}}$$

p = penetration depth of nail into frame members (member holding point), in.

F_{em} = dowel bearing strength of frame member (from NDS Table 12A), psi.

$R_e = F_{em}/F_{es}$

F_{yb} = bending yield strength for common nails, psi, which is defined as follows: *

$F_{yb} = 130,000 - 214,000 D$

* *Standard for Load and Resistance Factor Design (LRFD) for Engineered Wood Construction*, AF&PA/ASCE 16-95, American Forest and Paper Association, and American Society of Civil Engineers, 1996, "Commentary," Section C7.4.3, p 91.

The nominal nail lateral design capacity, Z , based on single-point nail bending and nail rotation in the OSB (Mode III_s), is calculated as follows (NDS, Eq 12.3-3):

$$\text{Mode III}_s \quad Z = \frac{k_2 D t_s F_{em}}{K_D (2 + R_e)} \quad [\text{Eq 3}]$$

where,

$$k_2 = -1 + \sqrt{\frac{2(1 + R_e)}{R_e} + \frac{2F_{yb}(2 + R_e)D^2}{3F_{em}t_s^2}}$$

The nominal nail lateral design capacity, Z , based on two-point nail bending (Mode IV, see Figure 17), is calculated as follows (NDS, Eq 12.3-4):

$$\text{Mode IV} \quad Z = \frac{D^2}{K_D} \sqrt{\frac{2F_{em}F_{yb}}{3(1 + R_e)}} \quad [\text{Eq 4}]$$

The nominal design capacities, Z , for each mode of failure for the OSB-to-frame member nail connections defined by Equations 1 through 4 above, are given in Tables 2 and 3. Table 2 shows the nominal capacities of these nail connections for the I_s and III_m failure modes. Table 3 gives the nominal capacities of these connections for the III_s and IV failure modes. Also, Table 3 displays two other failure conditions — strap/nailing plate tearing at the nail holes and nail shear strength. Tearing of the truss plate at a nail hole is calculated based on the nominal bearing strength of the nail holes, Z_b as follows, where deformation around the nail holes is a design consideration* (i.e., it represents a yield-type failure):

$$Z_b = 2.4D t_p F_u, \text{ lb} \quad [\text{Eq 5}]$$

where,

D = the diameter of the nails, in.

t_p = thickness of truss plate, in.

F_u = the ultimate strength of the truss plate assuming ASTM A653, Grade 33 steel, 45,000 psi

* *AISC Load and Resistance Factor Design*, 2nd Edition, 1994, J3.10, "Bearing Strength of Bolt Holes", p 6-85.

Table 2. Connection calculated capacities.

Panel Name	Side Member				K_D	l_s	Main Member			Dowel		Nail		III_m Nail Lateral Resistance Z (lb)
	Nail Size	Nail Dia D^1 (in)	Thickness of Side Member t_s (in)	Dowel Bearing Strength F_{es}^2 (psi)			Nail Lateral Resistance Z (lb)	Dowel Bearing Strength F_{em}^2 (psi)	Bearing Strength Ratio R_e	Nail Length L^1 (in.)	Nail Shank Penetration p (in)	Yield Strength in Bending F_{yb}^3 (ksi)	k_1	
P 3-1	8d	0.131	0.0598	33000	2.2	118	3350	0.10	2.5	2.4	102	0.508	205	
P 3-2	8d	0.131	0.5	5000	2.2	149	3350	0.67	2.5	2.0	102	0.882	150	
H4-Tie	8d	0.131	0.0359	33000	2.2	71	3350	0.10	2.5	2.5	102	0.507	207	
P 3-3	8d	0.131	0.5	5000	2.2	149	3350	0.67	2.5	2.0	102	0.882	150	
H4-Tie	8d	0.131	0.0359	33000	2.2	71	3350	0.10	2.5	2.5	102	0.507	207	
P 3-4	8d	0.131	0.5	5000	2.2	149	3350	0.67	2.5	2.0	102	0.882	150	
H4-Tie	8d	0.131	0.0359	33000	2.2	71	3350	0.10	2.5	2.5	102	0.507	207	
P 3-5	8d	0.131	0.5	5000	2.2	149	3350	0.67	2.5	2.0	102	0.882	150	
H4-Tie	8d	0.131	0.0359	33000	2.2	71	3350	0.10	2.5	2.5	102	0.507	207	
P 3-3M	8d	0.131	0.5	5000	2.2	149	3350	0.67	2.5	2.0	102	0.882	150	
H4-Tie	8d	0.131	0.0359	33000	2.2	71	3350	0.10	2.5	2.5	102	0.507	207	
P 3-6	8d	0.131	0.5	5000	2.2	149	3350	0.67	2.5	2.0	102	0.882	150	
H4-Tie	8d	0.131	0.0359	33000	2.2	71	3350	0.10	2.5	2.5	102	0.507	207	
P 3-7	8d	0.131	0.5	5000	2.2	149	3350	0.67	2.5	2.0	102	0.882	150	
H4-Tie	8d	0.131	0.0359	33000	2.2	71	3350	0.10	2.5	2.5	102	0.507	207	

1. Nail dimensions provided by manufacturer.
2. Assumes plywood and top plate is spruce-pine-fir with specific gravity of 0.42.

Table 3. Wood shear panel connections.

Panel Name	III_s Nail Lateral Resistance k_2	IV Nail Lateral Resistance Z (lb)	Strap/Plate Nominal Bearing Strength Z_b (lb)	Nail Nominal Shear Strength Z_v (lb)	Minimum Nail Lateral Resistance Z_{min} (lb)	Ultimate to Allowable Strength Ratio Q_u/Q_a	Yield to Load Duration Factor C_D	Yield to Ultimate Strength Ratio Q_y/Q_u	Nail Yield Strength Z_y (lb)	Nail Ultimate Strength Z_u (lb)	
P 3-1	14.04	80	112	846	687	80	2.16	1.6	0.8	220	276
P 3-2	1.950	73	91		687	73	2.16	1.6	0.8	201	252
H4-Tie	23.28	79	112	508	687	79	2.16	1.6	0.8	219	274
P 3-3	1.950	73	91		687	73	2.16	1.6	0.8	201	252
H4-Tie	23.28	79	112	508	687	79	2.16	1.6	0.8	219	274
P 3-4	1.950	73	91		687	73	2.16	1.6	0.8	201	252
H4-Tie	23.28	79	112	508	687	79	2.16	1.6	0.8	219	274
P 3-5	1.950	73	91		687	73	2.16	1.6	0.8	201	252
H4-Tie	23.28	79	112	508	687	79	2.16	1.6	0.8	219	274
P 3-3M	1.950	73	91		687	73	2.16	1.6	0.8	201	252
H4-Tie	23.28	79	112	508	687	79	2.16	1.6	0.8	219	274
P 3-6	1.950	73	91		687	73	2.16	1.6	0.8	201	252
H4-Tie	23.28	79	112	508	687	79	2.16	1.6	0.8	219	274
P 3-7	1.950	73	91		687	73	2.16	1.6	0.8	201	252
H4-Tie	23.28	79	112	508	687	79	2.16	1.6	0.8	219	274

However, the tearing capacity (Equation 5) is well above the other failure modes and therefore will probably not be a governing condition in these panels. Another

unlikely failure mode, nail shear strength, Z_v , was also checked. The nominal shear strength of a nail, Z_v , may be calculated as follows*:

$$Z_v = 0.5F_{yb}\pi\frac{D^2}{4}, \text{ lb} \quad [\text{Eq 6}]$$

where,

F_{yb} = the bending yield strength for common nails, psi, defined after Equation 2.

In Equation 6, nail yield strength, F_{yb} , was used instead of ultimate strength (as called for in the AISC specification) because ultimate values were unknown.

The minimum nominal capacity, Z_{\min} , which is the minimum value from Equations 1 through 6, representing the controlling mode of failure that determines the lateral capacity of the panels. The controlling mode of failure for all panels, III_s, is single-point bending in the nail with rotation in the nail through the entire thickness of the OSB, as shown in Figure 17. From these values the yield strengths, Z_y , and ultimate strengths, Z_u , were calculated according to Equations 7 and 8, respectively:

$$Z_y = \frac{Q_u}{Q_a} \frac{Q_y}{Q_u} C_D Z_{\min} \quad [\text{Eq 7}]$$

$$Z_u = \frac{Q_u}{Q_a} C_D Z_{\min} \quad [\text{Eq 8}]$$

where,

Q_u/Q_a = the ratio of ultimate over allowable strength, set equal to 2.16. This is based on the following from FEMA 274†, “the in-grade testing program conducted by AF&PA determined that the limit state or ultimate strength of the materials was, on average, 2.16 times the allowable strength”.

* AISC *Load and Resistance Factor Design*, 2nd Edition, 1994, J3.6, “Design Tension or Shear Strength,” and Table J3.2, pp 6-81 and 6-83.

† FEMA: Federal Emergency Management Agency; FEMA 274, National Earthquake Hazards Reduction Program (NEHRP), C8.3.2.5, p 8-6).

Q_y/Q_u = the ratio of yield load over ultimate load, set to equal 0.8 (FEMA 274, C8.3.2.5, p 8-6). This ratio may apply more to the overall panel behavior rather than an individual nail connection as it is being applied here. The overall panel resistance will increase after the nails in the corners first yield but continue to carry load. This is because the nails toward the panel interior will then pickup more load and eventually yield themselves, so that the overall panel resistance increases with further deformation. However, this increase is being represented entirely by the assumption that the yield strength of the nail connections is 20% less than their ultimate strength, because this effect can be easily incorporated into the analytical model.

C_D = load duration factor, which equals 1.6 for wind and earthquake load (NDS Table 2.3.2).

Table 3 presents nail yield strength, Z_y and nail ultimate strength Z_u values. Table 4 shows the panel width, W , height, H , and nail spacing between the OSB and top and bottom plates, s_B . The number of nails along the top and bottom plates, n , is determined as follows:

$$n = \frac{W}{s_B} + 1 \quad [\text{Eq 9}]$$

Plywood panel lateral capacity increases with vertical load. Therefore, in terms of lateral capacity, the most critical loading condition is a vertical load of zero. If no vertical load is applied, the only resistance to overturning rotation of the panel is due to the nails at the bottom and top plates of the panel. However, when vertical load is applied, the nails along the studs at the edge of the panel also contribute overturning moment resistance. Without vertical load, the plywood is free to rotate once the nail connections at the top and bottom have failed because the studs can only provide vertical resistance if they can act in bearing against the top and bottom plate. They can only provide axial resistance in compression because the nails at their ends to the top and bottom plates will provide no significant pullout resistance, especially along the axis of the stud fibers.

The spruce-pine-fir plates attached to the top frame allow for the zero load condition. As seen in Figure 2, the lateral load is applied to the panel over 4 ft away from the panel. This is a conservative approach because it eliminates any vertical load that could be transferred into the panel. Also, this approach conservatively allows for another failure condition — top plate bending — which is not modeled analytically. (See Chapter 2 for additional information on evaluating top plate bending failure.)

Overturning resistance was greatly increased by the installation of post-tensioned threaded rods (see Figure 2 for an example) at the panel edges. The rods allow the studs to develop vertical resistance in the same way as the vertical load, thus increasing overturning moment resistance.

Simpson Strong-Tie Hurricane Ties added additional overturning resistance capacity. The maximum overturning resistance is then equal to the holddown vertical capacity, HD, plus vertical load applied by the threaded rod, TR. The left side of Equation 10 is the applied overturning moment minus moment resistance provided by the OSB-to-stud nail connections. The right side of the equation is the overturning moment resistance provided by the nail connections between the plywood and the top and bottom plates. This assumes an identical nail pattern at the top and bottom.

$$PH - M_{sy} = \frac{2V_{\max} s_B^2}{W} \sum_{i=1}^n (n-i)^2 \quad [\text{Eq 10}]$$

where,

P = the total applied lateral load, lb.

H = the panel height, in.

M_{sy} = the overturning moment resistance, provided by the plywood-to-stud nail connections at their yield strength. This is defined as follows:

$$M_{sy} = \text{Min} \left[(TR_y + HD_y)W, \frac{H}{s_S} Z_{sy} W \right], \text{ lb-in.} \quad [\text{Eq 11}]$$

TR_y = the total applied vertical load, defined as follows for panels with threaded rods (for the PSP-Std baseline panel tested in Phase I, the actual total applied vertical load replaces TR_y):

$$TR_y = A_{nt} F_y, \text{ lb}$$

where,

$A_{nt} = 0.226 \text{ in}^2$, net tensile area for 5/8 in. threaded rod (*AISC Load and Resistance Factor Design*, 2nd Edition, 1994, Vol II, Table 8-7).

$F_y = 36,000$ psi, assumed to be AISI C-1008 – C-1012 steel based on ultimate strength values given by the supplier (McMaster-Carr Supply Company, Chicago, IL).

HD_y = the holddown yield capacity of a single stud anchor, defined by:

$$HD_y = \text{Min} \left[n_{HD} Z_y, T_{HD} \right], \text{ lb} \quad [\text{Eq 12}]$$

where,

n_{HD} = the number of nails in the holddown.

Z_y = the minimum yield strength for the nails connecting the holddown to the stud, defined by Equation 7, lb.

T_{HD} = the ultimate capacity of the holddown based on the critical net area of the steel. This is defined as:

$$T_{HD} = F_u A_n, \text{ lb} \quad [\text{Eq 13}]$$

where,

F_u = the ultimate strength of the Hurricane Tie steel, conservatively assumed to be A653 Grade 33 steel, 45,000 psi.

A_n = the net area of the holddown steel along the critical rupture surface, in².

W = the panel width, in.

ss = the vertical spacing between the nails at the studs along the edge of the panels, in.

Z_{sy} = the yield strength for the nails at the studs along the edge of the panels, lb.

V_{\max} = the maximum vertical load applied to the nails along the top and bottom plate due to overturning moment, lb. This assumes that all overturning moment resistance along the top and bottom plate is provided by the OSB-to-plate nails, i.e., it is assumed that the vertical nails at the ends of the studs provide no resistance.

s_B = the horizontal spacing between the nails along the top and bottom plate, in.

The right side of the series in Equation 10 can be rewritten in a polynomial form as follows:

$$PH - M_{sy} = \frac{2V_{\max} s_B^2}{W} \left[\frac{1}{3}(n-1)^3 + \frac{1}{2}(n-2)^2 + \frac{7}{6}(n-1) - \frac{1}{2} \right], \text{ lb-in.} \quad [\text{Eq 14}]$$

Equation 14 can be rewritten as:

$$\frac{V_{\max}}{PH - M_{sy}} = \frac{W}{2s_B^2 \left[\frac{1}{3}(n-1)^3 + \frac{1}{2}(n-2)^2 + \frac{7}{6}(n-1) - \frac{1}{2} \right]}, \text{ in}^{-1} \quad [\text{Eq 15}]$$

The lateral load applied to each nail along the top or bottom plate, T , is determined as follows:

$$T = \frac{P_y}{n}, \text{ lb} \quad [\text{Eq 16}]$$

Finally, the combined maximum vertical and lateral load applied to the nails at the panel corners, Z_{app} , is set equal to the nail yield strength, Z_y (see Equation 7), expressed as follows:

$$Z_y = Z_{app} = \sqrt{V_{\max}^2 + T^2}, \text{ lb} \quad [\text{Eq 17}]$$

The predicted panel lateral yield capacity, P_y , is determined by selecting values of P in an iterative process until Z_{app} is set equal to Z_y . Table 4 shows values of P_y for each panel. Similarly, the predicted panel lateral ultimate capacity, P_u , is determined by selecting values of P in an iterative process until Z_{app} is set equal to Z_u . Ultimate strength values are calculated for HD_u and M_{su} by modifying the expressions in Equations 10 through 12 and 14 through 16. Table 5 shows values of P_u for each panel.

Table 4. Predicted panel lateral yield capacity, P_y .

Panel Name	Threaded										Stud Nails					Applied				
	Panel/ Strap Width	Panel/ Strap Height	Nail Spacing at Base	Number of Nails at Base	Rod Yield Strength	Yield Holddown Capacity	Nail Spacing at Stud	Nail Yield Strength	Nail Yield Moment Resistance	V_{Max} PH- M_{sy}	P_y	V_{Max}	T	Nail Lateral Load	Nail Yield Strength					
	W (in.)	H (in.)	s_B (in.)	n	TR_y (lb)	HD_y (lb)	s_S	Z_y (lb)	M_{sy} (lb-in)		(lb)	(lb)	(lb)	Z_{app} (lb)	Z_y (lb)					
P 3-1	56	95.5		5	0			220			557									
P 3-2 H4-Tie	48	96	4	13	8136		4	201	232041	0.00231	2577	35	198	201.4	201.4					
P 3-3 H4-Tie	48	96	4	13	8136		3	201	348061	0.00231	2618	0	201	201.4	201.4					
P 3-4 H4-Tie	48	96	4	13	8136		4	201	232041	0.00231	2577	35	198	201.4	201.4					
P 3-5 H4-Tie	48	96	4	13	8136		3	201	348061	0.00231	2618	0	201	201.4	201.4					
P 3-3M H4-Tie	48	96	4	13	8136		2	201	432640	0.00231	2618	0	201	201.4	201.4					
P 3-6 H4-Tie	48	96	4	13	0		4	201	42112	0.00231	1240	177	95	201.4	201.4					
P 3-7 H4-Tie	24	96	4	7	0		8	201	21056	0.00824	460	190	66	201.4	201.4					

Table 5. Predicted panel lateral ultimate capacity, P_u .

Panel Name	Threaded						Stud Nails				Applied				
	Rod Ultimate Strength	Ultimate Holddown Capacity	Nail Spacing at Stud	Nail Ultimate Strength	Ultimate Moment Resistance	V_{Max} PH- M_{su}	P_u	V_{Max}	T	Nail Lateral Load	Nail Ultimate Strength				
	TR_u (lb)	HD_u (lb)	s_S	Z_u (lb)	M_{su} (lb-in)		(lb)	(lb)	(lb)	Z_{app} (lb)	Z_u (lb)				
P 3-1	0			276			697								
P 3-2 H4-Tie	13108		4	252	290051	0.00231	3222	44	248	251.8	251.8				
P 3-3 H4-Tie	13108	1097	3	252	435077	0.00231	3274	0	252	251.8	251.8				
P 3-4 H4-Tie	13108	1097	4	252	290051	0.00231	3222	44	248	251.8	251.8				
P 3-5 H4-Tie	13108	1097	3	252	435077	0.00231	3274	0	252	251.8	251.8				
P 3-3M H4-Tie	13108	1097	2	252	580102	0.00231	3274	0	252	251.8	251.8				
P 3-6 H4-Tie	0	1097	4	252	52640	0.00231	1550	222	119	251.8	251.8				
P 3-7 H4-Tie	0	1097	4	252	26320	0.00824	575	238	82	251.8	251.8				

For each OSB panel, the lateral capacity is limited by the single-point nail bending and nail rotation mode of failure (Mode III_s, see Figure 17). Nail bending is a ductile failure, but nail rotation in the plywood will be less ductile. Nail rotation in the plywood will result in bearing failure of the wood, which will provide no continued resistance in subsequent panel deformation cycles. This combined mode of failure will still produce ductile panel system behavior because of the sustained resistance, but the load/deflection hysteretic envelope will be badly pinched, because once the OSB is crushed it will not provide resistance at subsequent lower amplitude cycles.

(A pinched hysteretic envelope is where the cyclic plot of lateral load versus deflection is necked down near the zero deflection crossing.)

As noted previously, as soon as the nails begin to yield and rotate, the inset panels begins to bear up against the 2x6 frame, and this unaccounted-for load path increases lateral load resistance. Therefore, the ultimate capacity (or panel over-strength) for the inset panels should be significantly greater than for the baseline panels.

Diagonal Strap Shear Panel Model

The predicted strength of the P3-1 panel is based on a completely different model. The nail connection yield and ultimate capacities (Z_y and Z_u , respectively) were determined by Equations 7 and 8. The predicted lateral yield capacity, P_y and predicted lateral ultimate capacity, P_u , in this panel are determined as follows:

$$P_y = nZ_y \left(\frac{W}{\sqrt{W^2 + H^2}} \right), \text{ lb} \quad [\text{Eq18}]$$

$$P_u = nZ_u \left(\frac{W}{\sqrt{W^2 + H^2}} \right), \text{ lb} \quad [\text{Eq19}]$$

where,

n = the total number of nails at the diagonal strap connections to the top or bottom plate and studs.

W = the width of the panel, which for the P3-1 panels is the horizontal distance between the strap connections, in.

H = the height of the panel, in.

Figure 18 plots the predicted lateral yield and ultimate capacities for each Phase III OSB and diagonal strap shear panel. This plot assumes the lateral yield displacement, δ_y , equals 0.4 in. and the lateral ultimate displacement, δ_u , equals 2.0 in.

4 Test Configuration and Procedures

Test Apparatus

Figure 19 shows an overall view of the test frame (with a PSP-Adv I panel from Phase I tests) used to test all shear panels at CERL. The panels are anchored to the CERL structural load floor through a structural tube member (TS 12 x 16 x 5/8 in., with a 1 in. thick stiffener plate on top). The top of the panel is anchored to another structural tube (TS 10 x 14 x 5/8 in.). The load beam is loaded laterally with a long-stroke actuator (40 in. stroke) with a 140 kip capacity in compression, a 100 kip capacity in tension (see the left side of Figure 19), and a 2 in. per second velocity limit. Vertical load is applied through the top beam by means of two vertical actuators (25 kip capacity each) shown in Figure 19. One of the vertical actuators is tied to the other in stroke control in order to keep the top beam horizontal. Load control is used so that the total applied vertical load is held to zero. Restraining the beam horizontally represents the effect of the floor or roof diaphragm and it significantly influences the load path and panel behavior. The total vertical load is held constant through the control system software and feedback loop.* Horizontally oriented stub columns attached to the test frame prevent out-of-plane deflections. Teflon® plates are attached at the ends of the stub columns to provide a frictionless surface bearing against the polished areas of the structural tube load beam.

Test Procedure

The panels were tested following one of two protocols, monotonic or cyclical. One specimen of each panel configuration was tested monotonically. Based upon desirable monotonic performance, two more specimens of select panel configurations were tested cyclically.

* Because the load beam and half the lateral actuator weigh 2500 lb, the vertical actuator load was held at a constant 2500 lb in tension to achieve the desired zero vertical load.

Monotonic Test Protocol

Each panel configuration was tested monotonically by laterally loading in one direction in the absence of any applied vertical load. The lateral load was applied at a constant stroke rate of 0.5 in. per minute, as illustrated in Figure 20. The choice of load rate was slow enough to allow observation of panel performance and failure progression. Load was applied until the point of ultimate failure or a lateral displacement of at least 6 in.

CUREE/Caltech Wood Frame Project Cyclic Test Protocol

The Consortium of Universities for Research in Earthquake Engineering (CUREE) / Caltech Wood Frame Project developed a load history for cyclic testing of wood components that represent the seismic demands imposed by California earthquakes on wood frame buildings.* Although this protocol was developed with an emphasis on West Coast seismic motions, consideration was given to other seismic hazards. The basic loading history for component tests considering ordinary ground motions was used in the cyclic tests conducted for this study. This loading history was developed based on far more detailed study of the seismic demands and cumulative damage of structural systems than the cyclic protocols used in the Phase I and Phase II studies.† The basic CUREE/Caltech Wood Frame project load history (hereinafter called CUREE) was developed to represent the seismic demands imposed by Californian earthquakes on wood frame structures. Overall, the loading history consists of three types of cycles. The first range of loading cycles, or “initiation” cycles, comprises six low-amplitude cycles used to check the testing equipment and also serve to collect data on the initial stiffness. Very minimal damage may develop during the initiation cycles. This is characteristic of damage that an *in-situ* specimen may experience before the design earthquake. After the initial six cycles is the first “primary cycle,” which is then followed by six trailing cycles at 75% of the primary amplitude. The primary cycle amplitude increases and the sequence continues with fewer trailing cycles until the completion of the test. Table 6 shows the sequence and amplitudes of the cycles that were executed in all Phase III cyclical tests. The CUREE load history used in all the Phase III panel cyclic tests is plotted in Figure

* Krawinkler et al. 2001.

† Two cyclic protocols were used in the earlier studies, the Sequential Phased Displacement Protocol (SPD), defined in the City of Los Angeles Standard Method of Cyclic (Reversed) Load Test for Shear Resistance of Framed Walls for Buildings; and a modification to the SAC Joint Venture Testing Programs and Loading Histories, unpublished guidance, 1997.

21. The primary cycle amplitude is based on the reference deformation, Δ . The variable Δ is an estimate of the deformation capacity of a panel at ultimate load. For the tests performed, a Δ of 2 in. was chosen based on earlier tests of a similar panel (SK-7) and monotonic tests of the first specimen of each panel configuration. After viewing the test data, this estimate proved to be very accurate.

Table 6. CUREE load history cycles.

Load Step	Number of Cycles, n	Peak Amplitude	Displacement (in.) when $\Delta = 2.0$ in
1	6	0.050 Δ	0.10
2	1	0.075 Δ	0.15
3	6	(0.75) 0.075 Δ	0.11
4	1	0.1 Δ	0.20
5	6	(0.75) 0.1 Δ	0.15
6	1	0.2 Δ	0.40
7	3	(0.75) 0.2 Δ	0.30
8	1	0.3 Δ	0.60
9	3	(0.75) 0.3 Δ	0.45
10	1	0.4 Δ	0.80
11	2	(0.75) 0.4 Δ	0.60
12	1	0.7 Δ	1.40
13	2	(0.75) 0.7 Δ	1.05
14	1	1.0 Δ	2.00
15	2	(0.75) 1.0 Δ	1.50
16	1	1.5 Δ	3.00
17	2	(0.75) 1.5 Δ	2.25
18	1	2.0 Δ	4.00
19	2	(0.75) 2.0 Δ	3.00
20	1	2.5 Δ	5.00
21	2	(0.75) 2.5 Δ	3.75
22	1	3.0 Δ	6.00
23	2	(0.75) 3.0 Δ	4.50
24	1	3.5 Δ	7.00
25	2	(0.75) 3.5 Δ	5.25
26	1	4.0 Δ	8.00
27	2	(0.75) 4.0 Δ	6.00

The CUREE cyclic test protocol was thought to be more representative of the loading effects of real earthquakes than the Sequential Phased Displacement (SPD) protocol used in the related Phase I and II wood shear panel studies. For comparison purposes, the application of the SPD protocol to the Phase IV panels would have used a first major event (FME) of 0.4 in. to scale the cyclic load history; the CUREE protocol used a reference deformation, Δ , of 2.0 in. to scale its load history. These estimates of FME and Δ are based on either monotonic test results or earlier cyclic testing of similar panels. The SPD protocol results in an excessive number of large-amplitude (post-yield) cycles, when panels are tested to large ultimate deflections (i.e., large ductility). If panels were tested to a lateral deflection of one cycle at 5 in., they would have been subjected to 156 post-yield deflection cycles at a deflection equal to 12.5 times the FME. This is not an excessively large deflection, but the number of post-yield cycles is excessive. By comparison, the same panel tested fol-

lowing the CUREE protocol, using a Δ of 2.0 in., would have been subjected to only 20 post-yield (beyond 0.4 in. deflection) cycles. Even if the panels reached their ultimate deformation at just 4 times the FME (very poor ductility), they would still be subjected to 38 post-yield cycles. If the CUREE protocol were used, the panels would be subjected to only 11 cycles to reach this deformation. Clearly, the CUREE protocol results in a conservatively high yet much more reasonable number of post-yield cycles that one could expect in even a very severe, long-duration earthquake. Testing standard plywood shear panels in previous studies showed that the plywood-to-framing nails around the panel perimeter were subjected to so many bending cycles that the nails fractured due to low-cycle fatigue. Similar OSB panels (e.g., P3-6) tested according to the CUREE protocol exhibited no nail fractures. The authors are not aware of nail fracture ever being reported as a result of actual earthquakes, further indicating that the CUREE protocol is more appropriate. Because of the more rigorous basis for the development of the CUREE protocol and this comparison of number of post-yield cycles, the CUREE protocol was used for all Phase III cyclic tests.

The start of the tests ran at a cyclic rate of 0.1 Hz (10 seconds per cycle or 6 cycles per minute) until the primary cycle with 0.6 in. amplitude because no significant damage or modes of failure were expected before that amplitude. A cyclic rate of 0.05 Hz (20 seconds per cycle or 3 cycles per minute) was used beginning at the amplitude of 0.6 in. The cyclic rate was slowed to 0.05 Hz to provide adequate time to document panel performance and failure progression. Also, if extreme lateral deformations over 10 in. were reached, the cyclic rate would have had to be slowed further or else the horizontal actuator's limiting velocity of 2 in./sec would be exceeded.

As in the monotonic tests, the top beam test fixture was held horizontal and no net vertical load was applied during the CUREE cyclic tests.

Instrumentation

Table 7 lists the instrumentation used for the shear panel tests and describes the purpose of each sensor. Figure 22 shows the sensors' location and orientation. To ensure that no unwanted motion took place, most gages were used for test control. Table 7 shows that several of the deflection measurements were made using linear variable differential transformers (LVDTs). The primary data used in reporting panel performance were gathered from channels 0, 1, 2, and 4. The vertical actuator force measurements (FVS and FVN in Table 7 and Figure 22) are required to define total shear force when deflections reach large amplitudes, at which point the

horizontal components of these forces become significant. The total actuator vertical force, TVF, was held to a constant 2500 lb tensile force, which supported the weight of the test fixture and half the lateral actuator, so that a net vertical force of zero would be applied to test panels. In Equation 20, TVF equals 2500 lb, which reduces the total shear force, TSF, at large horizontal displacements. TSF is determined as follows:

$$TSF = FH - TVF \left\{ \sin \left[\arctan \left(\frac{SH}{L} \right) \right] \right\} \quad [\text{Eq 20}]$$

where,

FH = the measured horizontal actuator force, lb.

TVF = the total vertical actuator force, equal to FVS plus FVN, lb.

SH = the measured horizontal actuator displacement, in.

L = the length of the vertical actuators, with vertical load applied, but no horizontal displacement, equal to 53 in. for the CERL test frame, in.

Table 7. Wood shear panel instrumentation.

Channel	Name & Type	Location & Positive Direction	Purpose
0	SH, Stroke	Lateral actuator, In-plane horizontal, South	Horizontal actuator displacement
1	FH, Load	Lateral actuator, In-plane horizontal, South	Horizontal actuator load measurement
2	FVS, Load	South vertical actuator, up	Vertical Load control
3	SVS, Stroke	South vertical actuator, up	Vertical Stroke (tied to #5)
4	FVN, Load	North vertical actuator, up	Load (summed with #2 for a 0 kip load)
5	SVN, Stroke	North vertical actuator, up	Controlled by #4, stroke feedback
6	D1, LVDT	North Rod, up	North Rod Displacement
7	D2, LVDT	South Rod, up	South Rod Displacement
8	D3, LVDT	South side wood to base beam, In-plane horizontal, South	To ensure no slippage
11	DH, Disp	North side of top wood beam, in-plane horizontal, South	Panel horizontal deflection measurement
12	FRN, Load	North Load Cell, Compression	North Rod Load Measurement
13	FRS, Load	South Load Cell, Compression	South Rod Load Measurement

5 Test Results and Observations

Table 8 summarizes all Phase III wood shear panels tested at CERL by showing test dates, panel names, panel descriptions, vertical loads applied, and load protocols. Table 8 also includes Phase I results of two PSP-STD panels tested according to different protocols, used in this study to help establish the performance baseline. A more detailed discussion of panel configurations is provided in Chapter 2. Figures 1 through 15 present construction drawings of all panels tested, including the PSP-Std panel from Phase I.

Generally, three panels of each configuration were tested, beginning with one specimen tested monotonically followed by two tested using the CUREE cyclic protocol. Tests from previous phases demonstrated that applying zero vertical load is more critical for the plywood panels than actually applying a vertical load. Therefore, all of the panels were built to test without vertical load. The monotonic test results provided an estimate of predicted deformation capacity at ultimate load, Δ , which was used as the reference deformation for the subsequent CUREE cyclic tests.

The strength of wood products is reduced under moist service conditions.* Specified design values are applicable to dry service conditions where the moisture content in use will be a maximum of 19%. Wet service factors, C_M , are used to correct design values when moisture content of wood in service exceeds 19%. Therefore, the moisture content of various components of the test panels was measured before testing. Table 9 shows the maximum moisture content measured in the indicated component of each test panel. These values were measured using a Protimeter Mini Super Mk II moisture meter. All of the panels' maximum moisture levels were at 14% or below. Therefore, no correction of test results was needed for any measured strength values.

* NDS, Section 4.1.4, "Moisture Service Condition of Lumber."

The following sections provide test results and detailed observations on the performance of each panel type.

Table 8. Summary of panels tested.

Date Tested	Panel Name	Panel Description	Vertical Applied Load	Lateral Load Protocol
7/26/00	P 3-1 Mono	1-1/4" x 16 ga diagonal straps on 2 x 6 frame	0	Monotonic
7/27/00	P 3-1 C1	1-1/4" x 16 ga diagonal straps on 2 x 6 frame	0	CUREE
7/27/00	P 3-1 C2	1-1/4" x 16 ga diagonal straps on 2 x 6 frame	0	CUREE
7/21/00	P 3-2 Mono	Inset panel, 5/8" rods outside panel w/8000 lb pre-tension, out-of-plane frame, TP35 plates at top	0	Monotonic
7/26/00	P 3-2 C1	Inset panel, 5/8" rods outside panel w/8000 lb pre-tension, out-of-plane frame, TP35 plates at top	0	CUREE
7/26/00	P 3-2 C2	Inset panel, 5/8" rods outside panel w/8000 lb pre-tension, out-of-plane frame, TP35 plts at top	0	CUREE
7/24/00	P 3-3 Mono	Inset panel, 5/8" rods inside panel w/8000 lb pre-tension, out-of-plane frame, TP35 plts at top	0	Monotonic
7/25/00	P 3-4 Mono	Inset panel, 5/8" rods outside panel w/8000 lb pre-tension, in-plane frame, TP35 plts at top	0	Monotonic
7/25/00	P 3-5 Mono	Inset panel, 5/8" rods inside panel w/8000 lb pre-tension, in-plane frame, TP35 plts at top	0	Monotonic
7/31/00	P 3-3M Mono	Inset panel, 5/8" rods inside panel w/6000 lb pre-tension, out-of-plane frame, TP35 plts at top	0	Monotonic
7/31/00	P 3-3M C1	Inset panel, 5/8" rods inside panel w/6000 lb pre-tension, out-of-plane frame, TP35 plts at top	0	CUREE
8/2/00	P 3-3M C2	Inset panel, 5/8" rods inside panel w/6000 lb pre-tension, out-of-plane frame, TP35 plts at top	0	CUREE
8/1/00	P 3-6 Mono	Baseline panel w/1/2" OSB, 2 x 4 studs 16" o.c., double top plt, H4 & H6 hurricane clips	0	Monotonic
8/1/00	P 3-6 C1	Baseline panel w/1/2" OSB, 2 x 4 studs 16" o.c., double top plt, H4 & H6 hurricane clips	0	CUREE
8/1/00	P 3-6 C2	Baseline panel w/1/2" OSB, 2 x 4 studs 16" o.c., double top plt, H4 & H6 hurricane clips	0	CUREE
8/2/00	P 3-7 Mono	Narrow inset panel, no rods or nailing plates, out-of-plane frame	0	Monotonic
8/2/00	P 3-7 C1	Narrow inset panel, no rods or nailing plates, out-of-plane frame	0	CUREE
8/2/00	P 3-7 C2	Narrow inset panel, no rods or nailing plates, out-of-plane frame	0	CUREE
3/4/99	PSP-Std-SPD1	Phase I Baseline panel w/1/2" 5-ply Douglas Fir Grade I plywood, 2 x 4 studs 16" o.c., double top plt	2500 lb	SPD
3/4/99	PSP-Std-MS1	Phase I Baseline panel w/1/2" 5-ply Douglas Fir Grade I plywood, 2 x 4 studs 16" o.c., double top plt	8000 lb	Mod SAC

Table 9. Maximum measured moisture content for each test panel.

Date Tested	Panel & Test		Wall Bottom Plate	Wall Top Plate	Edge Studs	Plywood	Inset Panel	
							Top or Bottom Plate	Studs
7/26/00	P3-1	MONO	11%	8%	9%	-	-	-
7/27/00	P3-1	C1	11%	8%	11%	-	-	-
7/27/00	P3-1	C2	11%	9%	11%	-	-	-
7/21/00	P3-2	MONO	9%	11%	8%	4%	9%	11%
7/26/00	P3-2	C1	9%	9%	6%	N.A.	12%	9%
7/26/00	P3-2	C2	9%	11%	8%	6%	9%	9%
7/24/00	P3-3	MONO	9%	9%	8%	4%	4%	8%
7/25/00	P3-4	MONO	9%	11%	4%	4%	8%	9%
7/26/00	P3-5	MONO	9%	9%	N.A.	4%	8%	8%
7/31/00	P3-3M	MONO	11%	12%	N.A.	8%	9%	11%
7/31/00	P3-3M	C1	11%	12%	11%	6%	9%	9%
8/3/00	P3-3M	C2	9%	11%	11%	4%	6%	12%
8/1/00	P3-6	MONO	12%	12%	9%	4%	-	9%
8/1/00	P3-6	C1	9%	12%	N.A.	4%	-	8%
8/1/00	P3-6	C2	9%	12%	N.A.	6%	-	9%
8/2/00	P3-7	MONO	11%	8%	N.A.	8%	8%	9%
8/2/00	P3-7	C1	11%	12%	9%	6%	8%	9%
8/2/00	P3-7	C2	9%	11%	N.A.	9%	8%	11%
3/4/99	PSP-Std	SPD1	9%	9%	11%	9%	-	-
3/4/99	PSP-Std	MS1	11%	11%	9%	14%	-	-

Test Documentation Based on City of Los Angeles (LA) Guidance

The cyclic tests conducted in the current study were based on the CUREE load protocol defined in Chapter 4. However, for continuity with the Phase I and II studies, panel response is also documented in the format defined by the *City of Los Angeles Standard Method of Cyclic (Reversed) Load Test for Shear Resistance of Framed Walls for Buildings*. This guidance prescribes that cyclic tests be conducted according to the sequential phased displacement, SPD load history. As discussed in Chapter 4, the SPD protocol has many more post-yield cycles before reaching lateral deformations that correspond to the ultimate capacity of test panels. Therefore, documenting panel behavior based on the City of LA guidance, but tested according to the CUREE rather than SPD protocol, will result in greater strength and ductility values. Reporting this information was judged to be useful for subjective comparisons with earlier studies, but it was not used to form the basis for design rec-

ommendations. Chapter 8 of the City of LA guidance indicates that the parameters shown below should be defined as follows:

$$\text{Maximum Shear Strength, } S_{\max} = \frac{P_{\max}}{W} \left(\frac{12 \text{ in}}{\text{ft}} \right), \text{ lb/ft} \quad [\text{Eq 21}]$$

where,

P_{\max} = the average absolute value of strength limit states, lb.

W = the shear panel width, in.

$$\text{Shear Stiffness, } G' = \left(\frac{P}{\Delta} \right) \left(\frac{H}{W} \right), \text{ lb/in.} \quad [\text{Eq 22}]$$

and

P = the lateral shear force measured at the top edge of the wall, equal to TSF in Equation 20, at both the yield and strength limit states due to loading in both the positive and negative directions, lb. The yield limit state is defined as the point on the force-displacement relationship where the panel clearly begins to behave in a nonlinear manner, which is also the onset of panel damage. (The definition for the yield limit state in the City of LA guidance cannot be used for the CUREE test because a single primary cycle is followed by lower amplitude trailing cycles (75% of primary). The strength limit state is the point on the force-displacement plot where the maximum lateral capacity is reached.)

Δ = the lateral panel deflection at the top of the wall panel, equal to SH in Table 7 or Figure 22, at both the yield limit and strength limit state due to loading in both the positive and negative directions, in.

H = the height of the shear panels, equal to 97 in. for all panels tested in this phase, in.

For all monotonic or cyclically tested panels, the lateral force (TSF) is plotted with respect to the lateral displacement (SH). The lateral load versus deflection data are plotted from the cyclic tests to form hysteretic envelopes. The load versus deflection performance of the panels defined by these plots is compared with observation on the progression of failure to define the ductile behavior of the shear panels. From the cyclic data, the average maximum shear strength, S_{\max} ,; positive and negative

displacement at yield (yield limit state); positive and negative shear force at yield; and positive and negative shear modulus at yield are defined. The positive and negative displacement, shear forces, and shear modulus are also defined for the ultimate strength (strength limit state). The positive and negative yield and ultimate shear forces are plotted on the hysteretic envelopes of recorded data to create a bi-linear curve fit. The data described above are summarized in tables for each test panel.

Test Documentation Based on FEMA 273 Guidance

The *NEHRP Guidelines for Seismic Rehabilitation of Buildings* (FEMA 273), provides guidance for quantifying panel behavior from test data. For an experimental program like this it is important to report test data in a way that is useable by others outside the original project. FEMA 273 provides guidance for the evaluation of buildings, including a procedure for interpreting cyclic test data, and this procedure is applied as follows:

1. FEMA 273 indicates that a second cycle backbone curve (follow FEMA 273, 2.13.3, “Design Parameters and Acceptance Criteria,” pp 2-44 to 2-46) should be defined for both positive and negative deformation. The CUREE cyclic tests protocol uses a single primary deformation cycle followed by two trailing cycles at 75% of the primary. Therefore, the points of the backbone curve are defined by those points where a new primary cycle crosses over the previous primary cycle, achieving a similar reduced envelope as the second cycle plots. This backbone curve is plotted along with the cyclic test data for each test panel.
2. Determine if the panel conforms to a Type 1 or Type 2 force deformation curve, as defined by FEMA 273, Figure 2-4, p 2-32, where the deformation parameter, e , is at least twice g . If the force deformation curve conforms to Type 1, but e is not more than twice g , and d is at least twice g , the deformation curve may be redrawn as shown in Figure 2-7 of FEMA 273, p 2-46. If neither requirement is met, the panel is classified as Type 3, and a force controlled panel. All panels tested in this study should be Type 1 or 2.
3. Define the stiffness of the shear panel, K , for use in linear procedures from the slope of the first segment of the average backbone curve (FEMA 273, 2.13.3 paragraph 3, p 2-45).

4. The yield strength, Q_y , or expected strength, Q_{CE} , for deformation-controlled panels is the lateral load value at the end of the first segment of the average backbone curve (FEMA 273, 2.9.4, p 2-33 and Figure 2-4, p 2-32). This value was chosen at a location on the backbone curve that clearly indicates the panel has begun to behave in a nonlinear manner or the onset of damage has begun.
5. For deformation-controlled panels, determine the extent of post-yield deformation for life safety performance level, m_{LS} . This is calculated from the average backbone curve, where m_{LS} equals 0.75 times the deformation at point 2 (δ_2) (maximum deformation before lateral resistance has dropped to no less than 80% of ultimate) of the Type 1 or Type 2 deformation curves divided by the deformation at yield (δ_y , point 1) (FEMA 273, 2.13.3, paragraph 7, p 2-46). This is expressed as:

$$m_{LS} = 0.75 \frac{\delta_2}{\delta_y} \quad [\text{Eq 23}]$$

6. Determine the ultimate capacity, Q_u , as follows*:

$$Q_u = m_{LS} Q_{CE} \quad [\text{Eq 24}]$$

7. The data based on the FEMA 273 guidance are presented in tabular form. The data are provided only for the cyclically loaded specimens of each panel configuration. All Phase III panels were loaded with the CUREE protocol while one of the Phase I PSP-Std panels was loaded with the SPD protocol and the other was loaded with modified SAC.

Calculated Allowable Design Capacity

The allowable design capacity, P' , can be calculated based on the model presented in Chapter 3 if the observed panel behavior is controlled by the predicted nail connection failures (i.e., modes of failure) and the model reasonably, yet conservatively predicts panel capacity. The first condition can be determined by comparing the lo-

* Method derived using guidance from FEMA 273, 2.13.3, and training handout provided for *FEMA 273 Training – Examples of Applications to Wood Buildings* (FEMA, Washington, DC, February 2000).

cation and mode of failures of the test panels with those predicted (e.g., Mode III_s for P3-3). The second condition can be determined by comparing the measured data with the predicted yield and ultimate capacity. Using this model, the allowable capacity, P' , is determined similar to P_y and P_u by selecting values of P in an iterative process until the connection applied force, Z_{app} is set equal to the connection allowable design strength, Z' . Appendix A at the end of this report presents a modification of the model developed in Chapter 3 to calculate panel capacity using allowable strength design. The calculated allowable design capacities for all test panels with zero vertical loads are presented in Table 10.

Appendix A also shows that the panel allowable design resistance, D' , is the panel allowable capacity, P' , divided by the panel width, W . The calculated design capacities are also presented in the summary tables for each panel configuration as these may influence the definition of allowable design capacities. If this model effectively predicts allowable capacities that are consistent with other accepted design values, the model could be used in the development of design values for panels of similar configuration but with different variables.

Table 10. Calculated panel allowable strength design capacities.

Panel Name	Panel Width W (in.)	Panel Height H (in.)	Nail Spacing at Base s_B (in.)	Number of Nails at Base n	Applied Dead Load DL (lb)	Allow		Minimum		Allow		Allow		Applied		Allow	
						Design Capacity HD _a (lb)	Nail Spacing at Stud s_s	Nail Lateral Resistance Z_{min} (lb)	Load Duration Factor C_D	Nail Design Strength Z' (lb)	Stud Nails Moment Resistance M_{sa} (lb-in)	V_{Max}	P'	V_{Max}	T	Z_{app}	Z'
						PH-M _{sa}											
P 3-1	56	95.5		5	0			80	1.6	128				323			
P 3-2 H4-Tie	48	96	4	13	6102		4	73	1.6	117	134283	0.00231	1492	21	115	116.6	116.6
P 3-3 H4-Tie	48	96	4	13	6102		4	73	1.6	117	201424	0.00231	1516	0	117	116.6	116.6
P 3-4 H4-Tie	48	96	4	13	6102		4	73	1.6	117	134283	0.00231	1492	21	115	116.6	116.6
P 3-5 H4-Tie	48	96	4	13	6102		3	73	1.6	117	201424	0.00231	1516	0	117	116.6	116.6
P 3-3M H4-Tie	48	96	4	13	6102		2	73	1.6	117	268566	0.00231	1516	0	117	116.6	116.6
P 3-6 H4-Tie	48	96	4	13	0		4	73	1.6	117	24370	0.00231	717	103	55	116.6	116.6
P 3-7 H4-Tie	24	96	4	7	0		4	73	1.6	117	12185	0.00824	266	110	38	116.6	116.6

P3-1 Test Results

Table 11 summarizes the performance of all P3-1 shear panels tested following the monotonic and CUREE test protocols. The tests are documented using both the City of LA and FEMA 273 guidance. The calculated allowable strength design capacities defined in Appendix A and presented in Table 10 are included in Table 11.

P3-1 Monotonic

The first P3-1 panel was tested monotonically by loading it at 0.5 in. per minute laterally in the positive (south) direction. The top beam was held horizontal and forced to maintain a net vertical load of 0 lb. Figure 23 shows the lateral load versus deflection performance of this panel. This plot does not show a very well defined yield point. Between 1.0 in. and 2.5 in. lateral deflection, the slope of the lateral load versus deflection plot decreased. The steel strap attached to the frame from the top left to the bottom right was being tensioned by the lateral force, causing it to compress the top and bottom plates, which lead to crushing of the bottom plate as shown in Figure 24. At a deflection of 2.59 in. the panel reached its ultimate capacity of 1411 lb. After this point, the panel continued to behave in a ductile manner. Near 2.75 in. deflection, the nails holding the strap to the frame began to yield and pull out, causing the load capacity to decrease. By 3.7 in. deflection the nails holding the strap were almost completely pulled out, rendering the strap useless for load resistance (as seen in Figure 25). At 4.0 in. deflection, the load leveled off and remained fairly constant throughout the remainder of the test, which was halted at 7.0 in. deflection. There was still some residual capacity in the frame at the end of the test. This capacity was from a secondary load path between the strap and studs in weak axis bending. The strap under tension was still attached to the frame at the middle stud.

P3-1 CUREE1

This P3-1 panel was tested cyclically using the CUREE protocol, and the results were plotted in Figure 26. At 0.6 in. deflection, slight buckling in the top plate was noted. By 0.8 in. deflection, it was compressing near the strap attachment on the right side and the nails began to pull out on the left side. A popping noise was heard at 1.0 in. deflection, attributed to cracking of the bottom plate at the two strap attachments. At 2.0 in. deflection, the straps pulled and twisted the bottom plate, creating a gap of approximately $\frac{1}{4}$ in. similar to that seen in the monotonic test. At 3.0 in. deflection the straps started to bite into the top plate on the right side at 3.0, and by 4.0 in. the left side had begun to fail similarly. During this cycle, the maximum load in the positive direction (1661 lb) was reached at 3.40 in., and the nail that attached the strap to the narrow face of the top beam started to pull out of the beam. The second stud from the left began to lift significantly at 5.0 in. deflection and the strap on the left side of the top plate ripped the wood. The maximum load in the negative direction was reached at 5.64 in. (1798 lb), then the capacity continued to decrease as a result of nail yielding and pull-out. At 7.0 in. the strap connected to the top plate on the left side had pulled out completely, and the strap connected to the top plate on the right had pulled out of the top. By 8.0 in.

the strap had pulled out completely, as shown in Figure 27. Residual capacity remained in the system due to the bending of the studs and the resistance provided by the length of the strap still attached to the studs in the bottom half of the panel.

Table 11. Performance of P3-1 shear panels.

Parameter	P3-1 Mono	P3-1 CUREE1	P3-1 CUREE 2	Cyclic Average
Average Maximum Shear Strength, S_{max} (lb/ft)	353	432	443	
Positive Displacement at Yield Limit State, Δ (in.)	0.41	0.55	0.38	
Negative Displacement at Yield Limit State, Δ (in.)		-0.37	-0.59	
Positive Shear Force at Yield Limit State, P (lb)	538	630	458	
Negative Shear Force at Yield Limit State, P (lb)		-588	-759	
Positive Shear Modulus at Yield Limit State, G (lb/in)	2659	2297	2464	
Negative Shear Modulus at Yield Limit State, G (lb/in)		3225	2592	
Positive Displacement at Strength Limit State, Δ (in.)	2.59	3.40	6.71	
Negative Displacement at Strength Limit State, Δ (in.)		-5.64	-2.87	
Positive Shear Force at Strength Limit State, P (lb)	1411	1661	1812	
Negative Shear Force at Strength Limit State, P (lb)		-1798	-1736	
Positive Shear Modulus at Strength Limit State, G (lb/in)	810	731	432	
Negative Shear Modulus at Strength Limit State, G (lb/in)		464	865	
Idealized force vs deformation curve, FEMA 273, Fig 2-4				
		Type 2	Type 2	
Positive Shear Stiffness, K_+ (lb/in)		982	1268	
Negative Shear Stiffness, K_- (lb/in)		1126	1408	1196
Positive Expected Strength, Q_{CE+} (lb)		743	445	
Negative Expected Strength, Q_{CE-} (lb)		-895	-541	
Positive Yield Deformation δ_{y+}		0.76	0.35	
Negative Yield Deformation δ_{y-}		-0.79	-0.38	
Positive Deformation above 80% ultimate resistance δ_{2+}		4.97	7.03	
Negative Deformation above 80% ultimate resistance δ_{2-}		-6.01	-4.08	
Positive Post-Yield Deformation for Life Safety Perf, m_{LS+}		4.93	15.02*	
Negative Post-Yield Deformation for Life Safety Perf, m_{LS-}		5.67	5.92	
Positive Ultimate Capacity, Q_u+ (lb) =		3658		
Negative Ultimate Capacity, Q_u- (lb) =		-5077	-3201	
Average Ultimate Capacity, Q_u (lb)		4368	3201	3979
Calculated Allowable Design Capacity, P' (lb)	323	323	323	323
Calculated Allowable Design Resistance, D' (lb/ft)	69	69	69	69

* This calculated value of m_{LS} is not valid because the ultimate capacity was not reached in the CUREE cyclic test. Due to other failures, a defined ultimate load was not reached.

P3-1 CUREE2

The second cyclic test of the P3-1 panel yielded different results from those found in the first test. The modes of failure occurred in the same general pattern, but in the second test there was significantly more damage to the top plate at the right con-

nection, where cracks formed both perpendicular and parallel to the grain. This reduced the ultimate capacity during the negative stroke to 1736 lb at 2.87 in., as seen in the load-versus-displacement plot in Figure 28. The positive displacement capacity increased in this test since the failures (see Figure 29) permitted significant displacement without loss of capacity. In fact, the load resistance increased throughout the test, up to 1812 lb at 6.71 in. deflection. The load resistance did begin to level off toward the end of the test, at 8.0 in., because the nails pulled out where the strap was attached to the stud and top plate. The lines visible in Figure 30 were drawn after the test, and they show the cracks in the top plate at the right connection. Figure 31 shows an overall view of this damaged panel after the test.

The data plots shown in Figures 23, 26, and 28 show the predicted capacity of the P3-1 panels along with the measured data. The yield capacity is predicted well by the model. These plots reveal that the P3-1 panel had significant overstrength (capacity beyond yield) and fairly good ductility. Table 11 shows that an ultimate capacity of 3979 lb was determined, based on the measured data. Table 4 showed a predicted yield capacity of 557 lb, and the test data plots agrees well with this value. However, this panel has very good over-strength and fairly good ductility, so the calculated allowable design capacity shown in Table 10 and Table 11 (323 lb) appears to be too conservative.

P3-2 Test Results

Table 12 summarizes the performance of all P3-2 shear panels in the same format as Table 11.

P3-2 Monotonic

The monotonic load was applied laterally to the south (left in Figure 2). Figure 32 shows the lateral load versus deflection performance of this panel. This plot does not show a very well defined yield point. Between $\frac{1}{2}$ in. and 2 in. deflection the panel stiffness leveled off. The nails in the bottom right corner attaching the OSB to the panel frame began to yield, and the panel itself started to lift off of the bottom plate during this stage (see Figure 33). At a lateral deflection of 2.6 in. the panel reached its ultimate capacity of 5714 lbs. After this point, the panel lost strength but continued to behave in a ductile manner. Just after reaching its ultimate peak, bearing of the bottom left corner of the OSB caused the bottom plate to split, which then resulted in the OSB pulling out of the panel as shown in Figure 34. The next major event occurred at approximately 3.5 in. deflection. The top plate on the right side of the panel split longitudinally due to bending, which began at a deflection of

2.2 in. (see Figure 35). At 4.5 in. deflection, the OSB began to pull out of the panel frame more severely due to nail yielding. By a deflection of 6.2 in., all of the nails that connected the OSB to the panel frame along the left side and in the bottom right corner had pulled through. Toward the end of the test, the OSB sheared loose from the upper left TP35 nailing plate, as shown in Figure 36. The test was halted at 7 in. deflection. Minimal damage was done to the TP35 nailing plates and associated nails.

P3-2 CUREE1

The lateral force versus displacement for the first cyclic test on a P3-2 panel is plotted in Figure 37. This panel was observed to begin yielding at a deflection of 0.6 in., when the OSB began to lift off the bottom plate as shown in Figure 38. At 1.4 in. the upper right and left corners of the OSB started to crush and buckle. The nails connecting the upper corners and the bottom right corner began to pull out of the plates at 1.5 in. Upon reaching 3.0 in. deflection, the lower edge of the OSB pulled out of the lower portion of the frame (see Figure 39). The peak load was reached, resisting 5496 lb in the positive direction at 2.93 in. and 5481 lb in the negative direction at 2.99 in. At 4.3 in. the top plate split above the left edge of the OSB while the plate working back and forth chewed the top OSB corners (see Figure 40). The lower right OSB nails were observed to be bending and pulling away from the frame. At 5.0 in. the nails in the upper left and right plates showed signs of bending, and the test was halted after 6.0 in. deflection. Residual stresses were found in the studs, which were still capable of resisting lateral load through weak axis bending, and in the nailing system, which still allowed transfer of shear through nails that had not pulled out of the panel or yielded completely.

P3-2 CUREE2

The lateral force versus displacement for the second cyclic test on P3-2 is given in Figure 41. This test produced a pattern of failure similar to that in the first cyclic test, except the failures occurred at earlier stages. The peak load was reached at 5646 lb and 1.97 in. displacement in the positive direction, at which time the nails began to yield in the corner plates, some nails pulled out along the bottom, and the top plate began to split. The peak load in the negative direction occurred at 5877 lb and 2.74 in. displacement. The bottom left corner began to crush while nails pulled out of the bottom of the OSB and nailing plates on top. After the panel had deteriorated and load capacity was lost, the test was halted at 7.0 in. deflection.

Table 12. Performance of P3-2 shear panels.

Parameter	P3-2 Mono	P3-2 CUREE1	P3-2 CUREE2	Cyclic Avg
Average Maximum Shear Strength, S_{max} (lb/ft)	1429	1372	1440	
Positive Displacement at Yield Limit State, Δ (in.)	0.40	0.39	0.37	
Negative Displacement at Yield Limit State, Δ (in.)		-0.40	-0.18	
Positive Shear Force at Yield Limit State, P (lb)	2925	2893	3206	
Negative Shear Force at Yield Limit State, P (lb)		-2974	-2049	
Positive Shear Modulus at Yield Limit State, G (lb/in)	14911	14826	17296	
Negative Shear Modulus at Yield Limit State, G (lb/in)		14919	23356	
Positive Displacement at Strength Limit State, Δ (in.)	2.64	2.93	1.97	
Negative Displacement at Strength Limit State, Δ (in.)		-2.99	-2.74	
Positive Shear Force at Strength Limit State, P (lb)	5714	5496	5646	
Negative Shear Force at Strength Limit State, P (lb)		-5481	-5877	
Positive Shear Modulus at Strength Limit State, G (lb/in)	2513	2075	3089	
Negative Shear Modulus at Strength Limit State, G (lb/in)		1957	3015	
Idealized force vs. deformation curve, FEMA 273, Fig 2-4		Type 1	Type 1	
Positive Shear Stiffness, K+ (lb/in)		5078	8255	
Negative Shear Stiffness, K- (lb/in)		5190	6573	6274
Positive Expected Strength, Q_{CE+} (lb)		4075	3153	
Negative Expected Strength, Q_{CE-} (lb)		-4181	-3813	
Positive Yield Deformation δ_{y+}		0.80	0.38	
Negative Yield Deformation δ_{y-}		-0.81	-0.18	
Positive Deformation above 80% ultimate resistance δ_{2+}		3.01	2.96	
Negative Deformation above 80% ultimate resistance δ_{2-}		-1.96	-2.92	
Positive Post-Yield Deformation for Life Safety Perf, m_{LS+}		2.81	5.81	
Negative Post-Yield Deformation for Life Safety Perf, m_{LS-}		1.83	3.77	
Positive Ultimate Capacity, Q_{u+} (lb) =		11452	18310	
Negative Ultimate Capacity, Q_{u-} (lb) =		-7640	-14378	
Average Ultimate Capacity, Q_u (lb)		9546	16344	12945
Calculated Allowable Design Capacity, P' (lb)	1492	1492	1492	1492
Calculated Allowable Design Resistance, D' (lb/ft)	373	373	373	373

The data plots shown in Figures 32, 37, and 41 show the predicted capacity of these panels along with the measured data. The model underestimates the yield capacity of these panels because it does not account for the forces carried through bearing between the inset panel and the overall 2x6 frame. The data plots show that these panels have significant yield strength, but relatively less over-strength and ductility compared to the P3-1 panel. Table 12 shows that an ultimate capacity of 12,945 lb was determined based on the measured data. Table 4 showed that the predicted yield capacity of this panel was 2577 lb, but the test data plots show that this value underestimates the measured data. Therefore, the calculated allowable design ca-

capacity shown in Tables 10 and 12 (1492 lb) is too conservative. However, this predicted capacity may be useful for defining design values.

P3-3, P3-4, and P3-5 Monotonic Test Results

The P3-2 test panel performance revealed that cyclic testing did not substantially reduce the panel ductility or change the modes of failure relative to the monotonic tests, so it was decided to build only one specimen of the P3-3, P3-4, and P3-5 configurations. Each was tested monotonically to assess its relative ductile performance, and the results were compared with the P3-2 results to determine the most promising inset panel configuration. The best-performing panel design in this test series could be further optimized if needed and tested cyclically.

Table 13 provides a summary of the monotonic performance of the P3-3, P3-4, and P3-5 shear panels. These tests were documented following the City of LA guidance. The calculated allowable strength design capacities defined in Appendix A and presented in Table 10 are included in Table 13.

Table 13. Performance of P3-3, P3-4 and P3-5 Monotonic Shear Panels.

Parameter	P3-3 Mono	P3-4 Mono	P3-5 Mono
Average Maximum Shear Strength, S_{max} (lb/ft)	1645	1197	1587
Positive Displacement at Yield Limit State, Δ (in.)	0.40	0.37	0.40
Positive Shear Force at Yield Limit State, P (lb)	3447	2950	3358
Positive Shear Modulus at Yield Limit State, G (lb/in)	17,556	15,912	16,930
Positive Displacement at Strength Limit State, Δ (in.)	2.00	1.21	1.97
Positive Shear Force at Strength Limit State, P (lb)	6580	4788	6349
Positive Shear Modulus at Strength Limit State, G (lb/in)	3941	4455	3852
Calculated Allowable Design Capacity, P' (lb)	1516	1492	1516
Calculated Allowable Design Resistance, D' (lb/ft)	379	373	379

P3-3 Monotonic

For this monotonic test, the load was applied laterally to the south (left in Figure 3). Figure 42 shows the lateral load-versus-deflection performance of this panel plotted in terms of actuator displacement. The panel increased in strength fairly steadily until a deflection of 1.4 in. At this deflection, the top right corner began to crush around the TP35 nailing plate, as shown in Figure 43. The threaded rod visible in this figure in front of the panel, was for instrumentation only and was not a structural element of the panel. After the corner was crushed, the forces were redistrib-

uted and the panel capacity continued to increase until reaching 6580 lb at a deflection of 2.0 in. Immediately after reaching ultimate load, another drop in resistance occurred in the load deflection plot resulting from further compression-buckling failure of the OSB in the top right corner. Figure 42 shows that lateral forces were redistributed, as in other tests, and the panel continued to deform without loss of capacity until 3 in. deflection. Some top plate bending was also noted in conjunction with the OSB buckling, but no failure was observed, and it did not have a significant effect on the panel strength. After deflecting 3 in., the panel gradually lost strength in a ductile manner until the end of the test. The major failure mechanism after 3.5 in. was nail yielding and pull-out between the OSB and 2x4 inset panel framing, particularly along the right side. This permitted the OSB to move outside the overall panel 2x6 framing, resulting in a loss of bearing resistance between the two. Figure 44 shows that, by the completion of the test, the OSB was completely outside the 2x6 overall panel framing on the right side of the panel. The nails had pulled out of the inset panel top plate and both vertical studs (2x4 edge stud and stud on the other side of the threaded rod cavity). In the bottom left corner, the OSB pulled out slightly from its recessed position in the 2x6 frame at 2.6 in. deflection, but it did not work completely loose. The test was discontinued at 6 in. deflection. Minimal damage occurred to the TP35 nailing plates and associated nails.

P3-4 Monotonic

In this monotonic test the load was applied laterally to the south (left in Figure 4.) Figure 45 shows the lateral load versus deflection performance of this panel. The panel exhibited a linear load-deflection relationship until 0.8 in. deflection. At this point, the bottom left TP35 nailing plate began to buckle. However, the panel lateral resistance continued to increase until it reached its maximum of 4788 lb at 1.2 in. deflection. Following the peak load, lateral resistance dropped due to crushing of the lower left corner of the OSB (Figure 46), splitting of the hem-fir bottom plate, and nail yielding. Figure 47 shows splitting of the SPF 2x4 bottom plate and failure of the OSB and inset bottom frame member at the nail connections to the TP35 plate in the right-bottom corner much later in the test. As the test continued there were numerous other failures. The inset panel yielded the nails connecting it to the overall 2x6 frame and displaced independently of this frame at 1.8 in. The top plate split due to bending at 2.2 in. The nails attaching the 2x6 frame to the inset panel completely pulled out at 3.1 in. Figure 47 shows the complete failure of bottom right corner connection at 4.5 in. Figure 48 shows the complete failure of the top plate at the top right corner at 5.2 in. deflection. This failure occurred because the inset panel frame members are oriented in-plane with respect to the panel so that bearing forces are concentrated on only the outer 2 in. of the 2x6 top plate. This bearing force split the top plate because the plate washer at the top of the threaded rod is able to rotate, providing limited protection for the top

rod is able to rotate, providing limited protection for the top plate. The P3-4 panel proved to be the weakest of all the inset panels, primarily because the bearing surface of the inset panel on the 2x6 overall panel top plate is offset both out-of-plane and in-plane relative to the restraint provided by the threaded rod plate washer. The offset, particularly out-of-plane, makes the 2x6 top plate vulnerable to brittle failure as shown in Figure 48. The P3-5 panel has a similar problem with the out-of-plane offset because like the P3-4, it is only 2 in. deep; however, the threaded rod is mounted within the inset panel so a more direct load path is available in-plane. Nevertheless, the lateral resistance of this weaker panel did not drop significantly because the OSB and inset panel held together and racked within the overall frame. Although separated from the overall frame (see Figure 49), the inset panel still provided lateral resistance through bearing against the overall frame at all four corners. The test was stopped at 6.0 in. lateral deflection.

P3-5 Monotonic

For this monotonic test, the load was applied laterally to the north (right in Figure 5). Figure 50 shows the lateral load versus deflection performance of this panel. The panel behavior showed no distinct yield point as seen in the almost parabolic load-deflection plot. The sequence of failure mechanisms was similar to those occurring in the other inset panels. First, the nails between the OSB and inset panel frame began to yield as the panel lifted up on the bottom left corner. The lifting continued as the nails in the TP35 plate yielded and caused splitting in the bottom plate. Figure 51 shows that the top plate began to flex in bending at 1.7 in. deflection. The ultimate load of 6349 lb was reached at 2.0 in. deflection. As the deflection increased, the OSB began to work out of the recess and yield some of the nails in the TP35 plates. The top plate continued to bend until at 3.6 in. it cracked in both a splitting and bending failure (see Figure 52). The test ended at 4.0 in. deflection. All studs remained attached to the frame, and the connections between the OSB and inset panel studs remained intact after the test was halted, providing means of transferring lateral force through bearing against the overall 2x6 frame.

The top plate in this panel is less vulnerable to bending failure than in the P3-4 panel because the plate washer for the threaded rod is above the corners of the inset panel, where the bearing forces against the overall panel 2x6 top plate are the greatest. However, the top plate is still vulnerable because of the narrow 2 in. wide bearing surface and the offset out-of-plane, which twists and splits the top plate (see Figure 52). The P3-3 panel provided the best load path, both in-plane and out-of-plane, for the forces between the inset panel bearing surface and the resistance from the threaded rod plate washer. The P3-3 panel configuration was therefore the best

inset panel, especially when a single top plate was used (as was the case with all inset panels considered here).

P3-3M Test Results

As explained on page 20, the P3-3M panel is a modification of the P3-3, optimized to make it slightly stronger and more ductile, plus easier to install. Table 14 summarizes the performance of all P3-3M shear panels tested, documented according to both City of LA and FEMA 273 guidance. The calculated allowable strength design capacity is defined in Appendix A, and is presented in Tables 10 and 14.

P3-3M Monotonic

For this monotonic test the load was applied to the left in Figure 6. Figure 53 shows the lateral load versus deflection performance of this panel. The panel exhibited a linear load-deflection relationship until 0.8 in. deflection. At this point, the bottom left H4 tie began to buckle. However, the panel continued to pick up load until reaching the maximum of 6362 lb at 1.91 in. displacement. At this deflection a nail yielded and pulled out of the top left corner of the OSB, reducing the panel resistance. The load then increased to 6334 lb, nearly equal to the load prior to nail pullout, and then began to slowly drop for the rest of the test. This second decrease in load occurred at 2.25 in. and was caused by lumber crushing in the frame. The nails around the perimeter of the panel continued to yield and pull through the OSB causing a reduction in lateral resistance. At 3.4 in. deflection the bottom 2x6 plate split and the OSB crushed in the bottom left and top right corners, and by 3.8 in. the nails along the bottom left had pulled through completely. The 2x6 stud bearing against the OSB on the left edge began to split on the bottom at 4.2 in., and by 6.0 in. enough damage had occurred to the panel to end the test. Figure 54 through Figure 56 are photographs taken after the test, highlighting many of the failures that occurred in this panel.

Figure 56 shows the interior face of the P3-3M monotonic panel. The threaded rods are inside the 3-1/2 in. wide cavity between the inset panel studs. The coupling nuts can be seen a few inches above the inset panel bottom plate. The load in the threaded rods was measured using load cells. The load cell can be seen just above the nailing plates at the top left and right corners of the panel in Figure 54. The threaded rods of all P3-3M panels were post-tensioned to just over 6000 lb. These are the loads shown at zero displacement in Figure 57. Figure 57 shows both the north and south threaded rod tensile force, plotted with respect to panel lateral displacement during the P3-3M monotonic test. Because this panel is being pulled to

the south (left in Figure 54), the panel begins to rack and rotate to the left. As expected, Figure 57 shows that this panel rotation increases the tension in the north rod while the tension in the south rod decreases. Similar to the lateral load versus deflection plot in Figure 53, Figure 57 shows that the north rod tension increases almost linearly until a panel lateral displacement of 0.8 in. The north rod reaches its peak tension at a larger lateral deflection than the panel itself, and then the rod tension and panel lateral resistance decreases dramatically after 4 in. deflection.

Table 14. Performance of P3-3M shear panels.

Parameter	P3-3M Mono	P3-3M CUREE1	P3-3M CUREE2	Cyclic Avg
Average Maximum Shear Strength, S_{max} (lb/ft)	1590	1701	1987	
Positive Displacement at Yield Limit State, Δ (in.)	0.33	0.41	0.36	
Negative Displacement at Yield Limit State, Δ (in.)		-0.39	-0.38	
Positive Shear Force at Yield Limit State, P (lb)	3037	3710	3705	
Negative Shear Force at Yield Limit State, P (lb)		-3497	-3403	
Positive Shear Modulus at Yield Limit State, G (lb/in)	18615	18278	20576	
Negative Shear Modulus at Yield Limit State, G (lb/in)		17979	18289	
Positive Displacement at Strength Limit State, Δ (in.)	1.91	2.88	2.93	
Negative Displacement at Strength Limit State, Δ (in.)		-3.00	-2.97	
Positive Shear Force at Strength Limit State, P (lb)	6362	7547	8246	
Negative Shear Force at Strength Limit State, P (lb)		-6057	-7647	
Positive Shear Modulus at Strength Limit State, G (lb/in)	4239	3137	3578	
Negative Shear Modulus at Strength Limit State, G (lb/in)		1987	3309	
Idealized force vs. deformation curve, FEMA 273, Fig 2-4		Type 1	Type 1	
Positive Shear Stiffness, K+ (lb/in)		7708	8386	
Negative Shear Stiffness, K- (lb/in)		8680	8712	8372
Positive Expected Strength, Q_{CE+} (lb)		4677	4628	
Negative Expected Strength, Q_{CE-} (lb)		-3497	-3398	
Positive Yield Deformation δ_{y+}		0.61	0.55	
Negative Yield Deformation δ_{y-}		-0.40	-0.39	
Positive Deformation above 80% ultimate resistance δ_{2+}		2.89	2.89	
Negative Deformation above 80% ultimate resistance δ_{2-}		-1.96	-1.95	
Positive Post-Yield Deformation for Life Safety Perf, m_{LS+}		3.57	3.92	
Negative Post-Yield Deformation for Life Safety Perf, m_{LS-}		3.65	3.75	
Positive Ultimate Capacity, Q_{u+} (lb) =		16679	18157	
Negative Ultimate Capacity, Q_{u-} (lb) =		-12747	-12730	
Average Ultimate Capacity, Q_u (lb)		14713	15444	15078
Calculated Allowable Design Capacity, P' (lb)	1516	1516	1516	1516
Calculated Allowable Design Resistance, D' (lb/ft)	379	379	379	379

The loss of both lateral resistance and north rod tension after 4 in. deflection are both due to the OSB moving completely outside the 2x6 frame along the bottom of the panel.

Figure 58 shows the north threaded rod stress versus strain. The stress shown in this figure is the rod tension divided by the rod net tensile area, A_{nt} , which equals 0.226 in² (this area is defined after Equation 11 in Chapter 3). The threaded rod strain was calculated by measuring the rod elongation using linear variable differential transformers (LVDTs) and dividing by the 12 in. LVDT gauge length. Figure 56 shows the LVDT sensors attached to both threaded rods. Figure 58 shows that the north rod reached a maximum stress of 56 ksi. This mild steel rod has a design yield strength of 36 ksi and ultimate (tensile) strength between 58 and 80 ksi. The slope of the stress-versus-strain plot over the linear portion between 0.00012 and 0.00054 in./in. is 29,000 ksi, which equals the modulus of elasticity of steel. This indicates the threaded rod did not yield (within the LVDT gauge range) until a stress of 53 ksi, which equates to a rod force of 12,000 lb in Figure 57. However, the plot in Figure 57 suggests the north threaded rod may have yielded at a tensile force of 11,000 lb outside the LVDT gauge range.

P3-3M CUREE1

The lateral force versus displacement for the first cyclic test of P3-3M is given in Figure 59. The first observed failure occurred at 0.8 in. deflection. At this time a ¼ in. gap was seen between the OSB and 2x6 frame bottom plate, and also along the lower portion of the side studs. These gaps are indications of nail yielding between the OSB and inset panel 2x4 frame. At 1.4 in. deflection slight crushing occurred in all four corners of the OSB, as shown in Figure 60. The top left corner of the OSB finally failed at 2.0 in. At a 3.0 in. deflection, the 2x6 base plate began to splinter, the OSB pulled away from the frame, and the OSB in the upper right corner crushed. This P3-3M panel reached an ultimate capacity of 7547 lb at 2.88 in. in the positive direction and 6057 lb at 3.0 in. in the negative direction. By 4.0 in., the OSB was completely pulled out of the frame at the lower corners and across the entire panel bottom. Damage continued through 5 in. displacement, when the OSB was loosely attached to the frame by the nails on the top half of the panel. The bottom third of the nails had yielded and/or pulled out of the frame. The test continued until 7.0 in. Figure 61 is a photograph of the bottom of the panel after the test ended, showing that the stud to the interior of the threaded rod cavity on the right side of the panel had split. The residual capacity that remained at this point was from weak-axis bending of the studs that carried some load into the top portion of the panel. Most of the studs remained well attached to the top and bottom plates.

Figure 62 shows both the north and south threaded rod tensile force, plotted with respect to time in the P3-3M CUREE1 test. This figure shows that tensile force of both rods oscillates about the initial 6200 lb post-tension. Figure 62 shows that the tension in one rod increases while the tension in the other decreases as the panel racks back and forth. At 6.7 min (corresponding to 1.4 in. lateral deflection) in the south rod and 7.5 min (2.0 in. lateral deflection) in the north rod, Figure 62 shows the tensile forces drop to zero. No compressive resistance can be developed in the rods because the rod nuts simply rest on the plate washers at the top plate of the panels. This explains why the forces shown in Figure 62 reach zero force and flatten (force remains at zero for a period of time).

Figure 63 plots the stress-versus-strain of the heavier loaded north threaded rod. The smaller concentrated cycles at the center of this plot show that the threaded rod stress oscillated about 27 ksi (i.e., 6200 lb/ 0.226 in²). The slope of both the initial and later large stress cycles shown in Figure 63 equal 28,000 ksi, which is close to the modulus of elasticity of steel and indicates elastic response. Then at 9.4 min, at a panel lateral deflection of 2.8 in., the north rod appears to yield within the LVDT gauge range at a threaded rod tensile force of 10,300 lb. In the previous cycle this rod reached a tensile force of 13,100 lb (stress of 58 ksi in Figure 63) and likely yielded outside the LVDT gauge range. Figure 63 suggests the threaded rod may have yielded substantially, at a relatively small stress (31 ksi). However, closer inspection of the condition of the panel at this point (lateral deflection of 5 in.) reveals that the inset panel frame was badly damaged and was likely influencing the LVDT measurement. At 5 in. lateral displacement the threaded rod reaches a tensile force of only 6800 lb at 10.4 minutes (see Figure 62). The lateral resistance of the panel is only 3800 lb (see Figure 59) at this displacement, explaining why the threaded rod tensile force is only 6800 lb.

The threaded rod stresses never drop below zero in Figure 63 because no compressive force can be developed in these rods. The flat portions of the plot at zero stress in Figure 63 occur because the force remains at zero (see Figure 62) while the panel continues to deform and influence LVDT measurements. However, these later LVDT measurements only indicate movements in the LVDT gauge, not true changes in rod strain.

P3-3M CUREE2

The lateral force versus displacement for the second cyclic test on P3-3M is given in Figure 64. This panel performed similar to the CUREE1 test of P3-3M with very few exceptions. This panel did reach higher load capacities, withstanding 8246 lb at 2.93 in. in the positive direction and 7647 lb at 2.97 in. in the negative direction.

Figure 65 shows both the north and south threaded rod tensile force, plotted with respect to time during the P3-3M CUREE2 test. This figure shows that the tensile force of the rods oscillates about the initial 6100 lb post-tension. Figure 66 plots stress versus strain of the heavier loaded north rod. Both the initial cycle at the center of Figure 66 and later cycles on the right side have a slope equal to 28,000 ksi (i.e., close to the elastic modulus for steel), indicating elastic response. Then at 7.4 min, at a panel lateral deflection of 1.65 in. the North rod appears to yield within the LVDT gauge range at a threaded rod tensile force of 15,000 lb (stress of 66 ksi in Figure 66).

The P3-3 panel provided better performance than the P3-2 because of the more direct load path between the bearing surface of the inset panel and the bearing surface provided by the threaded rod plate washers, the latter of which protect the top plate from bending failure. The P3-3M panel has two improvements over the P3-3 panel: (1) a larger cavity for the threaded rods, making construction easier, and (2) a reduction in the nail spacing for the inset panel stud to the interior of the cavity from 8 in. to 4 in. o.c. Figure 67 shows the bottom corner of the back face of a P3-3M panel after the test ended. The figure shows the cavity between the two 2x4 inset panel studs that contains the threaded rod, and also shows the coupling nut near the bottom of the panel and the LVDT instrumentation on the threaded rod.

Table 14 shows that the P3-3M panel has greater strength than the P3-2 cyclically loaded panels (see Table 12 for comparison). The P3-3M panels had an average expected strength, Q_{CE} , of 4050 lb, an average m_{LS} value of 3.72 and an ultimate capacity, Q_u , of 15,078 lb, which are greater than the values for the P3-2 panel (3806 lb, 3.55, and 12,945 lb respectively). The ultimate capacity is not a true lateral capacity, but rather a quantity that expresses the combined lateral strength and ductile performance. This value will be scaled down to provide working stress allowable design values.

P3-6 Test Results

The P3-6 panel provides data for defining a baseline measured response that can be compared with accepted allowable strength design values to establish a reduction factor for scaling down measured data from other panel configurations. These tests establish the ductile system behavior of the baseline panel so that other panel performance can be appropriately compared. Table 15 documents the performance of all P3-6 panels tested following both the City of LA and FEMA 273 guidance. The calculated allowable strength design capacity is also included in Table 15.

Table 15. Performance of P3-6 shear panels.

Parameter	P3-6 Mono	P3-6 CUREE1	P3-6 CUREE2	Cyclic Avg
Average Maximum Shear Strength, S_{max} (lb/ft)	859	566	578	
Positive Displacement at Yield Limit State, D (in.)	0.40	0.38	0.55	
Negative Displacement at Yield Limit State, D (in.)		-0.38	-0.35	
Positive Shear Force at Yield Limit State, P (lb)	2080	1184	1505	
Negative Shear Force at Yield Limit State, P (lb)		-1546	-1614	
Positive Shear Modulus at Yield Limit State, G (lb/in)	10452	6231	5497	
Negative Shear Modulus at Yield Limit State, G (lb/in)		8309	9398	
Positive Displacement at Strength Limit State, D (in.)	3.26	1.37	2.75	
Negative Displacement at Strength Limit State, D (in.)		-2.93	-1.82	
Positive Shear Force at Strength Limit State, P (lb)	3438	1926	2264	
Negative Shear Force at Strength Limit State, P (lb)		-2601	-2358	
Positive Shear Modulus at Strength Limit State, G (lb/in)	959	1525	699	
Negative Shear Modulus at Strength Limit State, G (lb/in)		835	1024	
Idealized force vs. deformation curve, FEMA 273, Fig 2-4		Type 1	Type 1	
Positive Shear Stiffness, K_+ (lb/in)		2852	2532	
Negative Shear Stiffness, K_- (lb/in)		3033	4218	3159
Positive Expected Strength, Q_{CE+} (lb)		1120	1462	
Negative Expected Strength, Q_{CE-} (lb)		-1794	-1583	
Positive Yield Deformation d_{y+}		0.39	0.58	
Negative Yield Deformation d_{y-}		-0.59	-0.38	
Positive Deformation above 80% ultimate resistance d_{2+}		3.06	4.07	
Negative Deformation above 80% ultimate resistance d_{2-}		-4.00	-3.99	
Positive Post-Yield Deformation for Life Safety Perf, m_{LS+}		5.85	5.29	
Negative Post-Yield Deformation for Life Safety Perf, m_{LS-}		5.08	7.98	
Positive Ultimate Capacity, Q_{u+} (lb) =		6549	7733	
Negative Ultimate Capacity, Q_{u-} (lb) =		-9108	-12630	
Average Ultimate Capacity, Q_u (lb)		7829	10181	9005
Calculated Allowable Design Capacity, P' (lb)	717	717	717	717
Calculated Allowable Design Resistance, D' (lb/ft)	179	179	179	179

P3-6 Monotonic

The first P3-6 panel was tested monotonically by loading it at 0.5 in. per minute laterally, to the right in Figure 7. The top beam was held horizontal and forced to maintain a net vertical load of zero. Figure 68 shows the lateral load-versus-deflection performance of this panel. This panel shows a fairly linear relation between load and deflection to about 2000 lb, at 0.4 in. deflection, then softens and plateaus, reaching an ultimate load at 3438 lb and 3.26 in. displacement. The panel initially softened due to the lifting of studs from the frame (see Figure 69) and was

compounded by propagation of a crack in a stud, which existed before the start of the test.

The panel performed contrary to predicted performance by losing very little strength over the next 2 in. deflection. For the first 5 in. of lateral deflection, a block of wood was installed between the top plate and test fixture, just above a stud. This block was intended to represent the out-of-plane restraint provided by roof trusses or floor joists (of a two story building), which would prevent out-of-plane buckling of the top plate. However, it was observed that the block was preventing top plate rotation and was carrying lateral load, thus distorting the actual capacity of the panel. This block was not placed in the center, but was offset above one of the studs, where it clearly carried lateral load. The test was briefly stopped, the block was removed, the test was restarted, and the measured lateral resistance (Figure 68) revealed an 1800 lb drop in lateral force. As a result of this experience, the block was not used in the P3-6 cyclic tests.

After the drop in lateral resistance, the panel resistance increased as deflection increased mainly due to the performance of the panel components, which would have failed earlier if the block had not interfered with testing. The load leveled off after the gain. The test was halted at a deflection of 8 in. Since the panel had not completely failed at the end of the test, residual capacity remained and the panel and studs were still transmitting load. The top plate was damaged in bending, the OSB was significantly pulled away from the frame, and the H4 stud connection to the bottom plate in the left bottom corner had failed. Figure 70 shows the interior face of the P3-6 monotonic panel, where the Simpson Strong-Tie H4 seismic tie had torn, causing a loss of holddown resistance. The monotonic test results are normally used for defining the reference deformation, Δ , for the cyclic tests. However, because the block of wood inappropriately increased the ductility of this panel, the reference deflection was again set to 2.0 in., based on earlier tests of similar panels.

P3-6 CUREE1

The lateral force versus displacement plot of the first cyclic test of a P3-6 panel is shown in Figure 71. At a deflection of 0.4 in. the bottom right corner of the OSB began experiencing deformation due to nail yielding and rotation. The bottom plate began splitting and the right edge stud lifted off the bottom plate by approximately $\frac{1}{4}$ in. At 0.6 in. deflection, the OSB made conspicuous cracking sounds on both the positive and negative strokes, indicating the nails had begun to pull through the OSB on both bottom corners. When the deflection reached 0.8 in., the bottom plate at both edge studs was visibly splitting with each additional cycle. This panel reached an ultimate load of 1926 lb at 1.37 in. positive deflection. A loud cracking

noise occurred at this time, probably due to the nails continuing to pull through the OSB and additional splitting of the bottom plate. This cracking continued through 3 in. of deflection, when nail pull-through and nail yielding could clearly be seen at the bottom right corner of the OSB as shown in Figure 72. The load resisted by the negative cycles increased throughout the test until this point, reaching its maximum capacity of 2601 lb at 2.93 in. deflection. At 4.0 in. displacement, the top plate cracked above the right and left edge studs, as shown on the right edge in Figure 73. When the deflection reached 6.0 in., the panel lifted off the studs, except for at a loose connection at the top, and the panel swayed with the remaining cycles until the test was halted. A small residual capacity remained through weak-axis bending of the studs and some connection to the OSB near the panel top.

P3-6 CUREE2

Figure 74 shows the lateral force versus deflection of the P3-6 CUREE2 panel. This test produced results similar to the CUREE1 test except the panel damage and loss of capacity occurred at slightly larger deflections. At 2.0 in. deflection, the bottom plate began to split near the right edge stud and the OSB became detached from the bottom plate. The lateral load reached its maximum of 2264 lb at 2.75 in. positive deflection and 2358 lb at 1.82 in. in the negative direction. The photograph in Figure 75 was taken late in the test and it shows the OSB from the interior face, where it is almost completely pulled away from the bottom plate. This figure also shows the nails between the H4 tie and bottom plate pulled out of the bottom plate. At 5.0 in. deflection the top plate began to fail in bending above both the edge studs as shown in Figure 76, and at 7.0 in. the panel experienced massive failure, with the OSB barely remaining attached to the panel.

The P3-6 panel configuration is close to a baseline that will be used to scale to accepted allowable design capacities. However, the failure of the H4 ties eliminated the resistance provided by nails along the edge studs, because these failures completely remove the holddown resistance. This failure and the bending failure of the top plate, although realistic in real-world construction, was not permitted in the setup of the panel tests upon which established guidance is based. However, these failures did take place late in these tests, so the data collected from these test panels will provide useful data for defining the baseline

P3-7 Test Results

The P3-7 panel is essentially a narrow variation on the other inset panels, but without the threaded rods to provide stud holddown resistance. This panel was expected

to provide significantly less capacity, but also be much less costly to construct. The only stud holddown resistance along the bottom plate comes from the light H4 seismic ties. Because of the narrow panel width, this panel will also be much more vulnerable to overturning. **Error! Reference source not found.** provides a summary of the performance of all P3-7 shear panels in a similar format to the other cyclically tested panels.

P3-7 Monotonic

The first P3-7 panel was tested monotonically by loading it at 0.5 in. per minute laterally at the left in Figure 8. The top beam was held horizontal and forced to maintain a net vertical load of zero. Figure 77 shows the lateral load versus deflection performance of this panel. Like the others, this panel also has no definite yield point; the lateral stiffness slowly decreases, and although the test was carried out to deformations of 8 in., the maximum resistance was not reached. Therefore, the maximum resistance reached at 8 in. is reported here as the strength limit capacity. Initially the nails between the OSB and bottom plate yielded. The connection between the H4 ties, edge studs, and bottom plate failed, eliminating the holddown resistance and reducing overturning resistance. Then the nail connections between the OSB and bottom plate pulled completely through the OSB. As deformation continued, the single SPF 2x6 top plate began to fail in bending. Figure 78 shows that after 8 in. deflection the panel had essentially completely failed, and at that point the test was stopped.

The test configuration used in all Phase III panels applied load at only the extreme ends of the top plate, permitting almost unrestrained bending of the SPF top plate. For the tall, narrow P3-7 panel, a small amount of top plate bending deformation permitted very large lateral deflections once the bottom of the panel failed. Figure 78 shows that the bottom of the panel later in the test provides no moment restraint, but it does provide shear resistance. The limited top plate bending, together with the pinned support at the panel bottom, does provide a load path for panel resistance at extreme deformations. However, in actual construction the roof trusses or floor joists would restrain top-plate bending to some degree; panel capacity would increase slightly late in the test, but panel resistance would be lost much earlier.

P3-7 CUREE1

The P3-7 panels are very flexible and weak, and this first cyclic test produced confusing results in that the stiffness actually appeared to increase with increasing deflection. This appeared to be an atypical response of the panel frame, so the results

are not presented because of the confusion they may create. The second cyclic test produced much more reasonable results.

Table 16. Performance of P3-7 shear panels.

Parameter	P3-7 Mono	P3-7 CUREE2
Average Maximum Shear Strength, S_{max} (lb/ft)	272	324
Positive Displacement at Yield Limit State, Δ (in.)	0.41	1.35
Negative Displacement at Yield Limit State, Δ (in.)		-1.36
Positive Shear Force at Yield Limit State, P (lb)	377	614
Negative Shear Force at Yield Limit State, P (lb)		-814
Positive Shear Modulus at Yield Limit State, G (lb/in)	1852	917
Negative Shear Modulus at Yield Limit State, G (lb/in)		1211
Positive Displacement at Strength Limit State, Δ (in.)	7.95	7.70
Negative Displacement at Strength Limit State, Δ (in.)		-7.71
Positive Shear Force at Strength Limit State, P (lb)	1182	1194
Negative Shear Force at Strength Limit State, P (lb)		-1400
Positive Shear Modulus at Strength Limit State, G (lb/in)	216	185
Negative Shear Modulus at Strength Limit State, G (lb/in)		186
Idealized force vs. deformation curve, FEMA 273, Fig 2-4		Type 2
Positive Shear Stiffness, K+ (lb/in)		425
Negative Shear Stiffness, K- (lb/in)		552
Positive Expected Strength, Q_{CE+} (lb)		586
Negative Expected Strength, Q_{CE-} (lb)		-790
Positive Yield Deformation δ_{y+}		1.38
Negative Yield Deformation δ_{y-}		-1.43
Positive Deformation above 80% ultimate resistance δ_{2+}		8.03
Negative Deformation above 80% ultimate resistance δ_{2-}		-7.97
Positive Post-Yield Deformation for Life Safety Perf, m_{LS+}		4.37
Negative Post-Yield Deformation for Life Safety Perf, m_{LS-}		4.18
Positive Ultimate Capacity, Q_{u+} (lb) =		2560
Negative Ultimate Capacity, Q_{u-} (lb) =		-3300
Average Ultimate Capacity, Q_u (lb)		2930
Calculated Allowable Design Capacity, P' (lb)	266	266
Calculated Allowable Design Resistance, D' (lb/ft)	133	133

P3-7 CUREE2

Figure 79 shows the lateral force versus displacement plot for the P3-7 CUREE2 panel. The nails between the OSB and bottom plate yielded at very small deflections, and crushing of the OSB bearing against the 2x6 frame occurred. At 0.8 in. deflection, noticeable gaps formed between the OSB and the overall panel bottom

plate, top plate, and studs, revealing the growing nail yielding and OSB crushing. The bottom plate began to fail near the edge stud connections at 1.4 in. deflection. The top plate began to visibly bend at 2.0 in. deflection, and the H4 ties connecting the edge studs to the bottom plate started to yield. The gaps around the OSB perimeter grew as the nails pulled out of the inset panel frame members or pulled through the OSB. The H4 ties started pinching and tearing near the bottom plate. The inset panel 2x4 bottom frame member split in the later stages of the test. Figure 80 shows the complete fracture of the H4 tie at the bottom right corner as well as the OSB crushing and nail failure.

Figures 77 and 79 show that the P3-7 panel configuration is very flexible, and in many applications this lack of stiffness could limit its usefulness more so than the lack of strength. A lateral load system that lacks adequate stiffness may permit excessive drifts, causing significant nonstructural damage to a building even though the panel may have adequate strength. It should be possible to modify this narrow inset panel with more substantial holddown anchors at the tops and bottoms of both the 2x6 edge studs. This would greatly increase the panel's overturning resistance. Holddown anchors with greater capacities would increase the panel stiffness in addition to strength. Any modifications of the P3-7 panel must be tested again, however, to see if other modes of failure become critical.

PSP-Std Phase I Test Results

Similar to the P3-6 panel, the PSP-Std shear panels from the Phase I study provided data for defining baseline measured response. Table 17 documents the performance of both the PSP-Std-SPD1 and PSP-Std-MS1 panels, where the first was tested according to the City of LA sequential phased displacement (SPD) protocol and the second according to the modified SAC protocol (see Appendix B). Table 17 also shows the calculated allowable strength design capacities.

PSP-Std-SPD1

The PSP-Std panel was tested using the SPD protocol based on an FME of 0.6 in. and a cyclic rate of 6 cycles per minute. The top beam was held horizontal while the net vertical load was held to 2500 lb due to the weight of the test fixture and actuator. The other SPD-loaded PSP-Std panels had zero vertical load applied. The vertical load in these tests is not sufficient to resist the full overturning moment, so these results provide intermediate performance data between that of the SPD-loaded panels with no vertical load and the modified SAC-loaded panel (PSP-Std-MS1) with 8000 lb vertical load. The model presented in Chapter 3 indicates that

the overturning resistance provided by the 2500 lb vertical load is overcome at an applied lateral load of 1250 lb. When loaded laterally above 1250 lb, the nails along the top and bottom plate must provide additional overturning resistance. Figure 81 shows the lateral load versus deflection performance of this panel. As predicted by the model, failure begins at the corners of the panel due to single-point nail bending and nail rotation in the plywood (Mode III_s), as defined by Equation 3 (see Figure 17). Table 17 shows that the panel yields at a load of 920 lb under positive deflection and 1810 lb under negative deflection at lateral deflections of 0.27 and 0.24 in., respectively. The predicted yield capacity of this panel is 1924 lb, which is less than when loaded with 8000 lb vertical load because this lateral load is greater than the 1250 lb needed to overcome the vertical load overturning resistance.

This panel fails in a manner similar to the P3-6 CUREE-loaded panels, with the nails along the bottom yielding. The 2500 lb vertical load provided a similar overturning resistance as the P3-6 panel. In fact, based on the same analytical model, the predicted yield capacity of the P3-6 panel was 1240 lb compared to 1924 lb for this panel. The greater yield capacity is simply due to the vertical load. Therefore, these panels should provide similar lateral capacity and the progression of failure should be similar. Figure 82 shows that the overturning capacity provided by vertical load and nails along the bottom plate were quickly overcome when the nail connections failed and the studs lifted from the bottom plate. Table 17 shows that the panel reaches an ultimate capacity (strength limit) of 3112 lb under positive deflection and 3560 lb under negative deflection at lateral deflections of 1.33 and 1.59 in., respectively. The force and displacement values at the yield- and strength-limit states shown in Table 17 are plotted on Figure 81 to form the bilinear force (BLF) displacement response. Figure 81 also plots the predicted capacity of this panel with 2500 lb vertical load based on the model in Chapter 3, conservatively estimating the panel performance. Table 17 also presents the calculated allowable strength design capacity, which is conservative but reasonable. The plywood-to-bottom plate nail connection failures seen in Figure 82 progress into the center of the panel as deflections increase. Figure 82 shows that the 2x4 stud at the edge of the panel is beginning to lift up, demonstrating that the overturning resistance provided by the vertical load has been overcome. Deflections increase, and eventually lateral resistance drops (at approximately 2.5 in. in Figure 81) as the nail failures at the bottom plate progress toward the panel interior. Again, the studs then carry the load to the bottom plate in weak-axis bending.

Table 17. Performance of PSP-Std shear panels.

Parameter	PSP-Std SPD1	PSP-Std MS1
Average Maximum Shear Strength, S_{max} (lb/ft)	834	1141
Positive Displacement at Yield Limit State, Δ (in.)	0.27	0.52
Negative Displacement at Yield Limit State, Δ (in.)	-0.24	-0.52
Positive Shear Force at Yield Limit State, P (lb)	920	1481
Negative Shear Force at Yield Limit State, P (lb)	-1810	-3007
Positive Shear Modulus at Yield Limit State, G (lb/in)	6799	5730
Negative Shear Modulus at Yield Limit State, G (lb/in)	15287	11632
Positive Displacement at Strength Limit State, Δ (in.)	1.33	2.16
Negative Displacement at Strength Limit State, Δ (in.)	-1.59	-2.18
Positive Shear Force at Strength Limit State, P (lb)	3112	3698
Negative Shear Force at Strength Limit State, P (lb)	-3560	-5433
Positive Shear Modulus at Strength Limit State, G (lb/in)	4200	2730
Negative Shear Modulus at Strength Limit State, G (lb/in)	2624	2953
Idealized force vs. deformation curve, FEMA 273, Fig 2-4	Type 1	Type 1
Positive Shear Stiffness, K+ (lb/in)	3382	3264
Negative Shear Stiffness, K- (lb/in)	5537	6508
Positive Expected Strength, Q_{CE+} (lb)	1916	1498
Negative Expected Strength, Q_{CE-} (lb)	-2190	-2987
Positive Yield Deformation δ_{y+}	0.57	0.46
Negative Yield Deformation δ_{y-}	-0.40	-0.46
Positive Deformation above 80% ultimate resistance δ_{2+}	2.25	2.34
Negative Deformation above 80% ultimate resistance δ_{2-}	-2.25	-1.71
Positive Post-Yield Deformation for Life Safety Perf, m_{LS+}	2.98	3.83
Negative Post-Yield Deformation for Life Safety Perf, m_{LS-}	4.26	2.79
Positive Ultimate Capacity, Q_{u+} (lb) =	5710	5738
Negative Ultimate Capacity, Q_{u-} (lb) =	-9327	-8341
Average Ultimate Capacity, Q_u (lb)	7518	7040
Calculated Allowable Design Capacity, P' (lb)	1461	1557
Calculated Allowable Design Resistance, D' (lb/ft)	365	389

PSP-Std-MS1

The second baseline PSP-Std panel was loaded with the modified SAC protocol scaled to a δ_y equal to 0.6 in. while an 8000 lb vertical load was maintained. Figure 83 shows the lateral load versus deflection performance of this panel, demonstrating much greater maximum capacity due to the overturning resistance provided by the vertical load. Table 17 shows that the both the panel yield and strength limit values have increased considerably. Figure 83 plots the predicted capacity of this

panel with 8000 lb vertical load, reasonably estimating the panel performance. Table 17 gives the calculated allowable strength design capacity, P' and design resistance, D' .

Figure 84 shows that this panel actually begins to fail at the nail connections to the studs along the edge of the plywood, prior to failure along the bottom plate. This happens because these nails are heavily loaded due to the overturning resistance made possible by the larger vertical load. The nails at the panel corners, including at the studs, are subjected to the greatest relative displacements due to plywood rotation. Therefore the nails at the studs—particularly at the corners—fail early in the test when vertical load is applied. The nails in the corners at the bottom plate also begin to fail at the same time as those along the studs. The nails along the bottom are still subjected to vertical loads because of the plywood rotation, but the vertical load ensures that much greater load is applied to the plywood above the nails—where edge distance is not an issue—than below the nails where the edge distance to the bottom of the plywood is very small.

Table 17 shows that the PSP-Std MS1 panel has greater maximum lateral resistance (strength limit state in Table 17) than the PSP-Std-SPD1 panel. The greater vertical load, primarily due to the greater overturning resistance, provides the difference in lateral resistance. However, this panel is also stiffer and slightly less ductile, so that the average ultimate capacity, Q_u , is slightly less. However, the plots in Figures 81 and 83 reveal that this difference is misleading because the values for the measures of ductility are based on the second cycle backbone curve, which gives less credit to the PSP-Std-MS1 results because of the larger increments in displacement in the modified SAC protocol.

6 Recommended Allowable Shear Capacities

The ultimate capacity, Q_u , defined by Equation 24, does not represent a true capacity at all but rather a value of strength that accounts for both the panel lateral capacity and its ductile performance, the latter represented by m_{LS} . With these values, buildings can be evaluated for life-safety stability when the applied loads are defined based on linear analysis with no reduction for R factors or increase for importance factors (see FEMA 273).

The results reported here could eventually be used in deformation-based seismic design procedures. However, part of the purpose of this study is to develop design capacities for traditional force-based design of buildings. Therefore, all design capacities developed here are parallel the values presented in Table 2306.4.1 in the 2000 International Building Code (IBC), pp 564 and 565. The design values are given credit for ductile system behavior by using the values of Q_u (Equation 24). The values of Q_u are scaled so that the working stress design values, Q_D , for the baseline panels (P3-6 from this study and PSP-Std from Phase I) are set equal to the reported values in the 2000 IBC.

The values in the 2000 IBC are based on monotonic tests* conducted by the American Plywood Association (APA)†. The panel tests reported by the APA differ from the baseline panels presented in this report. In fact, all of the APA-tested panels were 8 ft x 8 ft, and that configuration will provide greater strength than the 4 ft x 8 ft panels tested in this study because the interior edge stud will not be vulnerable to overturning-related lifting. The 4 ft x 8 ft panels are more conservative, as explained at the beginning of Chapter 2. The test results reported here are not scaled to the APA panels directly, but rather to the 2000 IBC design values. However, the APA report (Adams 1987) does show the test fixture and key information on the test

* Panels were tested following ASTM E72 guidance, which is a force rather than deformation protocol. Load was applied in one direction only, but the load was applied and removed in cycles of 1200 lb increments.

† *Plywood Shear Walls*, American Plywood Association, Research Report 105, Noel R. Adams, January 1987.

configuration. Specifically, the APA test fixture did permit limited lifting of the edge studs from the top and bottom plates. APA personnel indicated that the edge studs typically lifted about $\frac{1}{4}$ in. from the base plate before the ultimate capacity was reached. The PSP-Std-SPD1 test panel, which had a 2500 lb vertical load, was constrained in a manner similar to those in the APA tests. However, the significantly greater overturning restraint provided with the 8000 lb vertical load in the PSP-Std-MS1 tests provided little additional benefit to the test panel. Conversely, in the other PSP-Std panels tested with no vertical load in the Phase I study, the top plate lifted vertically with no restraint. This condition is much different than the APA configuration and resulted in much weaker panel performance. The zero vertical load condition does provide a worst-case load condition for overturning resistance, but such a case would be exceptional and is not representative of the test conditions used to develop the design values in the 2000 IBC.

As will be seen, it is more conservative to assign larger values to a baseline test panel that is compared with 2000 IBC design values. Table 2306.4.1 in the 2000 IBC gives an allowable strength design (ASD) allowable shear of 430 lb/ft for 15/32 in. Structural I Sheathing with 8d nails 4 in. o.c. around the panel edges. However, a note to this table states that:

In Seismic Design Category D, E, or F, where shear design values exceed 490 plf (LRFD) or 350 plf (ASD), all framing members receiving edge nailing from abutting panels shall not be less than a single 3 in. nominal member. Plywood joint and sill plate nailing shall be staggered in all cases.

The baseline panel best fits the panel that gives the 430 lb/ft value, but the guidance developed here should be applicable in higher seismic design categories. Therefore, the baseline panel values should be scaled to the 350 lb/ft allowable strength value. Based on this note to Table 2306.4.1 in the 2000 IBC, design values are also provided for Load and Resistance Factor Design (LRFD), or ultimate strength design, by using the 490 lb/ft value. Note that the LRFD value of 490 lb/ft is simply 1.4 times the ASD value.

Two reduction factors are then developed, one for ASD, R_{ASD} , and one for LRFD design, R_{LRFD} . These factors are used to scale between the baseline test panel Q_u values and 2000 IBC allowable shear values. The average Q_u values from the positive and negative ultimate deflection for each baseline panel are taken from Tables 15 and 17, and are summarized in Table 18. The ASD and LRFD reduction factors are calculated as follows:

$$R_{ASD} = \frac{D_{uBaseline}}{350lb/ft} = \frac{Q_{uBaseline}}{W(350lb/ft)} \quad [Eq\ 25]$$

$$R_{LRFD} = \frac{D_{uBaseline}}{490lb/ft} = \frac{Q_{uBaseline}}{W(490lb/ft)} \quad [Eq\ 26]$$

where,

$Q_{uBaseline}$ = the average ultimate capacities Q_u of the baseline panels, shown in Table 18, lb.

W = the width of the baseline panel, ft.

$D_{uBaseline}$ = the average ultimate panel capacity per linear foot, lb/ft

Calculated values for R_{ASD} and R_{LRFD} are given in Table 18 for each baseline panel.

Table 18. Summary of baseline panel ultimate capacities.

Parameter	P3-6 CUREE1	P3-6 CUREE2	PSP- Std SPD1	PSP- Std MS1	Selected Reduction Factors
Average Ultimate Capacity, Q_u (lb)	7829	10181	7518	7040	
Test Panel Width, W (ft)	4.00	4.00	4.00	4.00	
Average Ultimate Shear per ft, D_u (lb/ft)	1957	2545	1880	1760	
2000 IBC ASD Baseline Allowable Shear (lb/ft)	350	350	350	350	
ASD Reduction Factor, R_{ASD}	5.59	7.27	5.37	5.03	5.6
2000 IBC LRFD Baseline Allowable Shear (lb/ft)	490	490	490	490	
LRFD Reduction Factor, R_{LRFD}	3.99	5.19	3.84	3.59	4.0

Table 18 shows that the P3-6 panels have the greatest ultimate capacities. However, the lateral load versus deflection of these test panels shown in Figures 71, 74, 81, and 83 reveal that the P3-6 panels have significantly less maximum lateral resistance (shear force at strength limit state in Tables 15 and 17) than either of the PSP-Std panels. The P3-6 panels also have smaller expected strength values, Q_{CE} . However, the P3-6 panels have much greater m_{LS} values, and this explains the greater Q_u values. The top plates of the P3-6 panels bent significantly during testing, permitting substantially greater lateral deflection without failure than if the top plates were not free to bend. The top plates of the P3-6 panels bent significantly more than any other panel except for the narrow P3-7 panel. The ductility of both of the P3-6 and P3-7 panels was exaggerated because of this bending, which would not be permitted in a real-world building. This top plate bending did not occur in the

P3-2 or the recommended P3-3M inset shear panel, nor in the P3-1 diagonal strap panel. Therefore, reduction factors R_{ASD} and R_{LRFD} should be based more on the PSP-Std panel tests than the P3-6 results. However, because higher values of baseline panel Q_u and reduction factors are conservative, reduction factors slightly greater than those based on the PSP-Std panels are used. Table 18 shows that the selected reduction factors are 5.6 and 4.0 for R_{ASD} and R_{LRFD} , respectively. These values are somewhat greater than those calculated for the PSP-Std panels but less than those for the P3-6 panels, for the reasons stated above.

From these selected reduction factors, calculated ASD shear values, D_{ASD} , and calculated LRFD shear values, D_{LRFD} , are determined for each panel according to Equations 27 and 28 respectively.

$$D_{ASD} = \frac{D_u}{R_{ASD}} = \frac{Q_u}{WR_{ASD}} \text{ lb/ft} \quad [\text{Eq 27}]$$

$$D_{LRFD} = \frac{D_u}{R_{LRFD}} = \frac{Q_u}{WR_{LRFD}} \text{ lb/ft} \quad [\text{Eq 28}]$$

Table 19 summarizes the test panel results and presents recommended design values for each shear panel tested cyclically in this project. The average maximum shear strength, S_{max} (Equation 21), is shown in the first row, followed by the measured shear stiffness, K , defined in step 2 of the FEMA 273 documentation guidance near the beginning of Chapter 5. These values are slightly reduced, based on a visual inspection of the test plots, to provide the recommended design stiffness, K_R , given in Table 19.

Table 19 also presents calculated ASD shear values, D_{ASD} , and calculated LRFD shear values, D_{LRFD} , based on Equations 27 and 28. Table 19 also presents recommended ASD shear values, D_{RASD} , and recommended LRFD shear values, D_{RLRFD} , by rounding down from the calculated values. The footnote in Table 19 indicates that the P3-2 and P3-7 panels are not recommended for use in construction because of their relatively poor performance. The P3-2 panel behaves reasonably well, as presented in Chapter 5 (page 49), but the P3-3M panel performs better and can be more easily installed in the field. The P3-3M panel may also be installed directly into a corner or against a door or window opening because the threaded rods are installed to the interior of the inset panel. The P3-3M panel may also be installed in a narrower opening than the P3-2 panel because of the threaded rod location and the need to place an additional stud to the exterior of the rod in the P3-2. The total width of the P3-3M panel is only 49.5 in., including the 2x6 edge studs, while the P3-2 panel is 57.5 in. wide.

The P3-7 panel is not recommended for design because of its extreme flexibility (i.e., very low stiffness), as described in Chapter 5 (page 62).

The recommended design values (D_{RASD} and D_{RLRFD}) for the P3-3M panel exceed the 350 lb/ft and 490 lb/ft values given in note i for Table 2306.4.1 in the 2000 IBC. These greater capacities are acceptable because this panel has twice the edge width (i.e., nailing surface) of the baseline type panel. In the P3-3M, the nailing surface between the OSB and inset stud is the full 1-½ in. width of the stud, as compared to ¾ in. for the baseline panel. The inset panel configuration also provides greater capacity directly through bearing.

Table 19. Wood shear panel recommended design values.

Parameter	P3-1	P3-2 [†]	P3-3M	P3-6	P3-7 [†]
Average Maximum Shear Strength, S_{max} (lb/ft)	438	1406	1844	572	324
Shear Stiffness, K (lb/in)	1196	6274	8372	3159	489
Recommended Design Stiffness, K_R (lb/in)	1000	6000	8000	3000	400
Average Ultimate Capacity, Q_u (lb)	3979	12945	15078	9005	2930
Test Panel Width, W (ft)	4.67	4.00	4.00	4.00	2.00
Average Ultimate Shear per ft, D_u (lb/ft)	853	3236	3770	2251	1465
ASD Reduction Factor, R_{ASD}	5.6	5.6	5.6	5.6	5.6
Calculated ASD Shear, D_{ASD} (lb/ft)	152	578	673	402	262
Recommended ASD Shear, D_{RASD} (lb/ft)	150	550	650	350	200
LRFD Reduction Factor, R_{LRFD}	4.0	4.0	4.0	4.0	4.0
Calculated LRFD Shear, D_{LRFD} (lb/ft)	213	809	942	563	366
Recommended LRFD Shear, D_{RLRFD} (lb/ft)	210	770	910	490	280

[†] The P3-2 and P3-7 shear panels are not recommended for construction, based on panel behavior and practicality of construction. Still recommended design values are provided for reference.

Table 8 in the referenced APA report (Adams 1987) provides load factors, which are the ultimate load divided by the design shear. The ultimate loads are based on 8 ft x 8 ft test panels that were loaded in one direction only. Both of these factors will lead to greater measured panel capacities than those measured in the tests conducted in the current study. The load factors provided in the APA report table vary between 3.3 and 5.0.* No comparison was made with the APA test data, but it is still of interest to note that a similar load factor could be calculated for each of the panels in Table 19. This comparison may be done by dividing the average maxi-

* Except where the test had to be stopped based on limitations of the test fixture or where or where additional capacity was measured based on the use of gypsum board.

mum shear strength, S_{\max} , by the recommended ASD shear, D_{RASD} (see Table 19 for these values). The resulting load factors would vary between a low of 1.62 for P3-6 and a high of 2.92 for the P3-1 panel. However, the S_{\max} values should not be used as a basis for design because they do not account for the ductile performance of the panels.

The recommended values in Table 19 can also be compared with the calculated values based on the analytical model presented in Appendix A. The calculation of these values is shown in Table 10. The last row of the summary table for each shear panel provides the calculated allowable design resistance, D' . Comparing these values with values for D_{RASD} in Table 19 shows that the analytical model is very conservative. The analytical model values are based on the allowable nail design resistance, Z' , in Table 10. These values also do not account for good ductile system behavior and are quite conservative. Therefore, although the analytical model is provided in Appendix A, it is not recommended for design.

7 Summary

In this investigation, alternative shear panel configurations for light wood construction were subjected to simulated seismic loads in order to document performance characteristics. The performance of each panel is documented in Chapter 5, including detailed observations of panel behavior. Four different variations of the basic inset panel were tested monotonically (P3-2, P3-3, P3-4, and P3-5). The P3-3 panel provided the best ductile behavior, was the strongest, and is the easiest to install on the job site. The P3-3 panel was further optimized into a configuration designated P3-3M (medium) panel. Light and heavy variations of the P3-3 panel were also developed but not tested during this phase of the work. The P3-3M panel performed very well and is recommended for construction purposes.

Chapter 6 presents design guidance for each of the recommended panels. The guidance directly parallels the 2000 IBC, Table 2306.4.1, and could be incorporated into future editions of the IBC. Chapter 6 also shows that the analytical predictive model, discussed in Chapter 3 and presented in Appendix A, is too conservative for design purposes. That model was based on design strengths of the materials used, which addresses the various modes of failure plus estimates of the yield and ultimate capacities. The model is limited to these configurations, with the variables indicated in Chapter 3. Although it is not recommended for design purposes, however, the model is a useful analytical tool for developing new, well proportioned panel configurations that provide ductile behavior.

The note to Table 19 (see Chapter 6) indicates that only the P3-1, P3-3M, and P3-6 panels are recommended for use in actual construction. However, two variations on the P3-3 configuration also were designed and should be evaluated experimentally. As indicated above, these configurations were as follows:

1. P3-3L – A light panel with no nailing plates at the top corners and increased nail spacing around the panel perimeter.
2. P3-3H – A heavy panel with nailing plates at both the top and bottom corners and nail spacing reduced.

The narrow P3-7 inset panel could be improved to include stronger holddown anchors at the tops and bottoms of both 2x6 edge studs. This would increase the over-

turning resistance, stiffness, and strength of the panel. An improved P3-7 panel should be designed and evaluated experimentally to confirm these hypotheses.

Additional design values could be provided for the P3-3L and P3-3H as well as an improved P3-7 panel if a new experimental study were to demonstrate good performance.

References

- 2000 International Building Code (IBC), International Code Council, Inc., Falls Church, VA. Table 2306.4.1, pp 564-565.
- Adams, Noel R. January 1987. “*Plywood Shear Walls*,” American Plywood Association, Tacoma, WA, Research Report 105.
- American Institute of Steel Construction (AISC), *AISC Load and Resistance Factor Design*, 2nd Edition, Vol II, 1994.
- American Forest and Paper Association (AF&PA) and American Society of Civil Engineers 16-95. 1996. *Load and Resistance Factor Design (LRFD) for Engineered Wood Construction*, “Commentary,” Section C7.4.3, p 91.
- American National Standards Institute (ANSI)/AF&PA NDS-1997, *National Design Specification (NDS) for Wood Construction*, 1997 Edition, American Forest and Paper Association, Washington, DC.
- American Society for Testing and Materials (ASTM) E72, “Test Methods of Conducting Strength Tests of Panels for Building Construction,” 1998.
- ANSI/AF&PA NDS-1997, *National Design Specification (NDS) for Wood Construction* (American Forest and Paper Association, 1997), sec 4.1.4.
- ASTM D 1165, vol 04.10, *Standard Nomenclature of Domestic Hardwoods and Softwoods* (2000), p 194.
- “City of Los Angeles Standard Method of Cyclic (Reversed) Load Test for Shear Resistance of Framed Walls for Buildings” (Structural Engineers Association of Southern California and the City of Los Angeles, revised 9 September 1997).
- Coil, John (instructor), *FEMA 273 Training – Examples of Applications to Wood Buildings* (FEMA, Washington, DC, February 2000), pp 14-15.
- FEMA 273, *NEHRP Guidelines for Seismic Rehabilitation of Buildings*. National Earthquake Hazards Reductions Program (NEHRP).
- FEMA 274, *NEHRP Commentary on the Guidelines for the Seismic Rehabilitation of Buildings*, C8.3.2.5, p 8-6.
- Krawinkler, Helmut, F. Parisi, L. Ibarra, A. Ayoub, and R. Medina. 2001. *Development of a Testing Protocol for Wood Frame Structures*, Stanford University, CUREE W-02.

SAC Joint Venture Testing Programs and Loading Histories, unpublished guidance (Structural Engineers Association of California; the Applied Technical Council; and California Universities for Research in Earthquake Engineering, 1997).

Figures

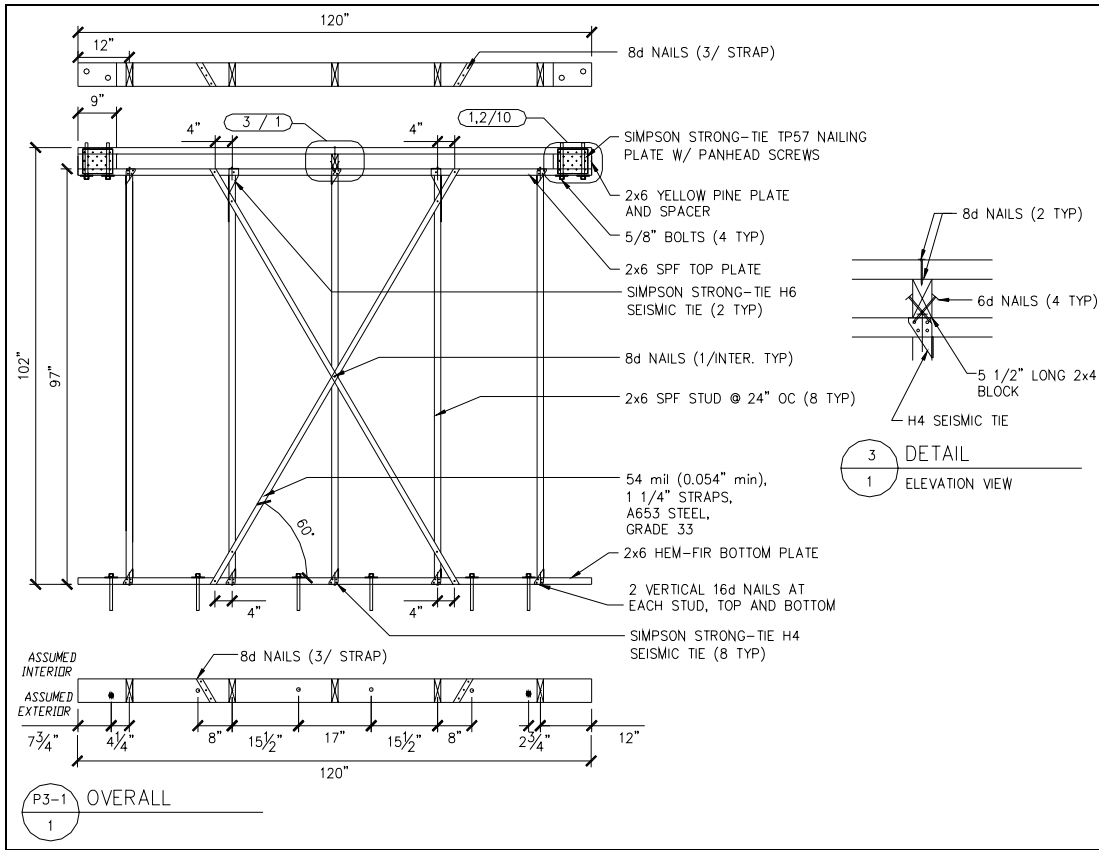


Figure 1. P3-1 diagonal strap shear panel.

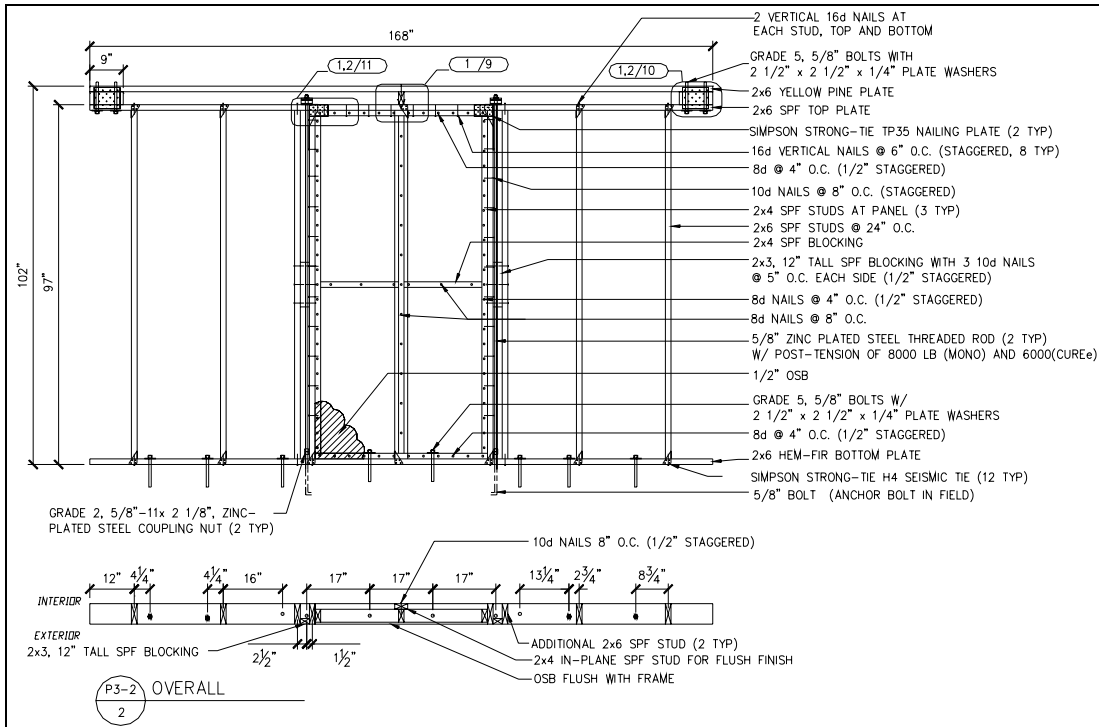


Figure 2. P3-2 OSB shear panel.

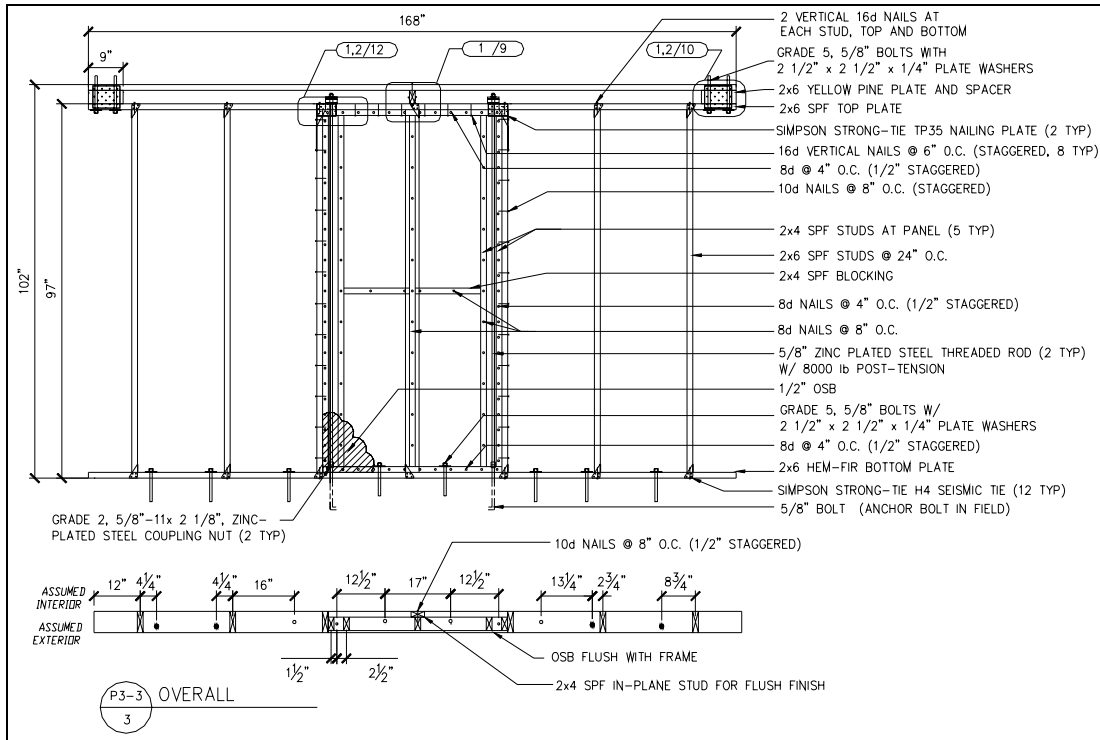


Figure 3. P3-3 OSB shear panel.

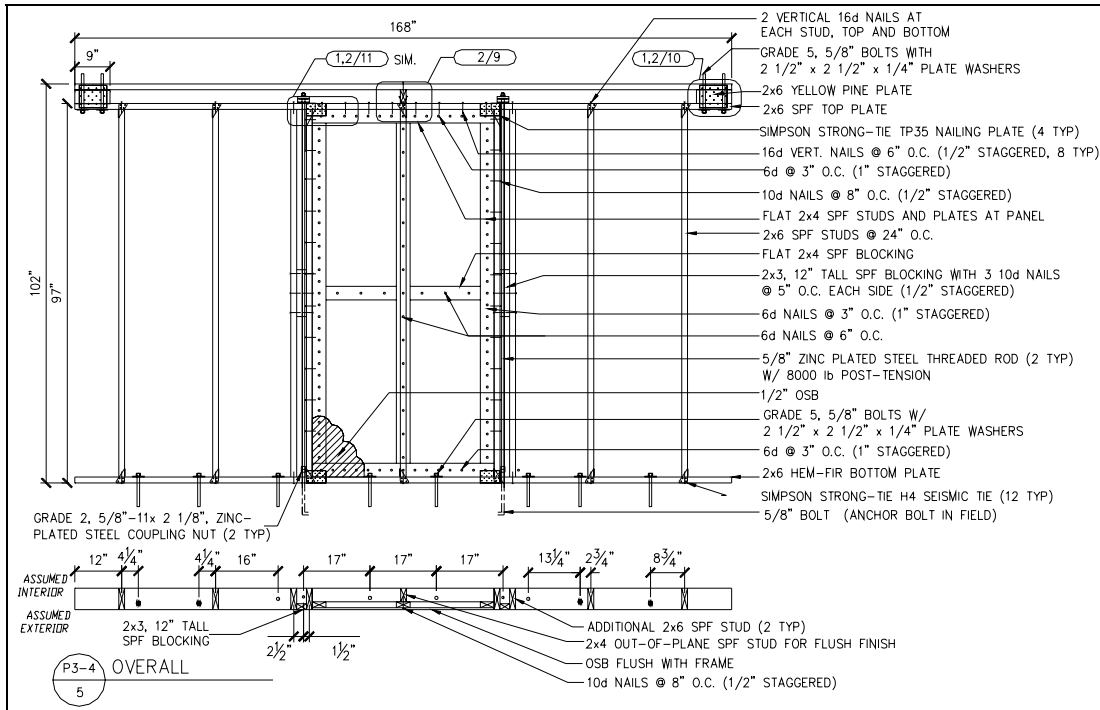


Figure 4. P3-4 OSB shear panel.

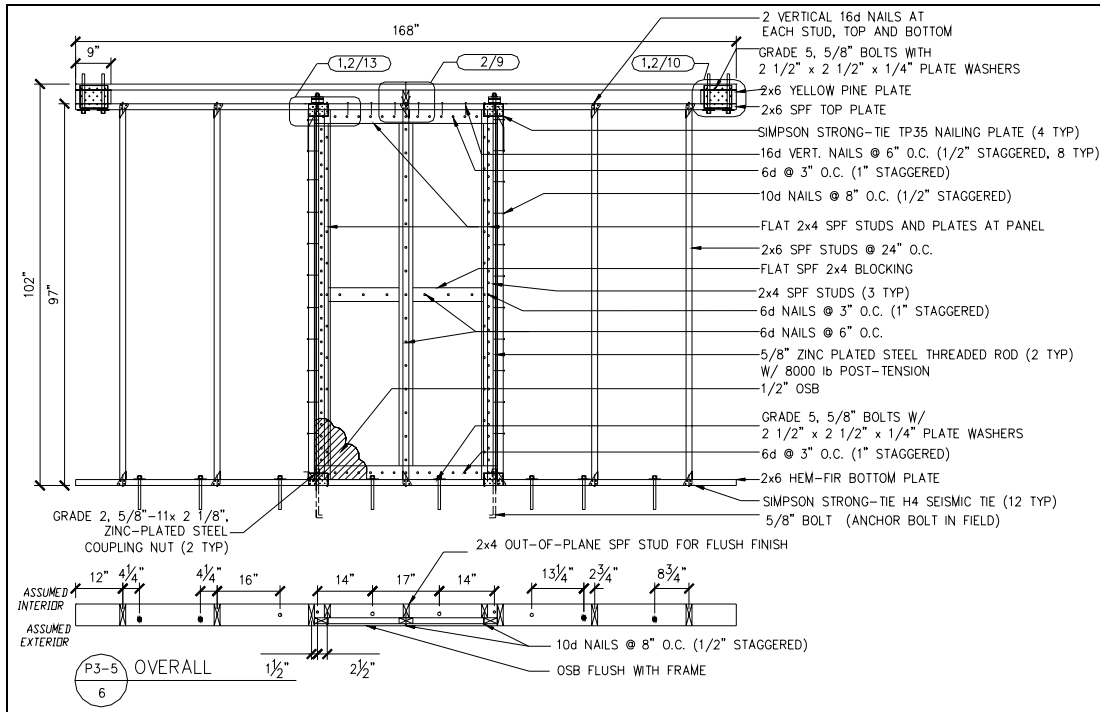


Figure 5. P3-5 OSB shear panel.

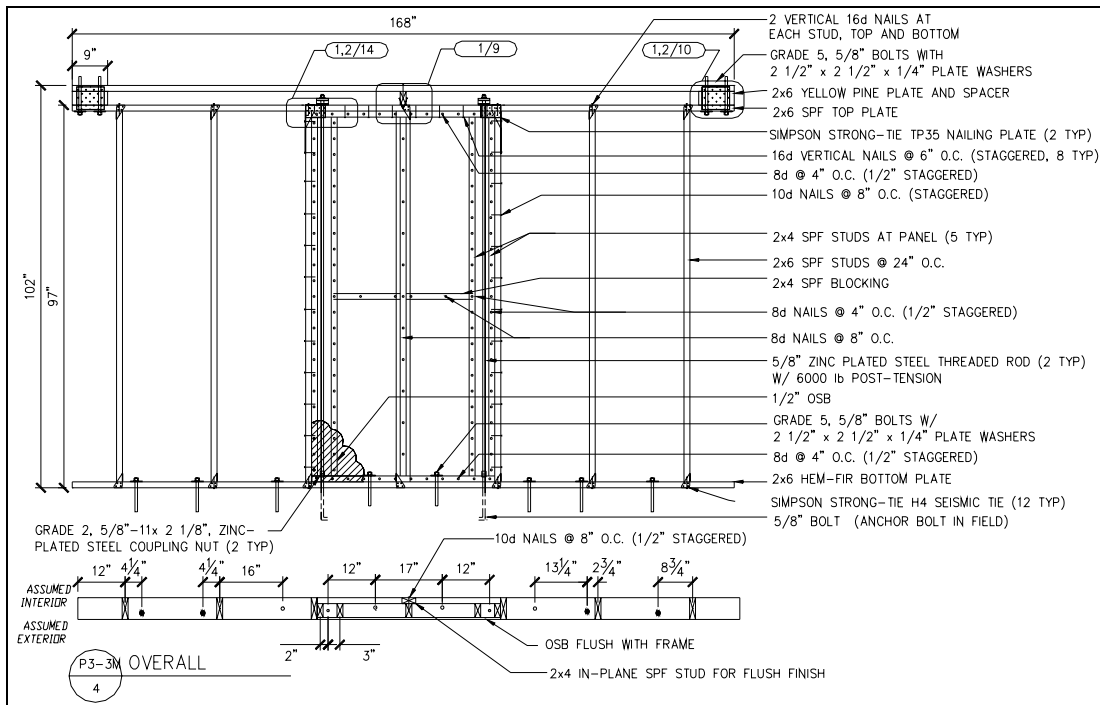


Figure 6. P3-3M medium-strength OSB shear panel.

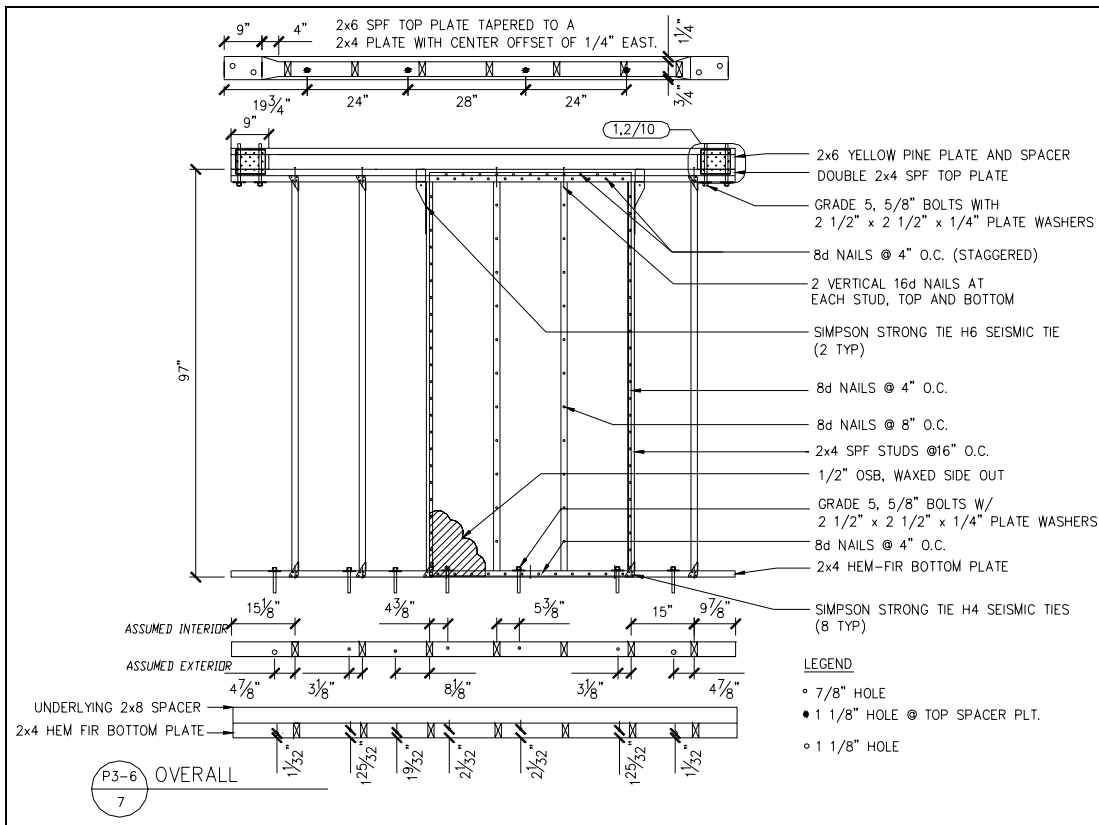


Figure 7. P3-6 OSB shear panel.

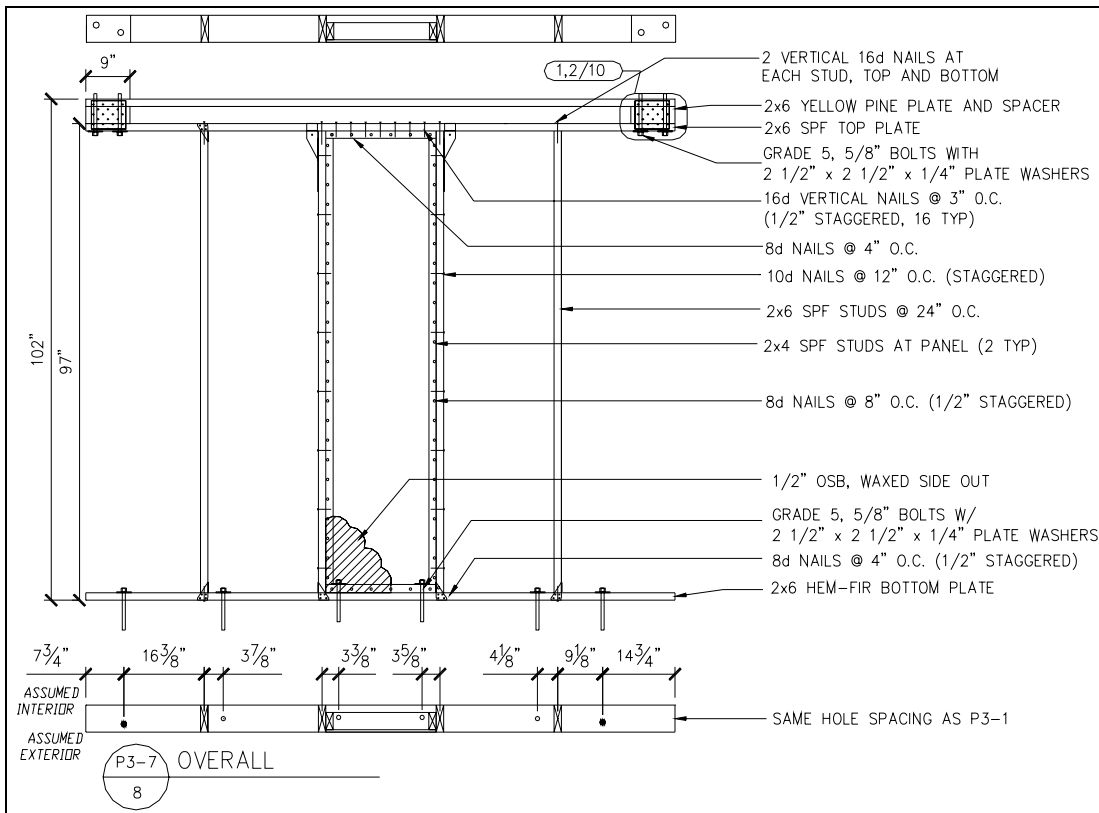


Figure 8. P3-7 OSB shear panel.

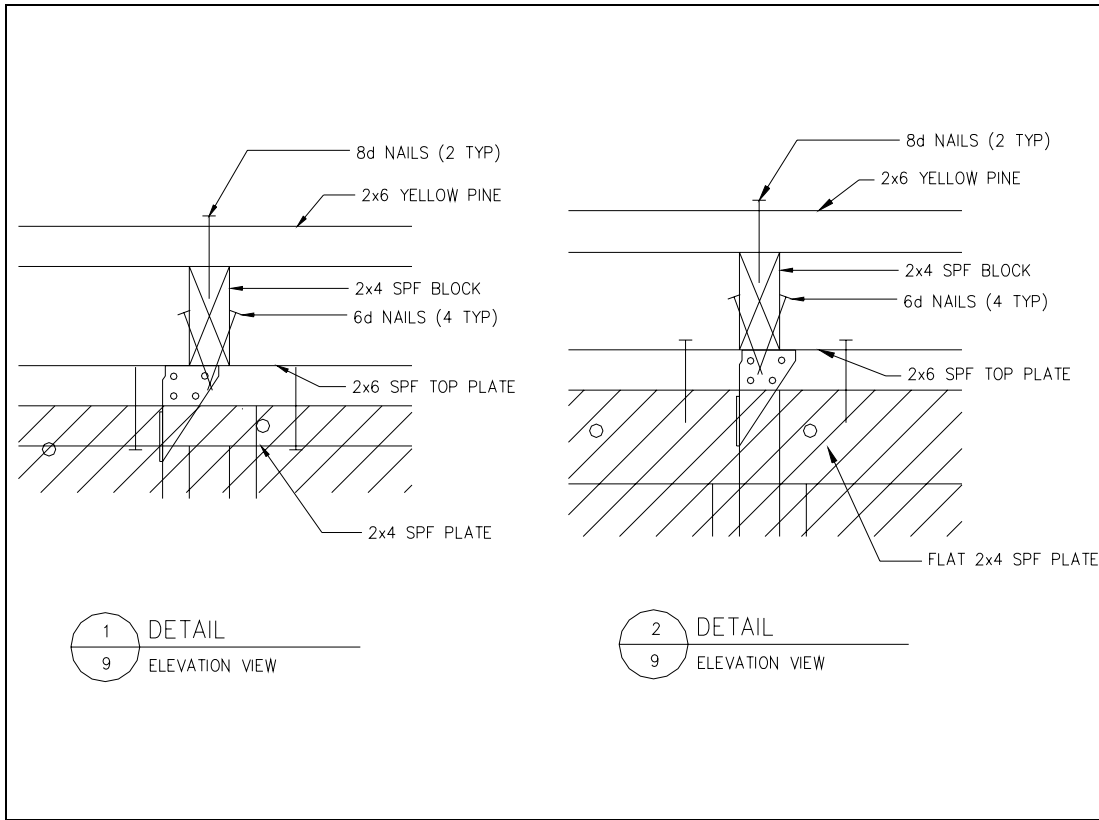


Figure 9. P3 OSB shear panel details.

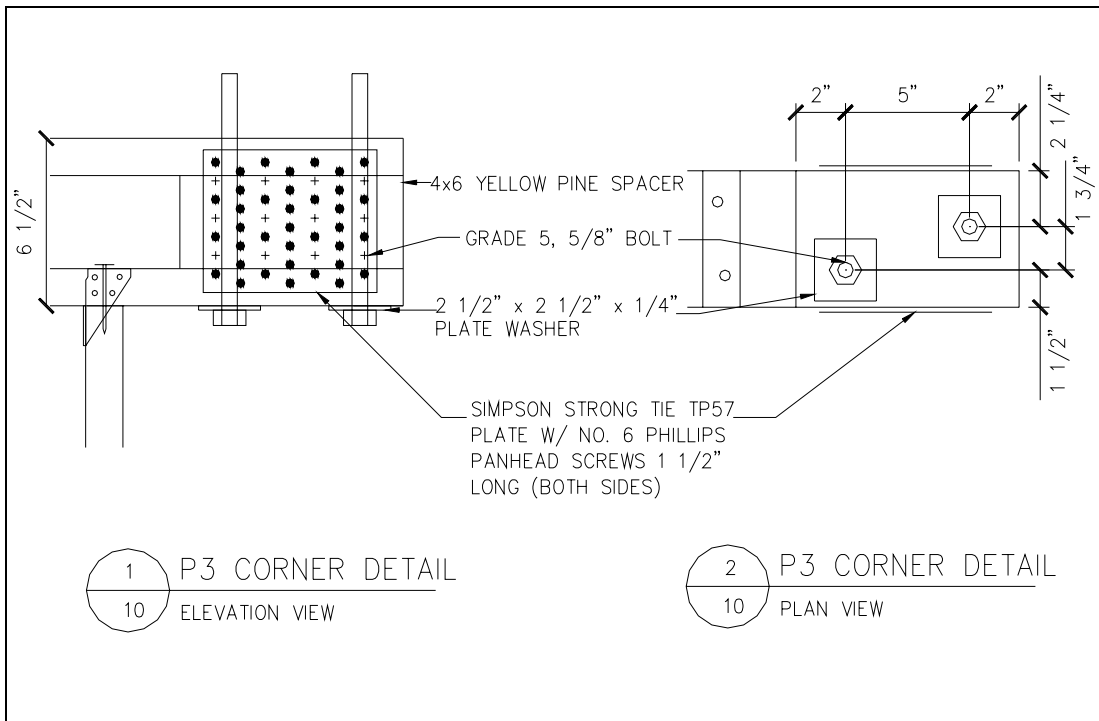


Figure 10. P3 OSB shear panel fastener details.

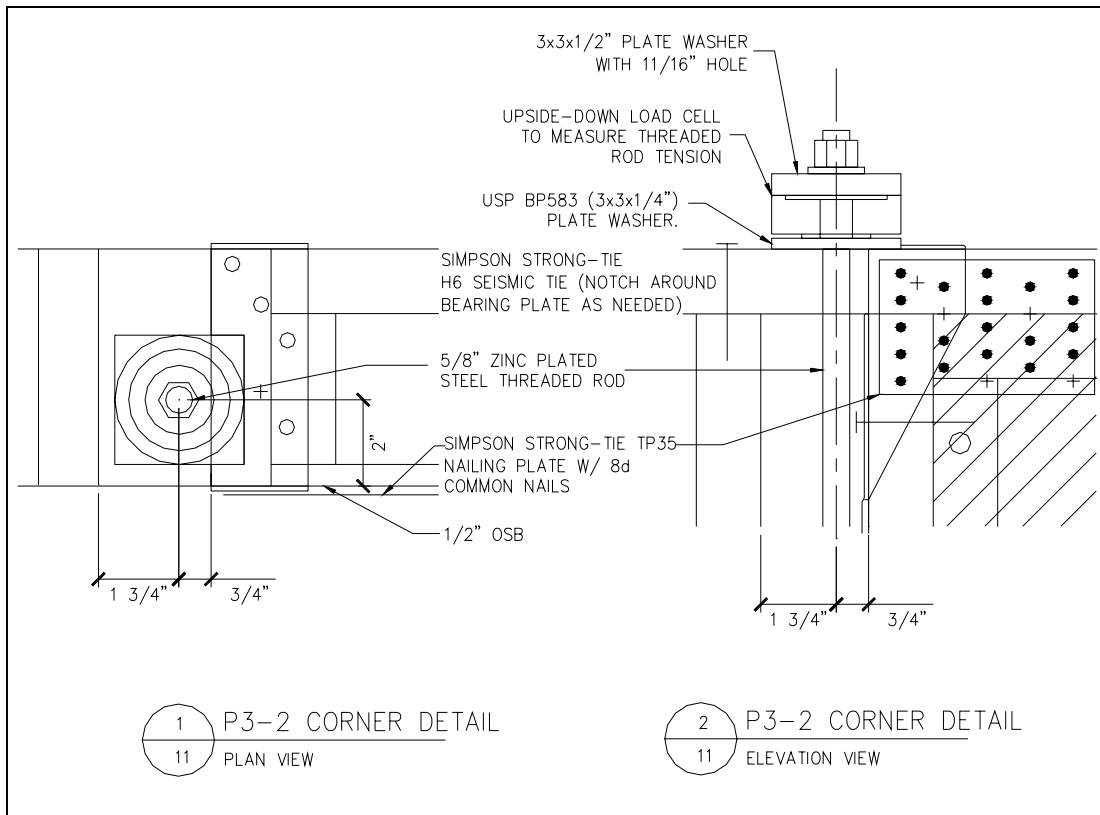


Figure 11. P3-2 OSB shear panel corner details.

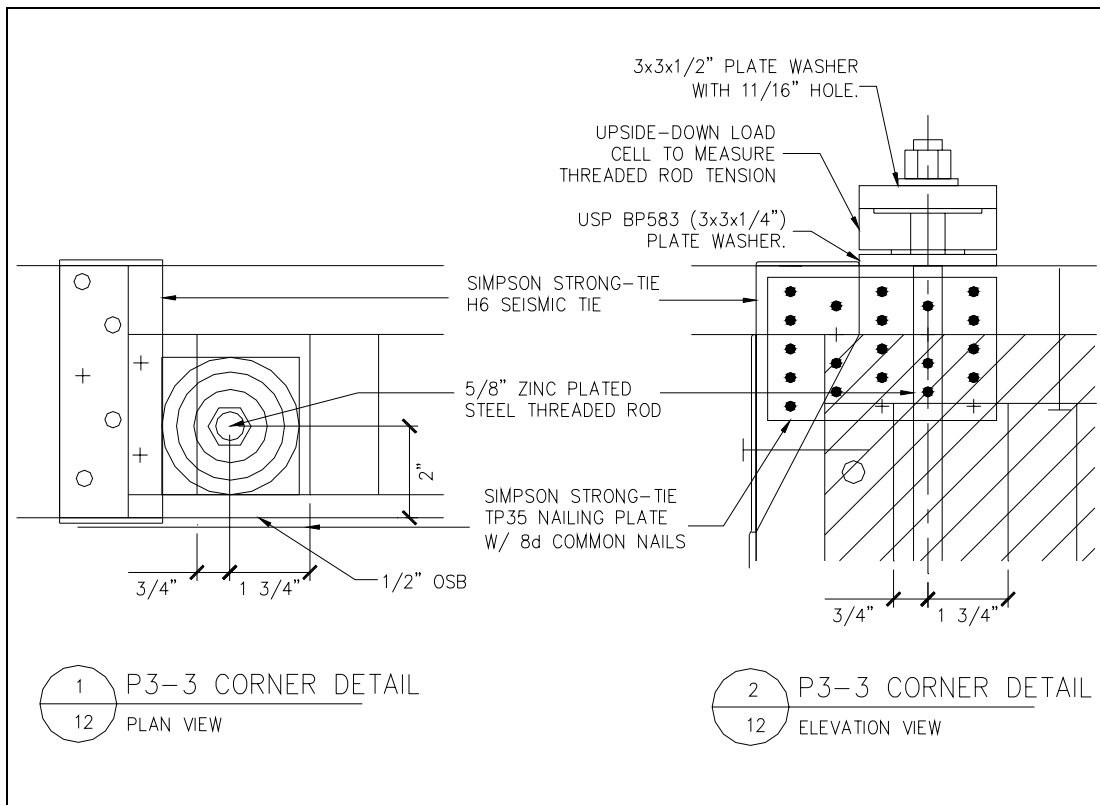


Figure 12. P3-3 OSB shear panel corner details.

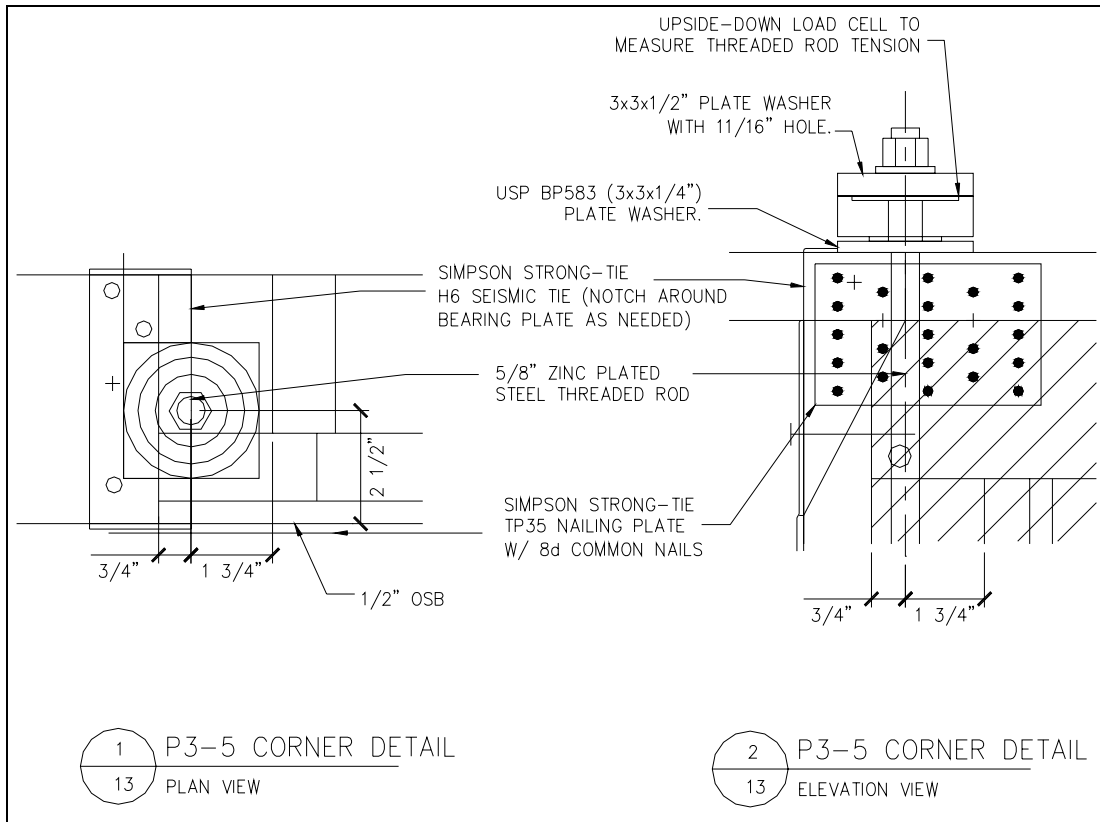


Figure 13. P3-5 OSB shear panel corner details.

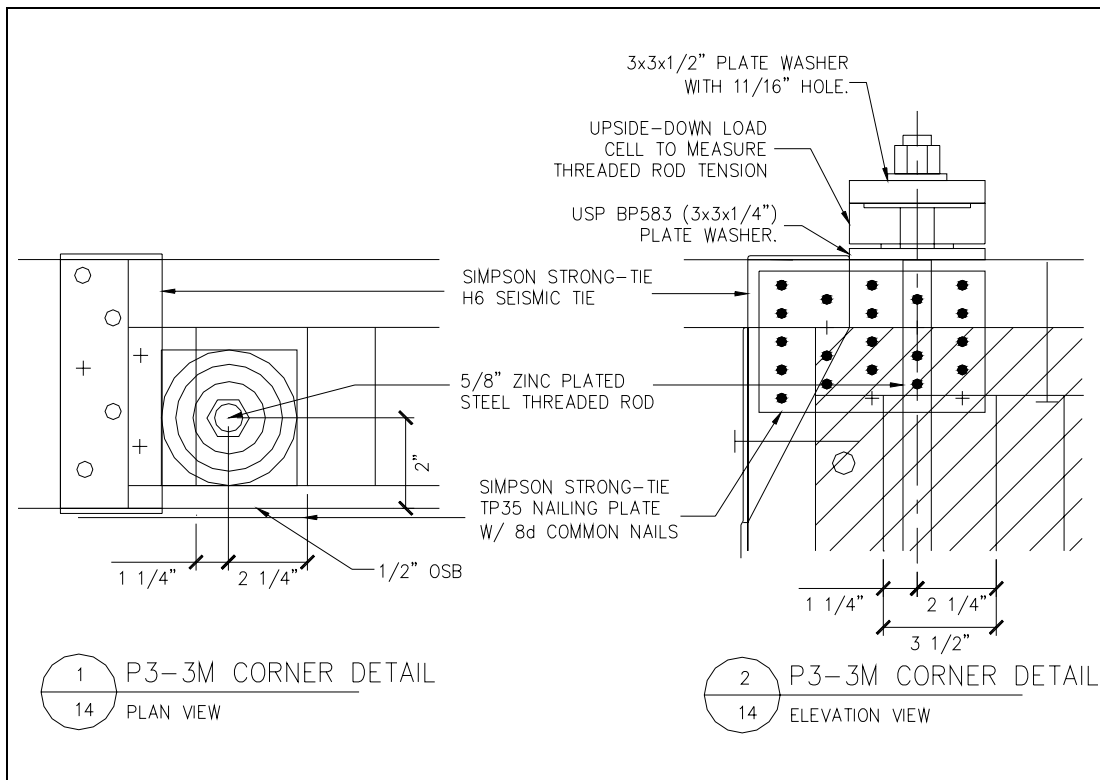


Figure 14 . P3-3M OSB shear panel corner details.

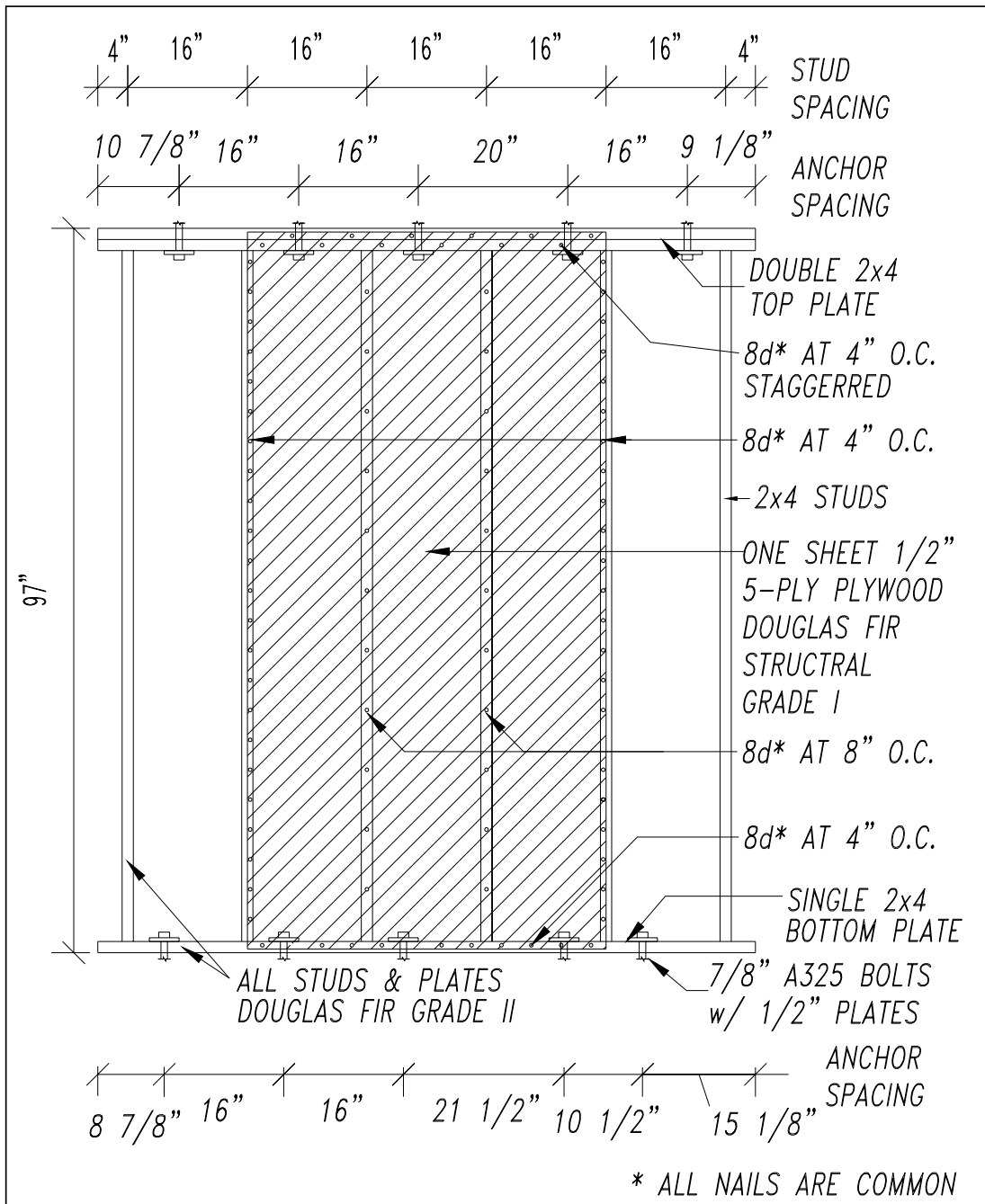


Figure 15. PSP-Std plywood shear panel tested in Phase I.

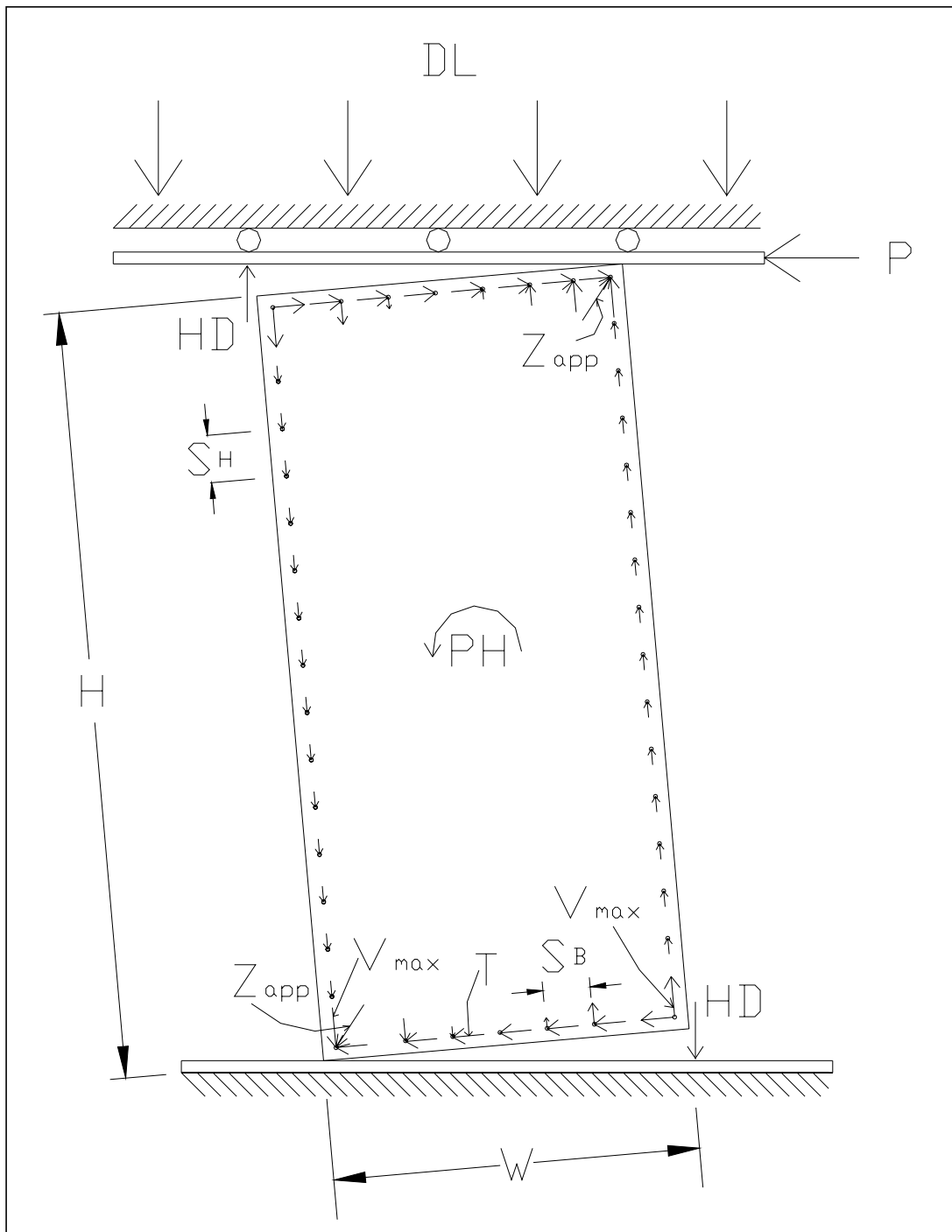


Figure 16. Wood shear panel showing forces applied to the panel and nails.

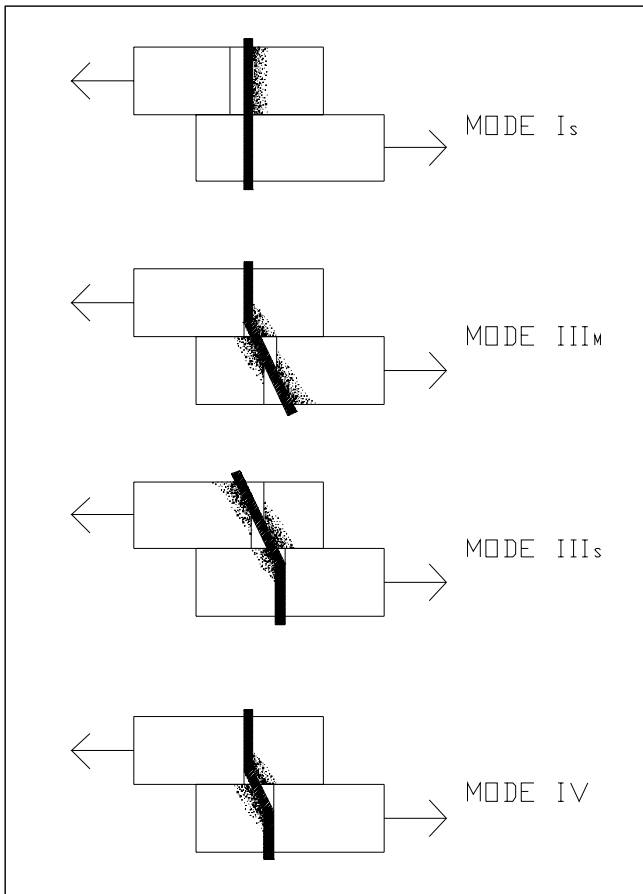


Figure 17. Graphical illustration of connection yield modes.

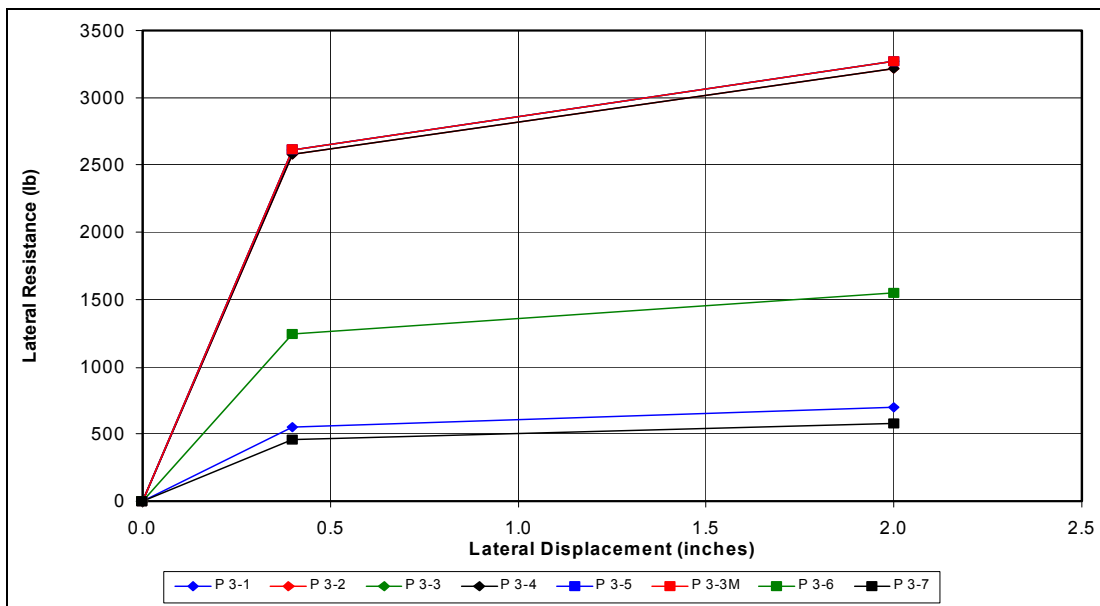


Figure 18. Predicted lateral yield and ultimate capacities for the Phase III shear panels.

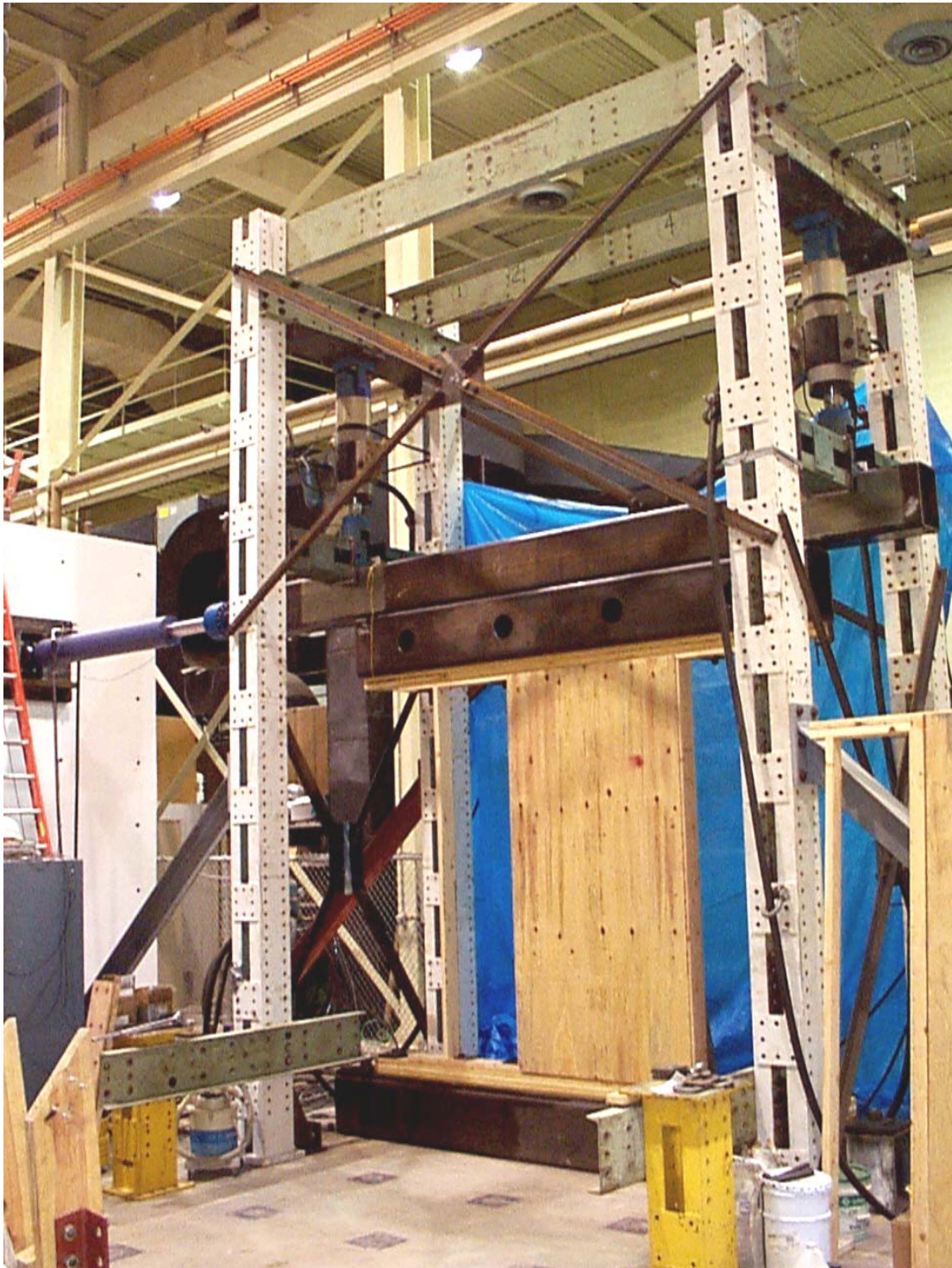


Figure 19. Overall view of test frame for testing shear panels at CERL.

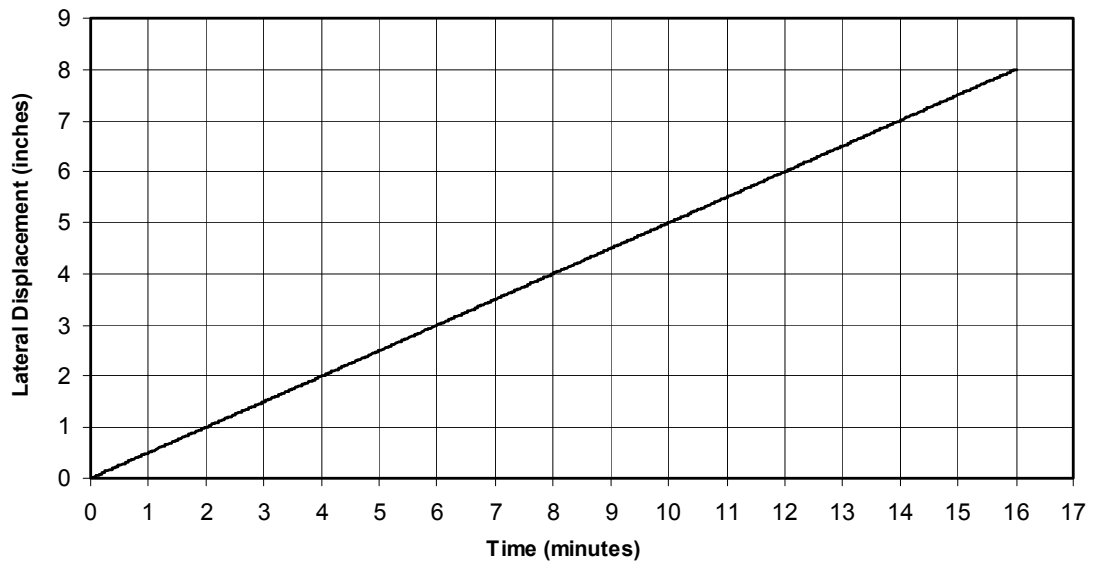


Figure 20. Monotonic load history with 0.5 inches per minute stroke rate.

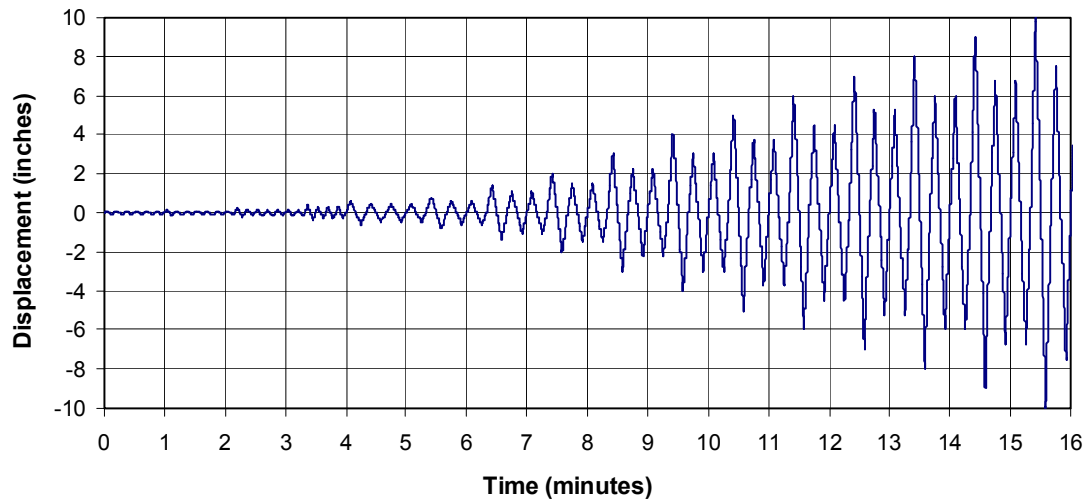


Figure 21. CUREE loading history with $\Delta = 2$ in., 0.1 Hz initial cyclic rate and 0.05 Hz later rate.

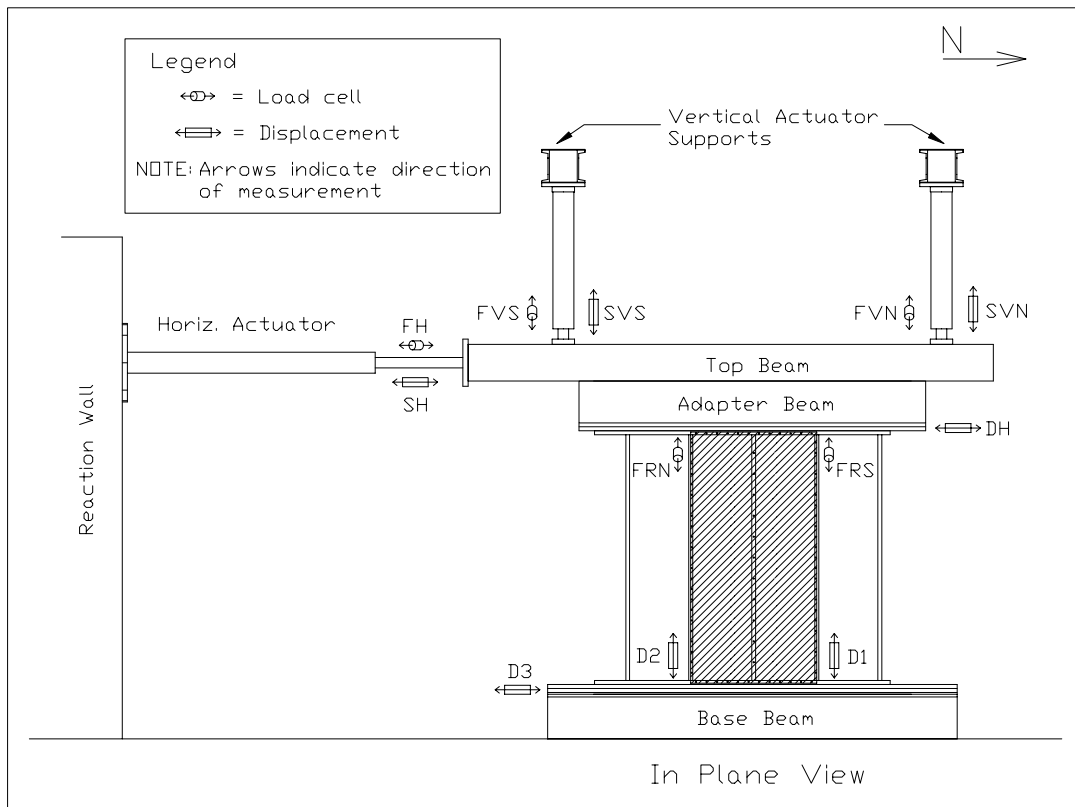


Figure 22. Schematic drawing showing sensor locations on wood shear panels.

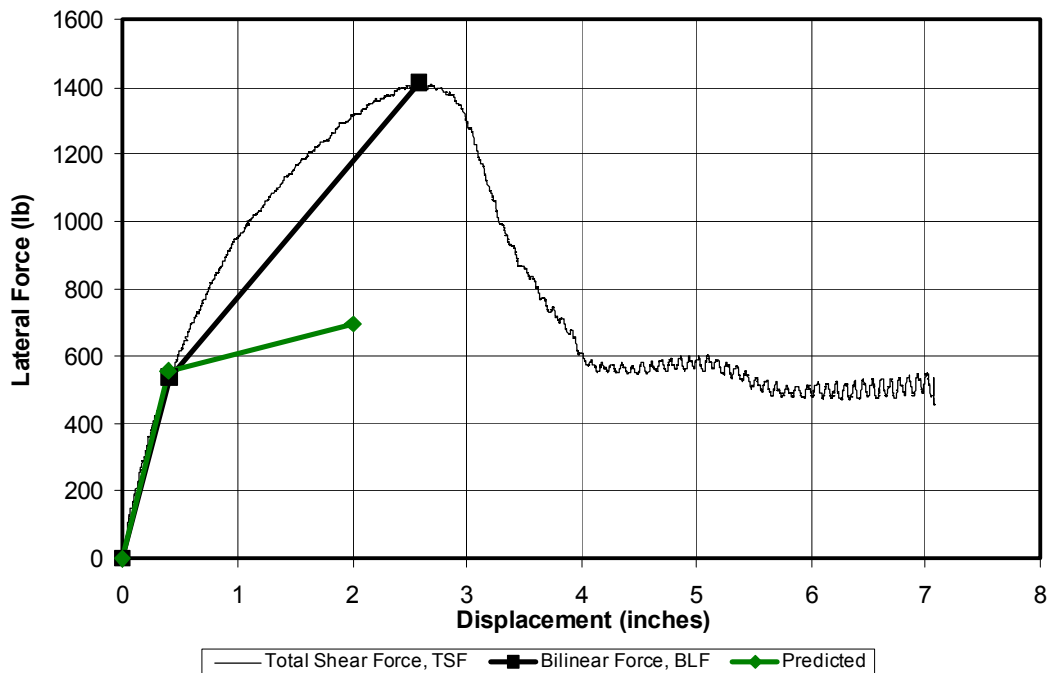


Figure 23. Lateral force (TSF) vs deflection for the P3-1 monotonic panel.

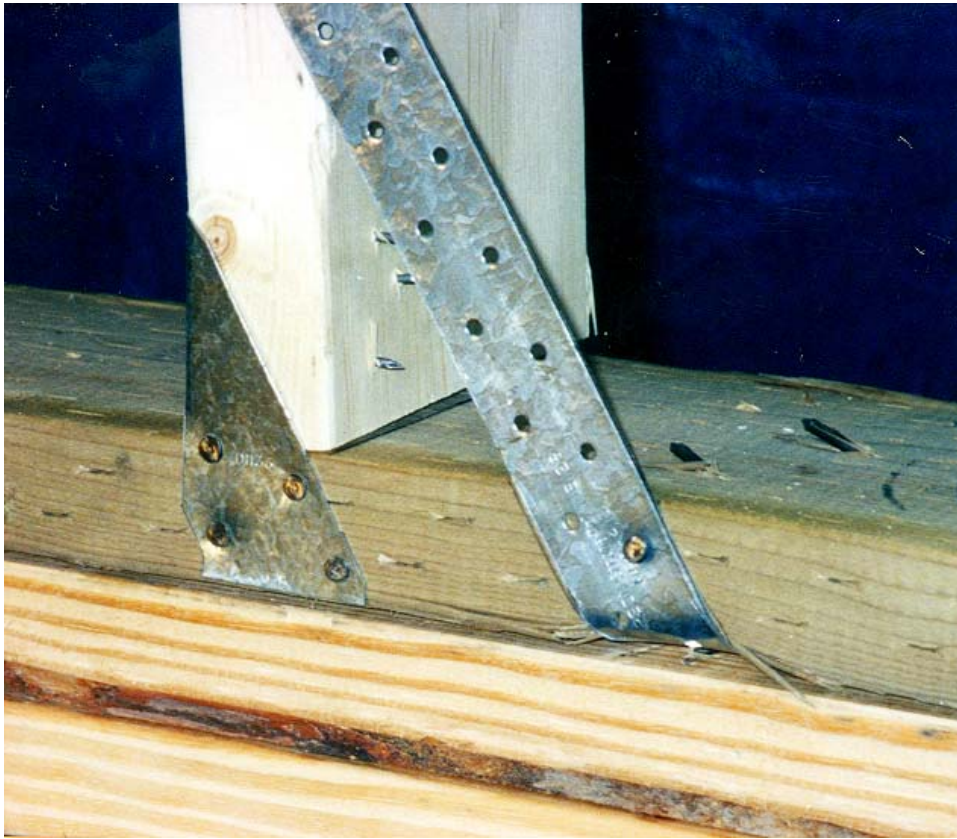


Figure 24. Crushing of bottom plate due to tensioning of steel strap.



Figure 25. Nails attaching steel strap to top plate yielded and pulled out.

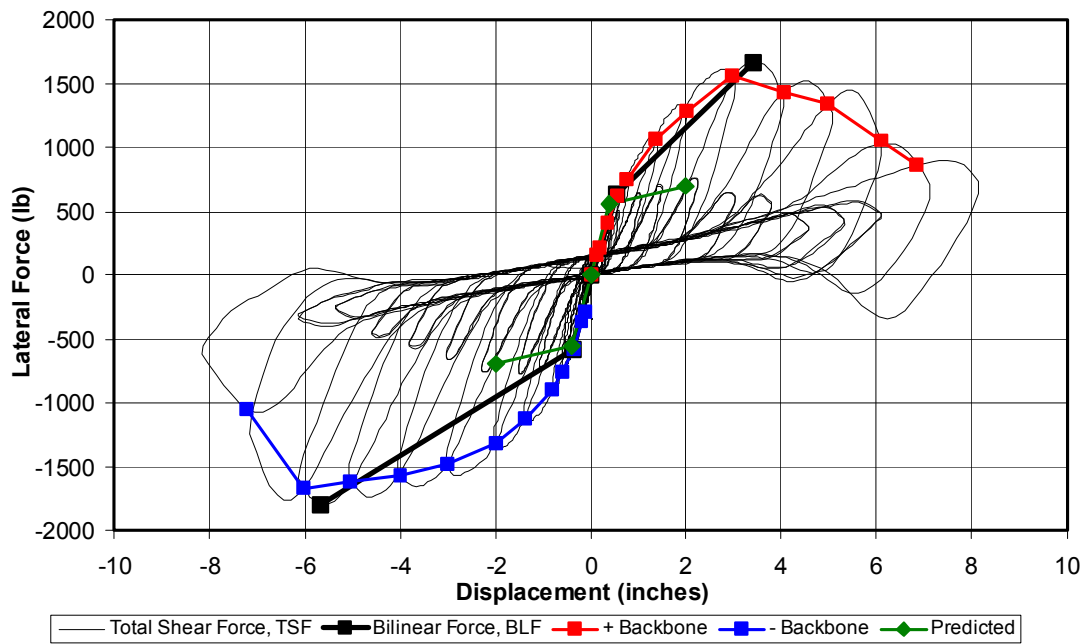


Figure 26. Lateral force (TSF) vs deflection hysteretic behavior of the P3-1 CUREE1 panel.



Figure 27. P3-1 CUREE1 panel strap failure showing straps still attached at the bottom and middle.

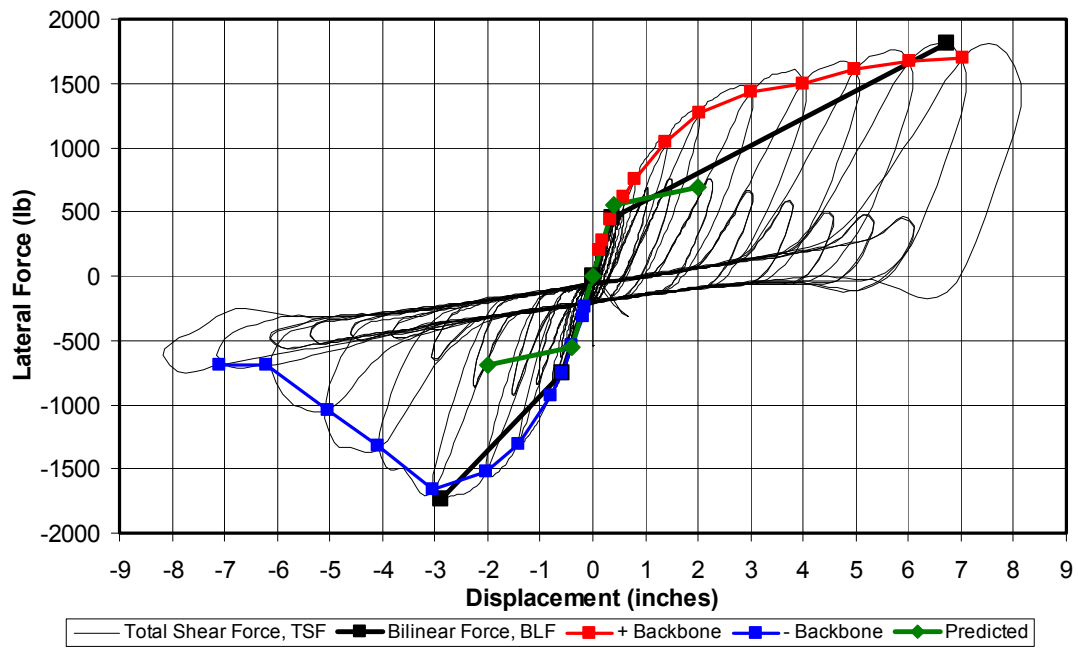


Figure 28. Lateral force (TSF) vs deflection hysteretic behavior of the P3-1 CUREE2 panel.



Figure 29. Damage in bottom plate due to tensioning of steel strap.



Figure 30. Damage in top plate at location of steel strap connection (P002987).



Figure 31. Damage state after completion of P3-1 CUREE2 test (7-7).

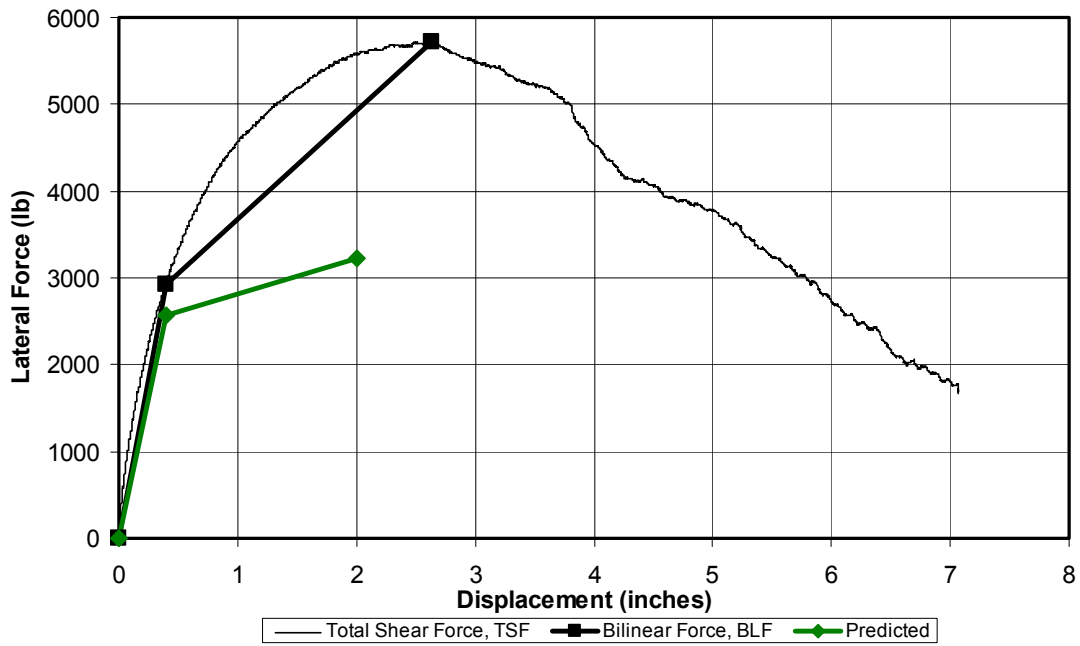


Figure 32. Lateral force (TSF) vs deflection for the P3-2 monotonic panel.



Figure 33. Gap at bottom of panel (right side) due to nail yielding.

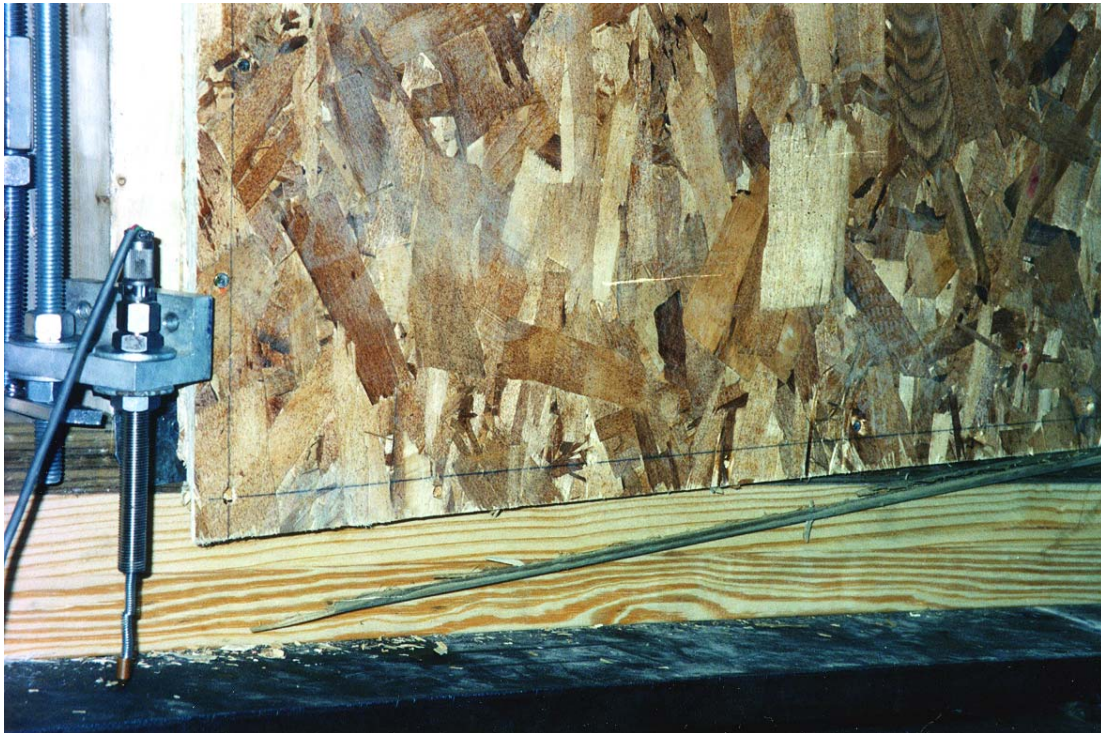


Figure 34. OSB pulling out of inset and crushing of hem-fir bottom plate.



Figure 35. Longitudinal split in top plate due to bending.



Figure 36. Block shear pullout of OSB from TP35 nailing plate.

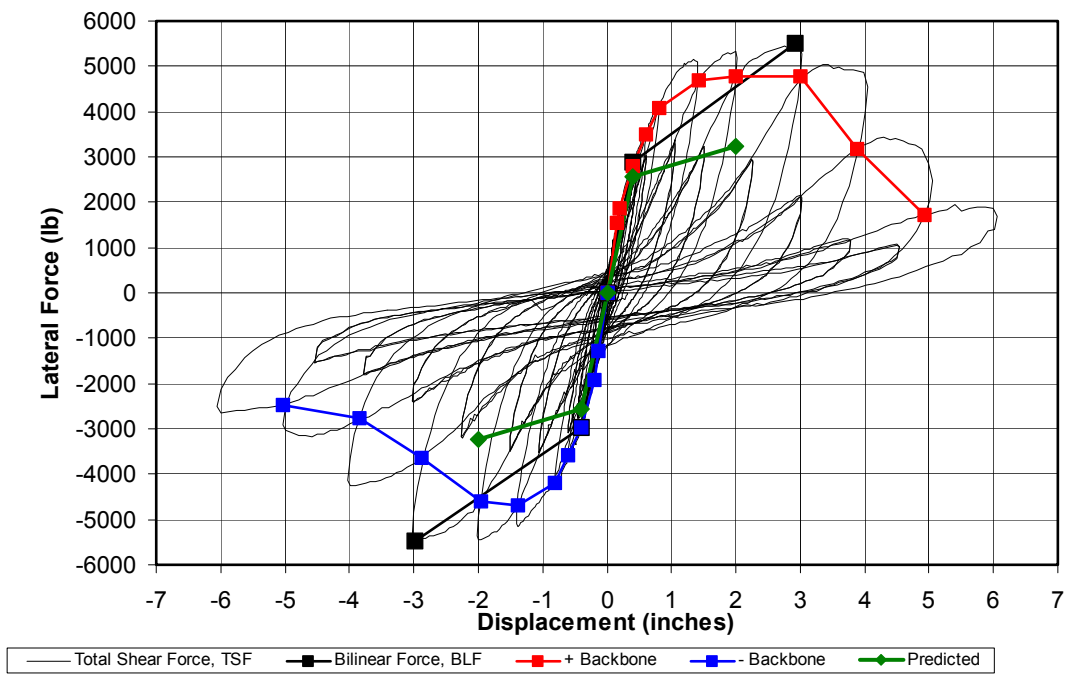


Figure 37. Lateral force (TSF) vs deflection hysteretic behavior of the P3-2 CUREE1 Panel.



Figure 38. Gap in inset panel due to nails yielding in OSB to panel connection.



Figure 39. OSB pulling out of frame in lower right corner.



Figure 40. Top plate splitting above the right side of the OSB.

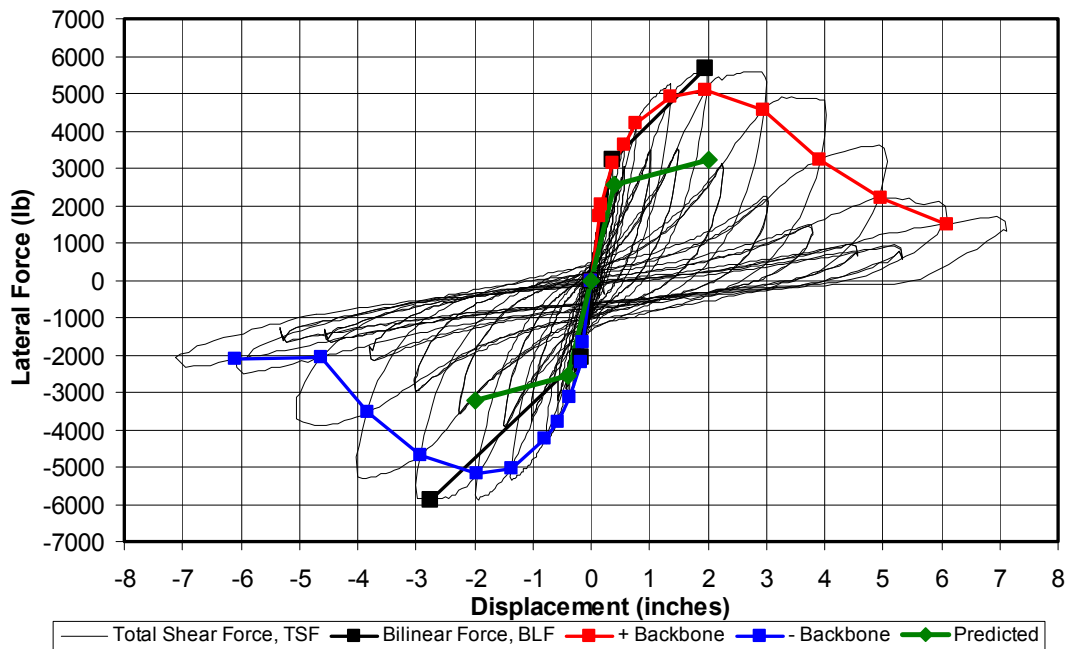


Figure 41. Lateral force (TSF) vs deflection hysteretic behavior of the P3-2 CUREE2 panel.

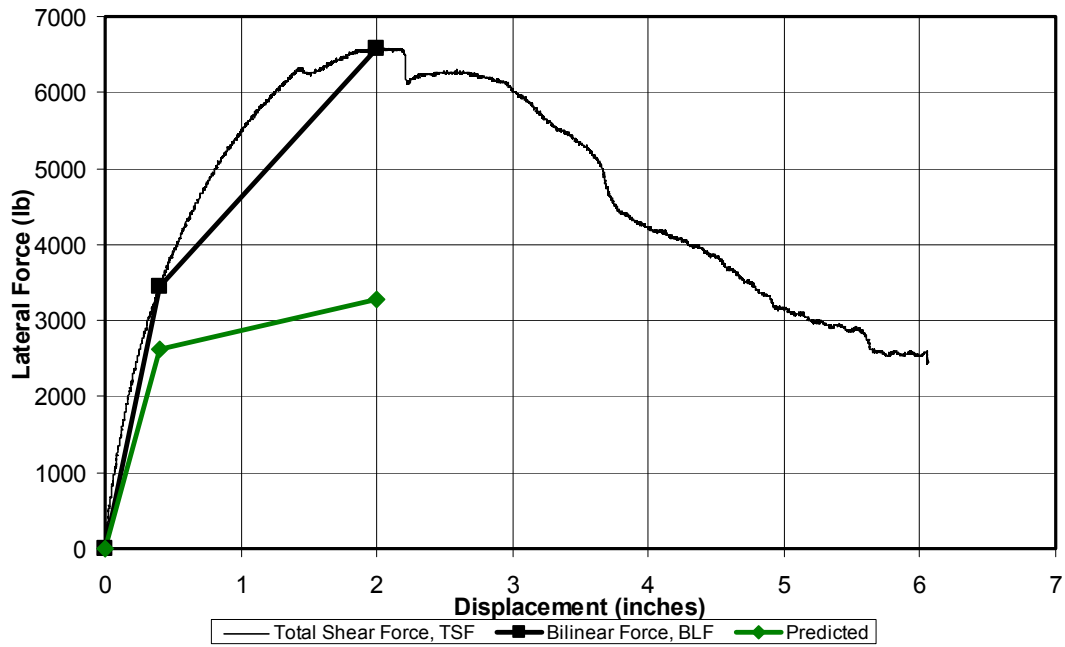


Figure 42. Lateral force (TSF) vs deflection for the P3-3 monotonic panel.

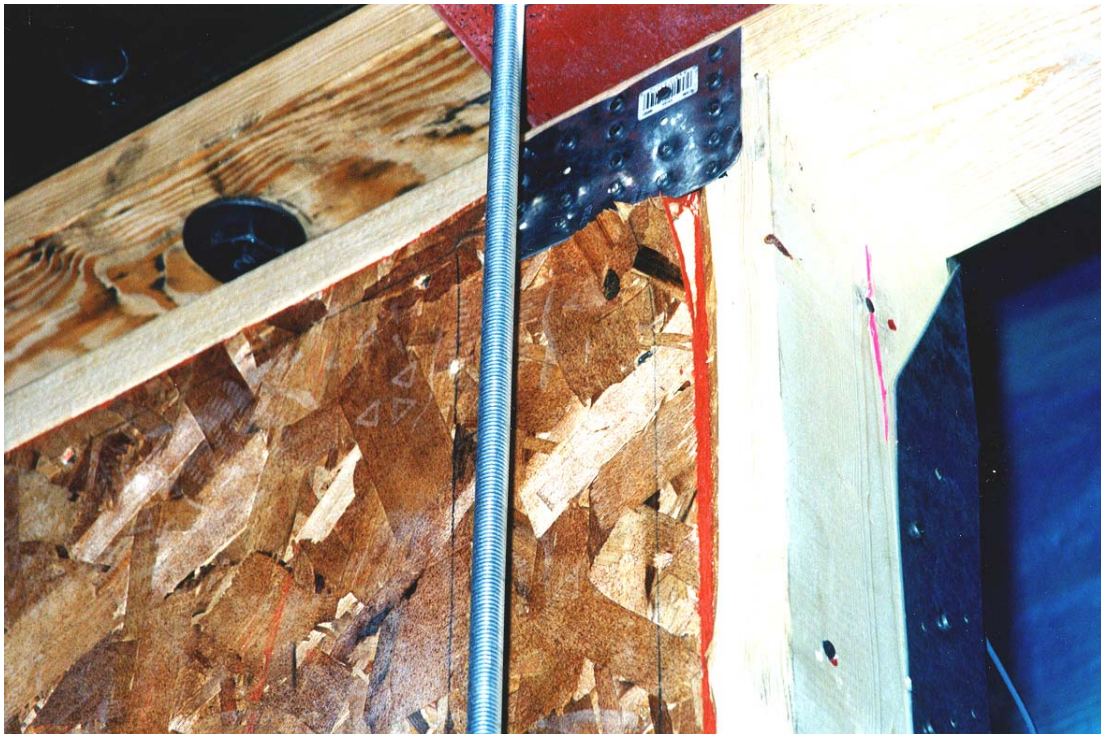


Figure 43. Crushing of top-right corner of OSB in the P3-3 mono panel.



Figure 44. OSB outside the 2x6 frame and nail pullout along right vertical edge of panel.

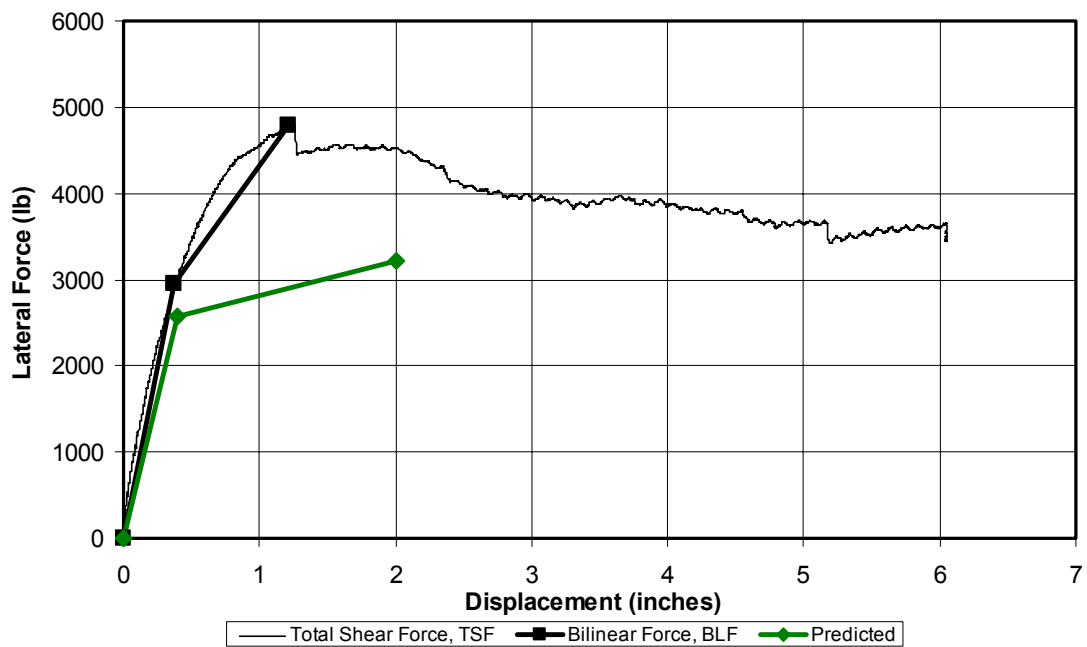


Figure 45. Lateral force (TSF) vs deflection for the P3-4 monotonic panel.

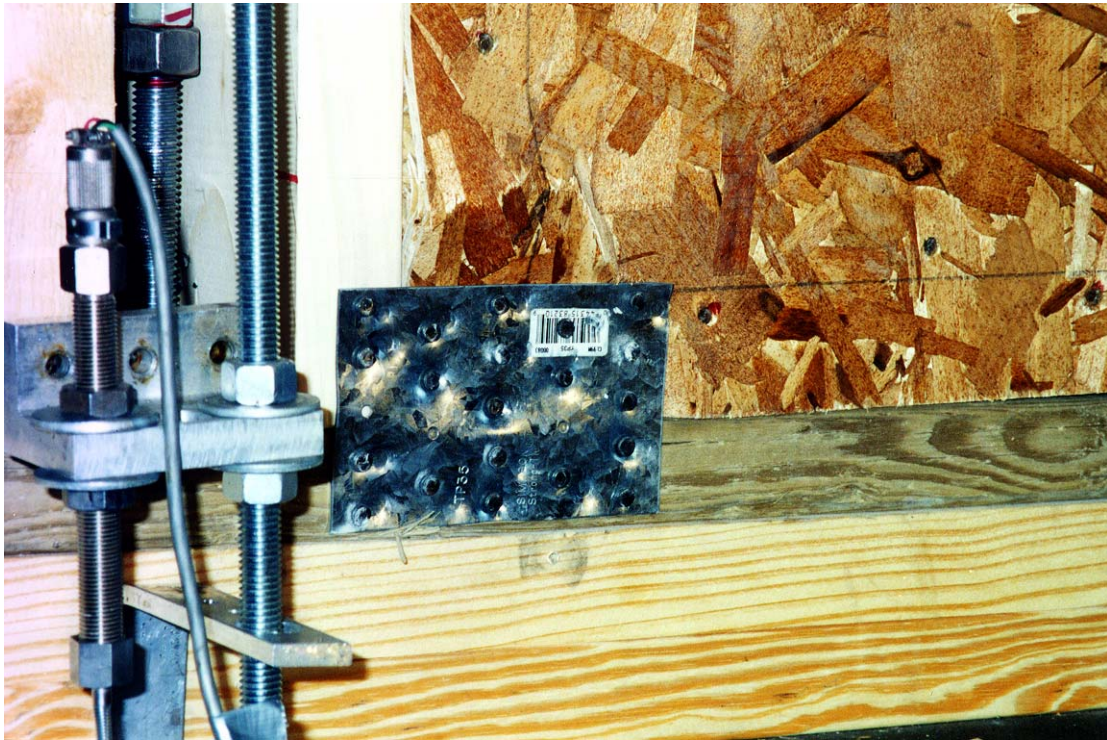


Figure 46. Crushing and buckling of lower left corner of OSB in the P3-4 mono test.



Figure 47. Damage to OSB and inset panel bottom plate at right corner of P3-4 mono panel.



Figure 48. Torsion and bending in top plate.



Figure 49. Inset panel detached from 2x6 frame.

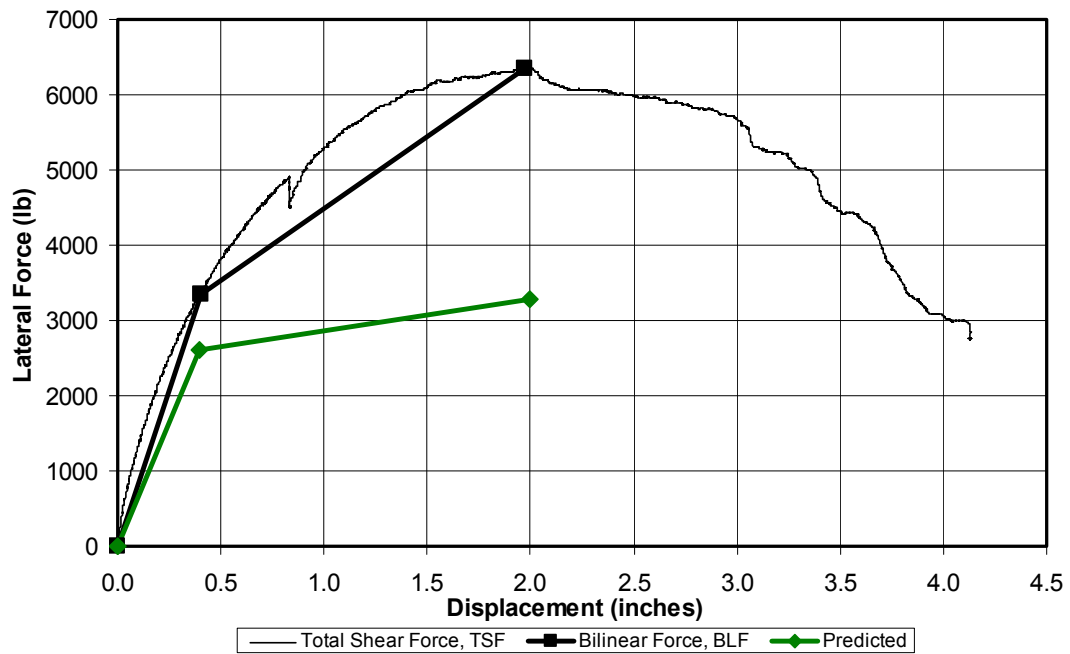


Figure 50. Lateral force (TSF) vs deflection for the P3-5 monotonic panel.



Figure 51. Top plate bending and nail yielding along OSB left edge.



Figure 52. Splitting and bending failure of P3-5 mono top plate.

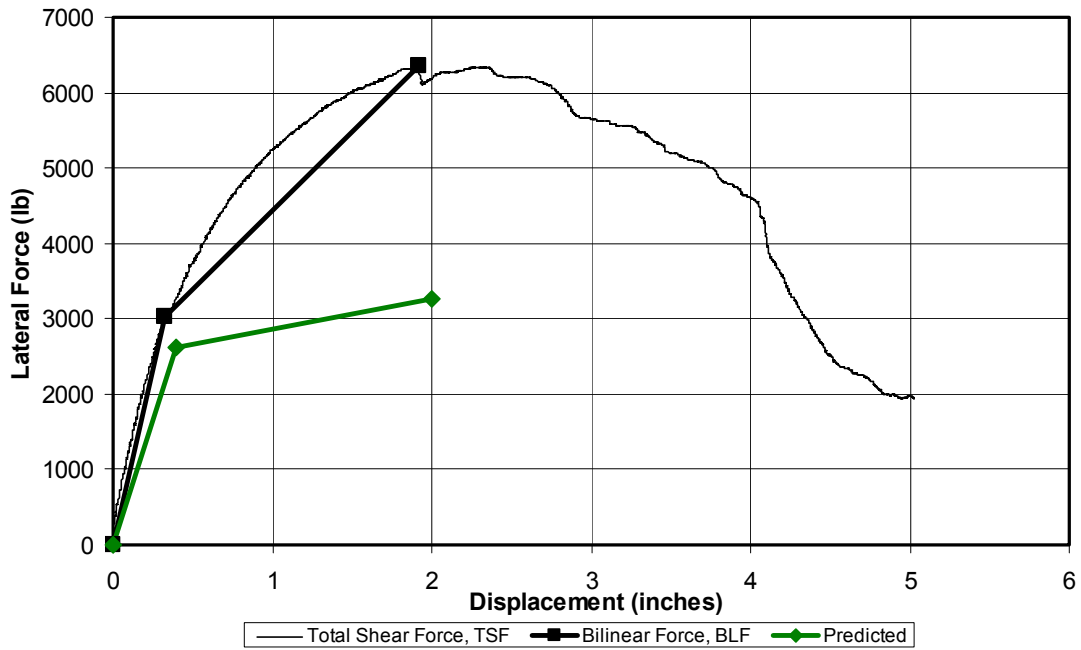


Figure 53. Lateral force (TSF) vs deflection for P3-3M monotonic panel.



Figure 54. Overall view of damaged P3-3M mono test panel.



Figure 55. Bottom of P3-3M mono panel showing the OSB pulled away from frame.



Figure 56. Interior face of P3-3M mono panel showing threaded rods.

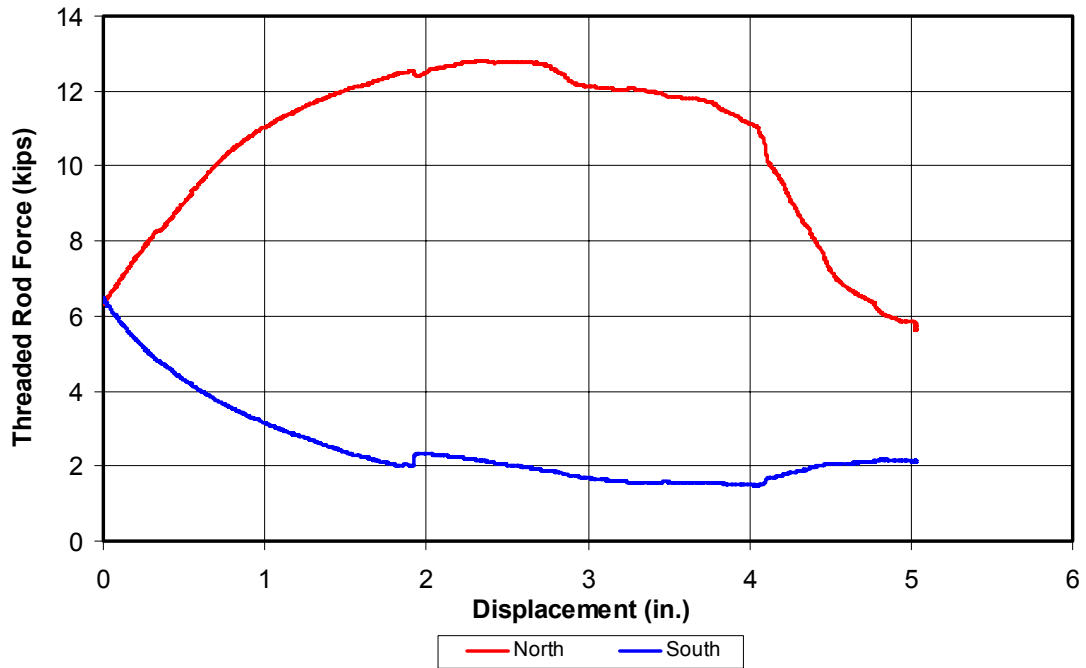


Figure 57. Load cell force vs lateral deflection in the P3-3M mono test.

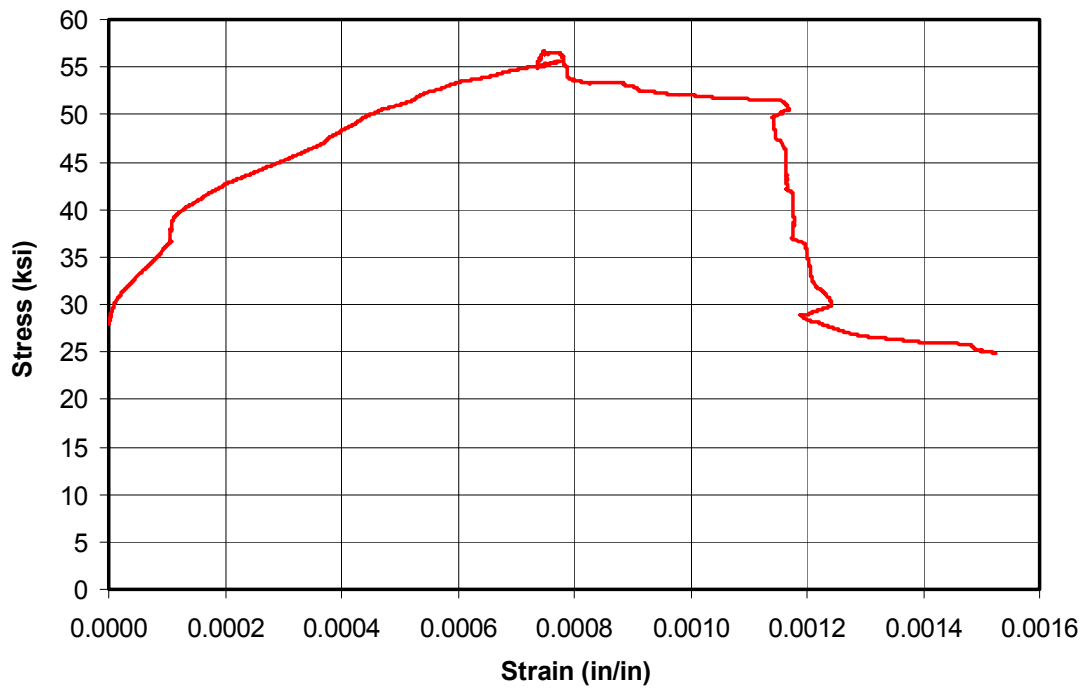


Figure 58. Stress vs strain plot for the north threaded rod.

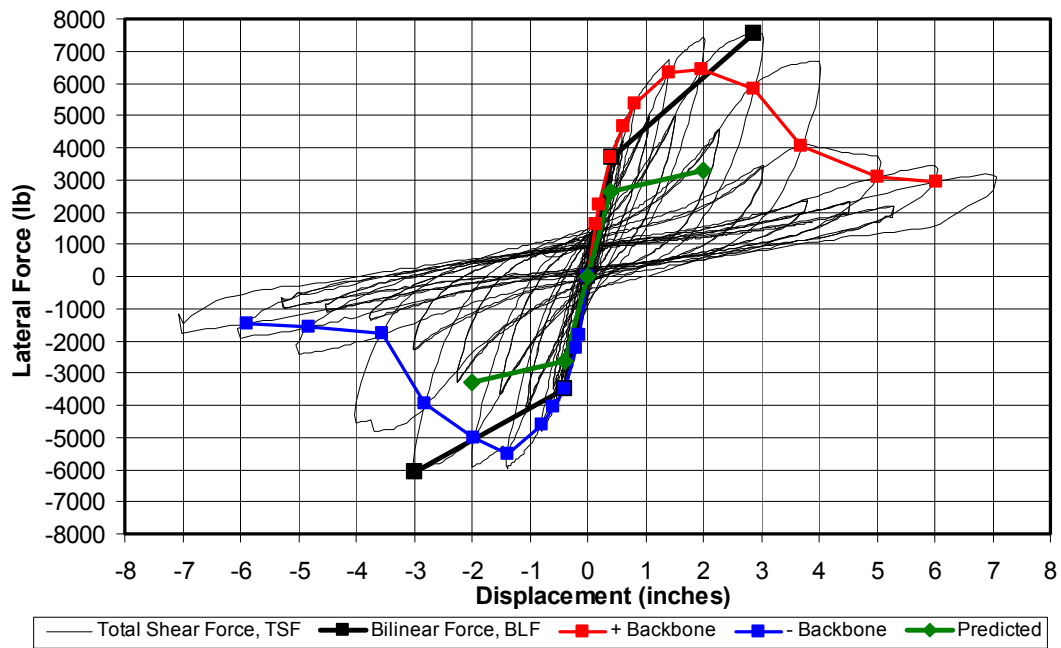


Figure 59. Lateral force (TSF) vs deflection hysteretic behavior of P3-3M CUREE1 panel.



Figure 60. Nail yielding and OSB crushing in P3-3M CUREE1 test.



Figure 61. Stud to interior of the threaded rod cavity split in P3-3M CUREE1 test.

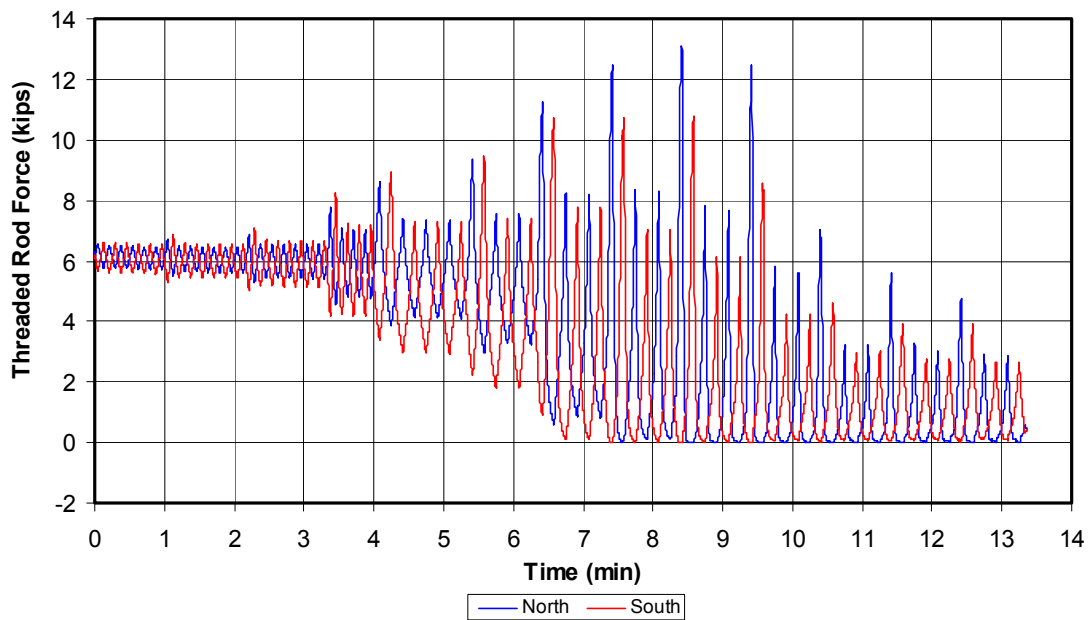


Figure 62. Threaded rod tension measured by north and south load cells in P3-3M CUREE1 test.

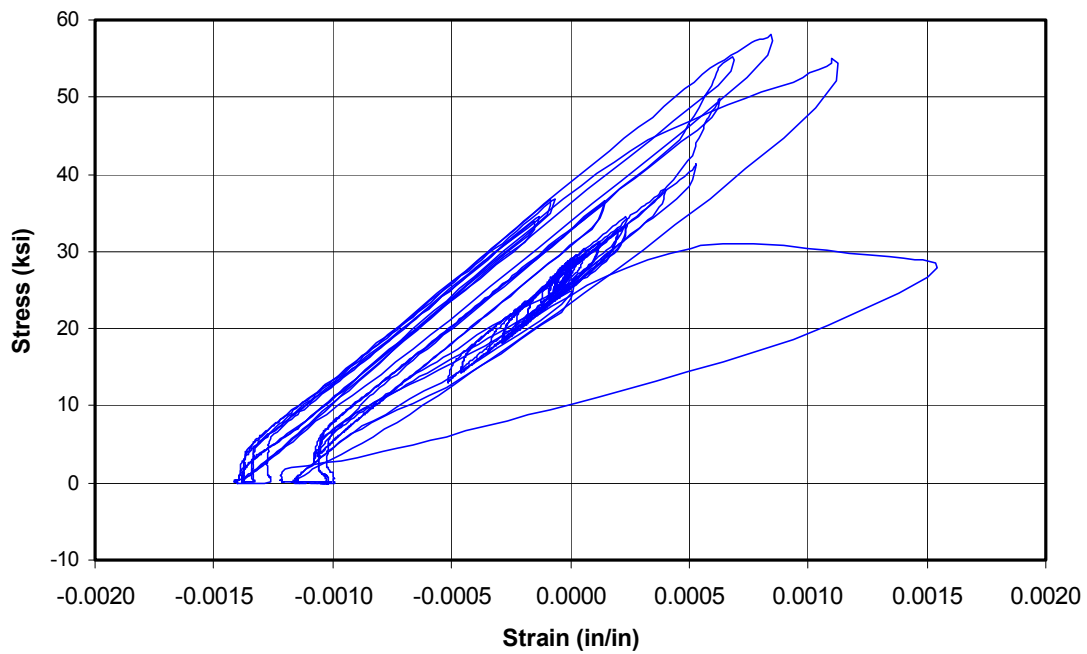


Figure 63. Stress vs strain plot for north threaded rod in P3-3M CUREE1 test.

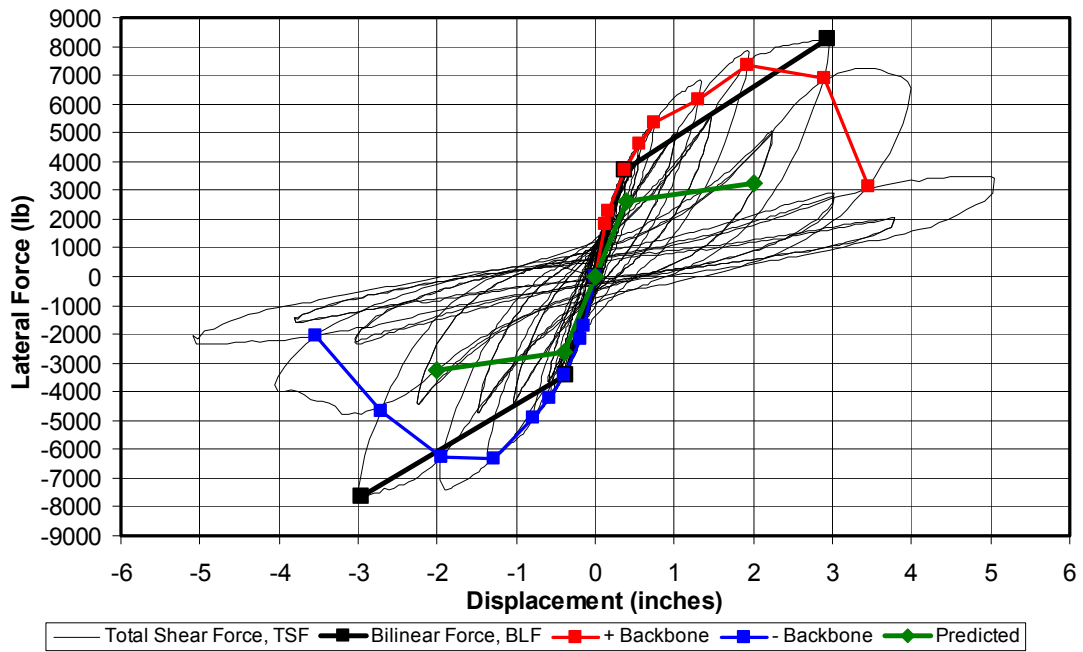


Figure 64. Lateral force (TSF) vs deflection hysteretic behavior of P3-3M CUREE2 panel.

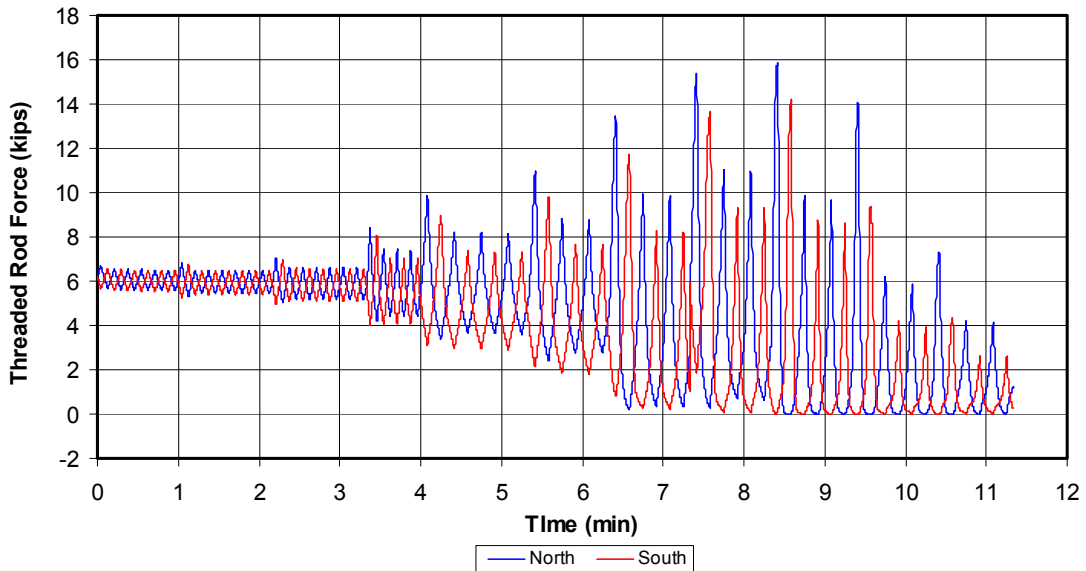


Figure 65. Threaded rod tension measured by north and south load cells in P3-3M CUREE2 test.

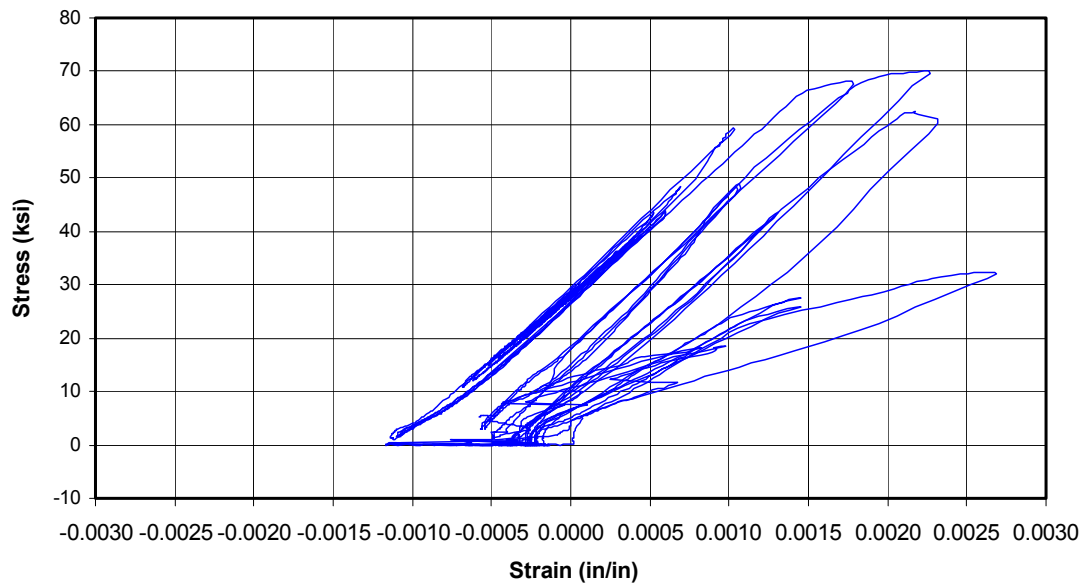


Figure 66. Stress vs strain plot for the north threaded rod in the P3-3M CUREE2 test.



Figure 67. Back face corner of P3-3M panel showing stud cavity and threaded rod.



Figure 68. Lateral force (TSF) vs deflection for P3-6 monotonic panel.



Figure 69. Stud lifting off of bottom plate in P3-6 monotonic test.



Figure 70. Shear failure of hurricane tie and nail yielding.

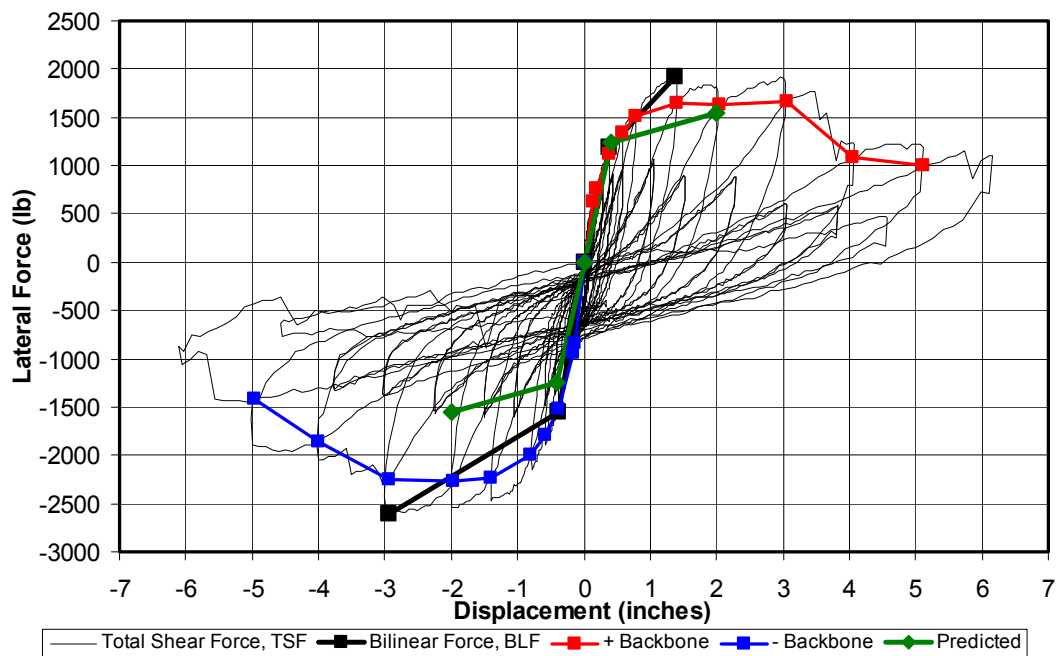


Figure 71. Lateral force (TSF) vs deflection hysteretic behavior of P3-6 CUREE1 panel.



Figure 72. Nails pulled through bottom right corner of the OSB of P3-6 CUREE1 panel.



Figure 73. Bending failure (cracking) of the top plate above the right edge stud.

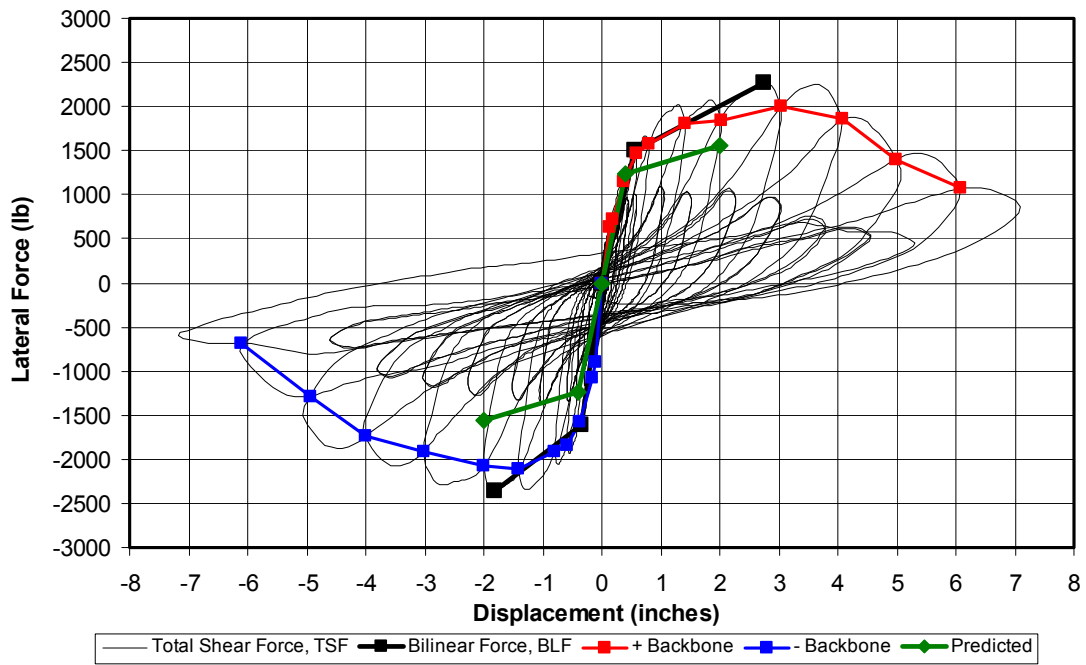


Figure 74. Lateral force (TSF) vs deflection hysteretic behavior of P3-6 CUREE2 panel.

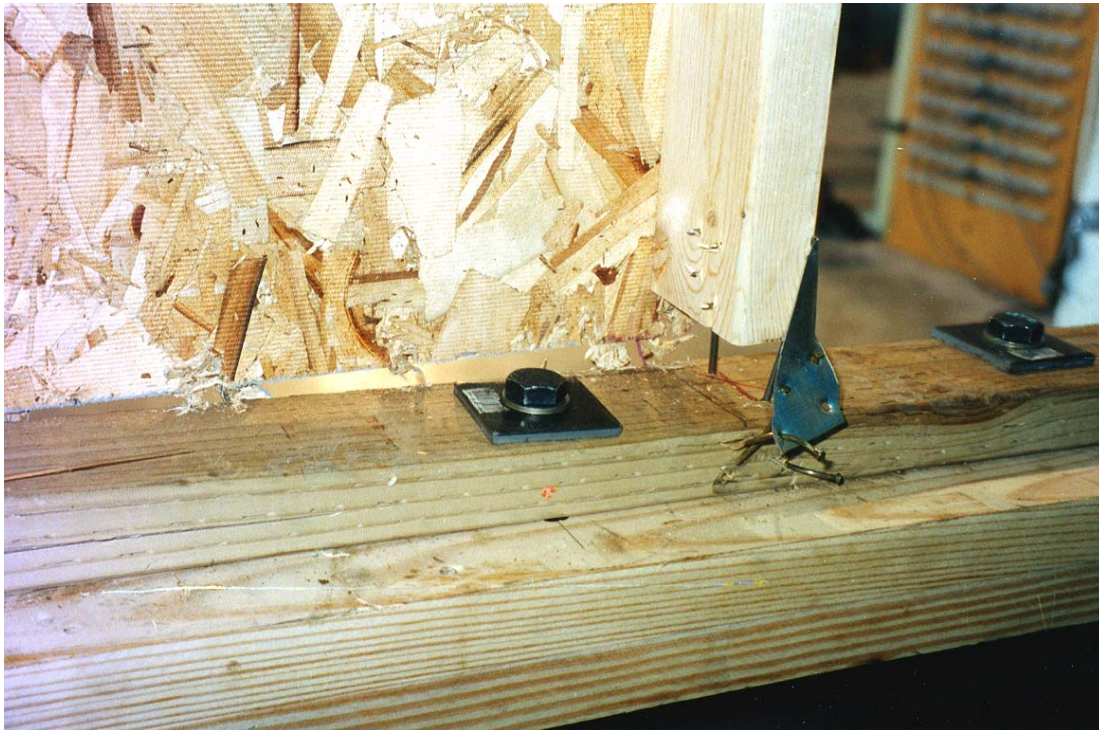


Figure 75. Interior face of P3-6 CUREE2 panel showing OSB nail and H4 tie nail failure.



Figure 76. Bending failure of the 2x4 top plate on P3-6 CUREE2 panel.

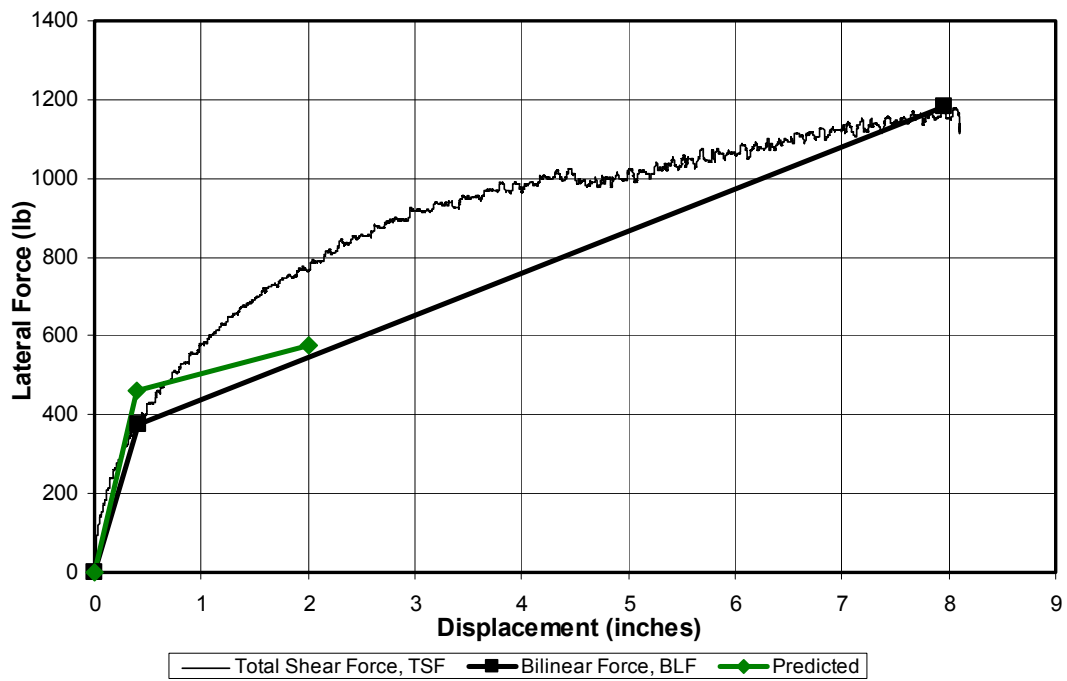


Figure 77. Lateral force (TSF) vs deflection for P3-7 monotonic panel.



Figure 78. Overall view of damaged P3-7 mono panel at the end of test.

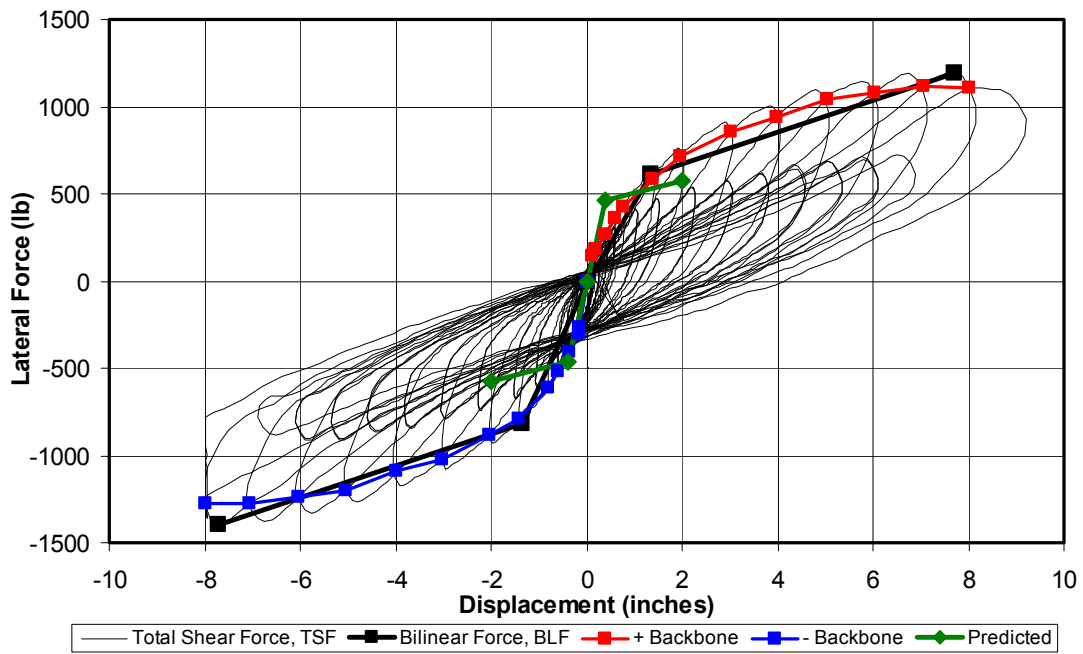


Figure 79. Lateral force (TSF) vs deflection hysteretic behavior of P3-7 CUREE2 panel.



Figure 80. Failure of H4 ties, OSB, bottom plate, and nail connections of P3-7 CUREE2 panel.

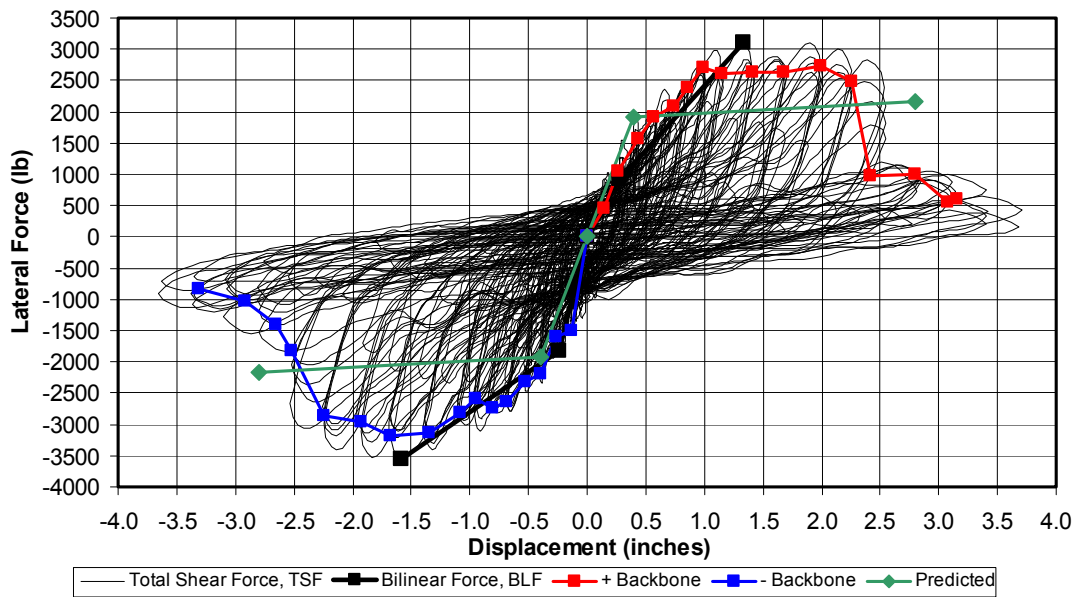


Figure 81. Lateral force (TSF) vs deflection hysteretic behavior of PSP-Std SPD1 panel.



Figure 82. Bottom left corner of the PSP-Std-SPD1 panel showing plywood to bottom plate nail connection failure and stud lifting.

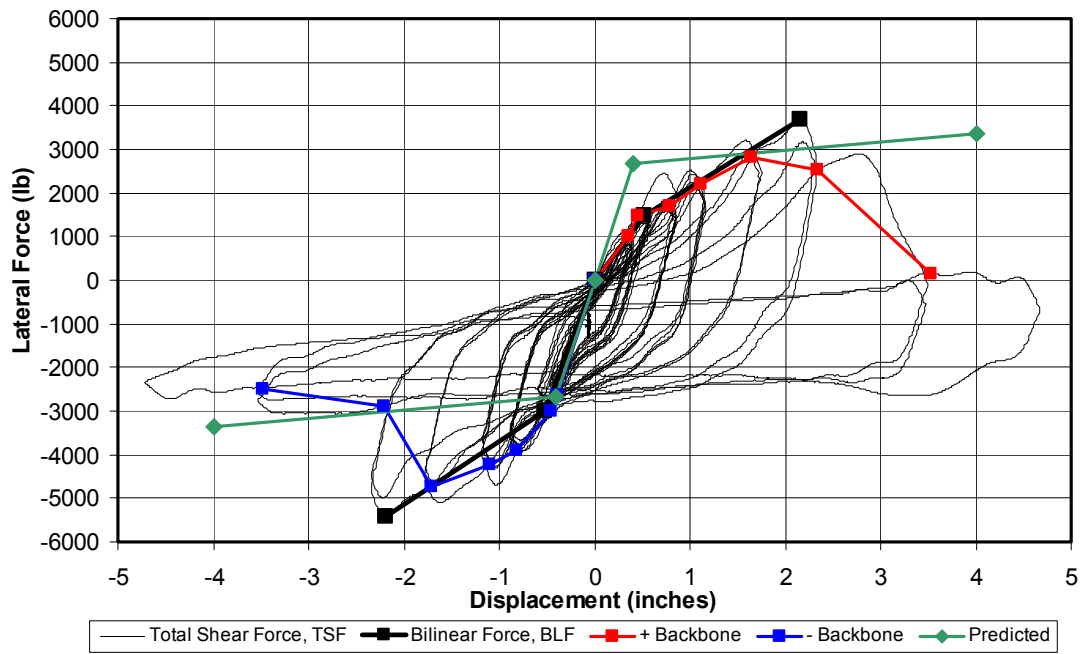


Figure 83. Lateral force (TSF) vs deflection hysteretic behavior of the PSP-Std MS1 panel.



Figure 84. Bottom of the PSP-Std-MS1 panel showing plywood to stud nail connection failure.

Appendix A: Predicted Allowable Strength Design Capacities

Wood Shear Panel Model

Chapter 3 described an analytical model developed to estimate wood shear panel behavior. As stated in Chapter 3, this model will be reliable only if the failure modes that define the model control test panel performance. Table 2 showed the minimum nominal capacity, Z_{\min} , which is the minimum value from Equations 1 through 4, representing the controlling mode of failure that determines the lateral capacity of the panels. From these values the allowable strengths, Z' , are calculated as follows:

$$Z' = C_D Z_{\min} \quad [\text{Eq A1}]$$

where,

C_D = load duration factor, which equals 1.6 for wind and earthquake load (NDS Table 2.3.2).

Table 10 provides the nail allowable strength, Z' , values, plus panel width, W , height, H , and nail spacing between the plywood and top and bottom plates, s_B . The number of nails along the top and bottom plates, n , is determined as follows:

$$n = \frac{W}{s_B} + 1 \quad [\text{Eq A2}]$$

The allowable strength design lateral capacity, P' , of the shear panels was calculated by modifying Equations 10 through 17 in Chapter 3. This was done for each test panel for applied dead loads, DL , of zero. The overturning resistance is equal to the allowable holddown vertical capacity, HD_a plus any applied vertical load, DL , times the panel width, W . Equation A3, below, accounts for the holddown and vertical load contribution to overturning resistance. The left side of Equation A3 is the applied overturning moment, minus the moment resistance provided by the plywood to stud nail connections. The right side of Equation A3 is the overturning moment

resistance provided by the nail connections between the plywood and top and bottom plates. This assumes an identical nail pattern at the top and bottom:

$$PH - M_{sa} = \frac{2V_{\max} S_B^2}{W} \sum_{i=1}^n (n-i)^2 \quad [\text{Eq A3}]$$

where,

P = the total applied lateral load, lb.

H = the panel height, in.

M_{sa} = the overturning moment resistance, provided by the plywood-to-stud nail connections at their allowable strength. This is defined as follows:

$$M_{sa} = \text{Min} \left[(TR_a + HD_a)W, \frac{H}{S_s} Z_{sa}W \right], \text{ lb-in.} \quad [\text{Eq A4}]$$

TR_a = the total applied vertical load, lb, which is defined as follows for panels with threaded rods (for the PSP-Std baseline panel tested in Phase I, the actual total applied vertical load replaces TR_a):

$$TR_a = A_{nt} 0.75F_y, \text{ lb} \quad [\text{Eq A5}]$$

A_{nt} = 0.226 in², net tensile area for 5/8 in. threaded rod (*AISC Load and Resistance Factor Design*, 2nd Edition, 1994, Vol II, Table 8-7).

F_y = 36000 psi, assumed to be A36 steel based on ultimate strength values given by the manufacturer.

HD_a = the holddown allowable capacity of a single stud anchor, defined by

$$HD_a = \text{Min}[n_{HD}Z_a, T_{HDa}], \text{ lb} \quad [\text{Eq A6}]$$

n_{HD} = the number of nails in the holddown.

Z_a = the minimum allowable strength for the nails connecting the holddown to the stud, defined by Equation A1, lb.

T_{HDa} = the allowable capacity of the holddown based on the net area of the steel. This is defined as:

$$T_{HD} = \phi F_u A_n, \text{ lb} \quad [\text{Eq A7}]$$

ϕ = the tensile rupture resistance factor, equal to 0.75.

F_u = the ultimate strength of the Hurricane tie steel. Conservatively assume to be A653 Grade 33 steel, 45,000 psi.

A_n = the net area of the holddown steel along the critical rupture surface, in².

W = the panel width, in.

s_s = the vertical spacing between the nails at the studs along the edges of the panels, in.

Z_{sa} = the allowable strength for the nails at the studs along the edges of the panels, lb, defined by Equation A1.

V_{max} = the maximum vertical load applied to the nails along the top and bottom plate due to overturning moment, lb. This assumes that all overturning moment resistance along the top and bottom plate is provided by the wood-to-plate nails, i.e., the vertical nails at the ends of the studs provide no overwhelming resistance.

s_B = the horizontal spacing between the nails along the top and bottom plate, in.

The right side of the series in Equation A3 is rewritten in a polynomial form as follows:

$$PH - M_{sa} = \frac{2V_{max}s_B^2}{W} \left[\frac{1}{3}(n-1)^3 + \frac{1}{2}(n-2)^2 + \frac{7}{6}(n-1) - \frac{1}{2} \right], \text{ lb-in.} \quad [\text{Eq A8}]$$

Equation A8 can be rewritten as:

$$\frac{V_{max}}{PH - M_{sa}} = \frac{W}{2s_B^2 \left[\frac{1}{3}(n-1)^3 + \frac{1}{2}(n-2)^2 + \frac{7}{6}(n-1) - \frac{1}{2} \right]}, \text{ in.}^{-1} \quad [\text{Eq A9}]$$

The lateral load applied to each nail along the top or bottom plate, T , is determined as follows:

$$T = \frac{P}{n}, \text{ lb} \quad [\text{Eq A10}]$$

The combined maximum vertical and lateral load applied to the nails at the panel corners, Z_{app} , is set equal to the nail allowable strength, Z' (see Equation A1), expressed as follows:

$$Z' = Z_{app} = \sqrt{V_{\max}^2 + T^2} \quad [\text{Eq A11}]$$

The panel allowable strength design lateral capacity, P' , is determined by selecting values of P in an iterative process until Z_{app} is set equal to Z' . Table 10 shows values of P' for each panel, with DL equal to zero. The panel allowable design resistance, D' , is calculated as follows:

$$D' = \frac{P'}{W} \quad [\text{Eq A12}]$$

Diagonal Strap Shear Panel Model

The P3-1 panel predicted strength is based on a different model than the one used for the wood panels. The nail connection allowable strength, Z' , is determined by Equation A1. The panel allowable strength design lateral capacity, P' , is determined as follows:

$$P' = nZ' \left(\frac{W}{\sqrt{W^2 + H^2}} \right), \text{ lb} \quad [\text{Eq A13}]$$

where,

n = the total number of nails at the diagonal strap connections to the top or bottom plate and studs.

W = the width of the panel, which for the P3-1 panels is the horizontal distance between the strap connections, in.

H = the height of the panel, in.

Table 10 also shows the value for P' of the P3-1 panel, plus the allowable design resistance, D' , calculated according to Equation A12.

Appendix B: Cyclic Test Protocols for Phase I Wood Shear Panels

Two cyclic test protocols were used to test the PSP-Std panels in the Phase I study. Details of the content of those protocols are discussed here.

Sequential Phase Displacement Protocol

Two specimens of each Phase I panel configuration were tested following the sequential phase displacement (SPD) protocol.* A cyclic rate of 0.1 hertz was used (10 seconds per cycle) because this rate provided adequate time to observe panel performance and failure progression. Table B1 defines the amplitude of each load cycle in terms of the first major event (FME). The FME is the yield limit state, defined as the point on the force-displacement relationship where the difference in the forces in the first and fourth cycle, at the same displacement, does not exceed 5%. The value for FME was estimated from the monotonic test results based on the point where non-linear response of the force-displacement relationship began. For most of the tests FME was set equal to 0.4 in. However, FME was 06 in. for the PSP-Std-SPD1, whose data is presented in the body of this report. Table B1 presents the displacement amplitudes for each cycle when FME equals 0.4 in. Figure B1 shows the lateral deformation time history for the SPD protocol using a cyclic rate of 0.1 hertz and FME equal to 0.4 in. The displacement amplitudes would be 50 percent greater than those shown in Tables B1 and Figures B1, when FME equals 0.6 in.

* This test procedure was defined in the City of Los Angeles Standard Method of Cyclic (Reversed) Load Test for Shear Resistance of Framed Walls for Buildings. This document was developed by the Structural Engineers Association of Southern California Ad Hoc Committee Testing Standards for Structural Systems and Components in conjunction with the City of Los Angeles, dated 1 August 1996, and revised 9 September 1997.

Table B-1. Sequential Phased Displacement (SPD) Protocol, FME = 0.4 in.

Cycle No.	% FME	Displacement (in.)	Cycle No.	% FME	Displacement (in.)	Cycle No.	% FME	Displacement (in.)
0	0%	0.00	66	400%	1.60	129	850%	3.40
1	25%	0.10	67	300%	1.20	130	638%	2.55
2	25%	0.10	68	200%	0.80	131	425%	1.70
3	25%	0.10	69	100%	0.40	132	213%	0.85
4	50%	0.20	70	400%	1.60	133	850%	3.40
5	50%	0.20	71	400%	1.60	134	850%	3.40
6	50%	0.20	72	400%	1.60	135	850%	3.40
7	75%	0.30	73	450%	1.80	136	900%	3.60
8	75%	0.30	74	338%	1.35	137	675%	2.70
9	75%	0.30	75	225%	0.90	138	450%	1.80
10	100%	0.40	76	113%	0.45	139	225%	0.90
11	75%	0.30	77	450%	1.80	140	900%	3.60
12	50%	0.20	78	450%	1.80	141	900%	3.60
13	25%	0.10	79	450%	1.80	142	900%	3.60
14	100%	0.40	80	500%	2.00	143	950%	3.80
15	100%	0.40	81	375%	1.50	144	713%	2.85
16	100%	0.40	82	250%	1.00	145	475%	1.90
17	125%	0.50	83	125%	0.50	146	238%	0.95
18	94%	0.38	84	500%	2.00	147	950%	3.80
19	63%	0.25	85	500%	2.00	148	950%	3.80
20	31%	0.13	86	500%	2.00	149	950%	3.80
21	125%	0.50	87	550%	2.20	150	1000%	4.00
22	125%	0.50	88	413%	1.65	151	750%	3.00
23	125%	0.50	89	275%	1.10	152	500%	2.00
24	150%	0.60	90	138%	0.55	153	250%	1.00
25	113%	0.45	91	550%	2.20	154	1000%	4.00
26	75%	0.30	92	550%	2.20	155	1000%	4.00
27	38%	0.15	93	550%	2.20	156	1000%	4.00
28	150%	0.60	94	600%	2.40	157	1050%	4.20
29	150%	0.60	95	450%	1.80	158	788%	3.15
30	150%	0.60	96	300%	1.20	159	525%	2.10
31	175%	0.70	97	150%	0.60	160	263%	1.05
32	131%	0.53	98	600%	2.40	161	1050%	4.20
33	88%	0.35	99	600%	2.40	162	1050%	4.20
34	44%	0.18	100	600%	2.40	163	1050%	4.20
35	175%	0.70	101	650%	2.60	164	1100%	4.40
36	175%	0.70	102	488%	1.95	165	825%	3.30
37	175%	0.70	103	325%	1.30	166	550%	2.20
38	200%	0.80	104	163%	0.65	167	275%	1.10
39	150%	0.60	105	650%	2.60	168	1100%	4.40
40	100%	0.40	106	650%	2.60	169	1100%	4.40
41	50%	0.20	107	650%	2.60	170	1100%	4.40
42	200%	0.80	108	700%	2.80	171	1150%	4.60
43	200%	0.80	109	525%	2.10	172	863%	3.45
44	200%	0.80	110	350%	1.40	173	575%	2.30
45	250%	1.00	111	175%	0.70	174	288%	1.15
46	188%	0.75	112	700%	2.80	175	1150%	4.60
47	125%	0.50	113	700%	2.80	176	1150%	4.60
48	63%	0.25	114	700%	2.80	177	1150%	4.60
49	250%	1.00	115	750%	3.00	178	1200%	4.80
50	250%	1.00	116	563%	2.25	179	900%	3.60
51	250%	1.00	117	375%	1.50	180	600%	2.40
52	300%	1.20	118	188%	0.75	181	300%	1.20
53	225%	0.90	119	750%	3.00	182	1200%	4.80
54	150%	0.60	120	750%	3.00	183	1200%	4.80
55	75%	0.30	121	750%	3.00	184	1200%	4.80
56	300%	1.20	122	800%	3.20	185	1250%	5.00
57	300%	1.20	123	600%	2.40	186	938%	3.75
58	300%	1.20	124	400%	1.60	187	625%	2.50
59	350%	1.40	125	200%	0.80	188	313%	1.25
60	263%	1.05	126	800%	3.20	189	1250%	5.00
61	175%	0.70	127	800%	3.20	190	1250%	5.00
62	88%	0.35	128	800%	3.20	191	1250%	5.00
63	350%	1.40						
64	350%	1.40						
65	350%	1.40						

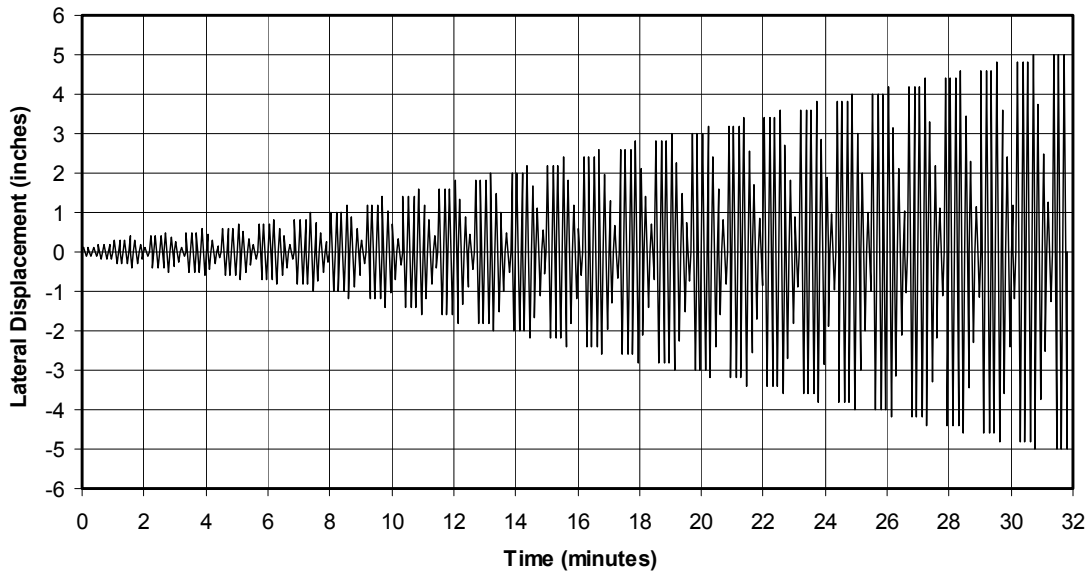


Figure B-1. Sequential Phase Displacement (SPD) time history at 0.1 Hz cyclic rate and 0.4 inch FME.

Modified SAC Protocol

Two specimens of each panel type were tested following a modification to another standard cyclic test method. This protocol is similar to SAC* guidelines that have been modified to scale to the lateral yield deflection described in ATC-24.† The SAC recommended loading histories call for loading with a deformation parameter based on interstory drift angle, θ defined as interstory height over interstory displacement. The commentary to the SAC document explains that the interstory drift angle of 0.005 radians corresponds to a conservative estimate of the value that would cause yield deformation. Therefore, the load protocol defined by SAC in terms of drift angle are scaled to the measured lateral yield deflection, δ_y to define the cyclic test steps as defined in Table B2. This protocol calls for a set number of cycles at each of the deformation amplitudes shown in Table B2. This protocol is illustrated by the deformation time history shown in Figure B2, which is based on a lateral yield deformation, δ_y of 0.4 in. and stroke rate of 12 in. per minute. However, the

* SAC Joint Venture Testing Programs and Loading Histories, unpublished guidance, 1997. SAC is a joint venture of three non-profit organizations: The Structural Engineers Association of California, the Applied Technical Council, and California Universities for Research in Earthquake Engineering.

† Applied Technical Council (ATC) 24, Guidelines for Cyclic Seismic Testing of Components of Steel Structures, 1992.

FME used for the PSP-Std-MS1 test was 0.6 in., such that the amplitudes shown in Table B2 and Figure B2 were 50 percent greater for this test.

Table B-2. Modified SAC Cyclic Test Protocol, FME = 0.4 in.

Load Step #	SAC-2		Modified SAC Amplitude	Modified SAC Amplitude at FME = $\delta_y = 0.4$ in. (in.)
	Number of Cycles, n	Peak Deformation, θ (radians)		
1	6	0.00375	$0.75\delta_y$	0.3
2	6	0.005	$1.0\delta_y$	0.4
3	6	0.0075	$1.5\delta_y$	0.6
4	4	0.01	$2\delta_y$	0.8
5	2	0.015	$3\delta_y$	1.2
6	2	0.02	$4\delta_y$	1.6
7	2	0.03	$6\delta_y$	2.4
8	2	0.04	$8\delta_y$	3.2
9	2	0.05	$10\delta_y$	4.0
10	2	0.06	$12\delta_y$	4.8
11	2	0.07	$14\delta_y$	5.6

The net vertical load for the modified SAC tests was held constant at 8000 lb, while holding the top beam horizontal. BSC indicated this vertical load is a possible upper limit for field conditions, based on a distributed load of 1000 lb per foot along an 8-foot wide wall. A constant stroke rate of 12 in. per minute was used for all modified SAC tests, as this rate provided adequate time to make observations on panel performance and failure progression.

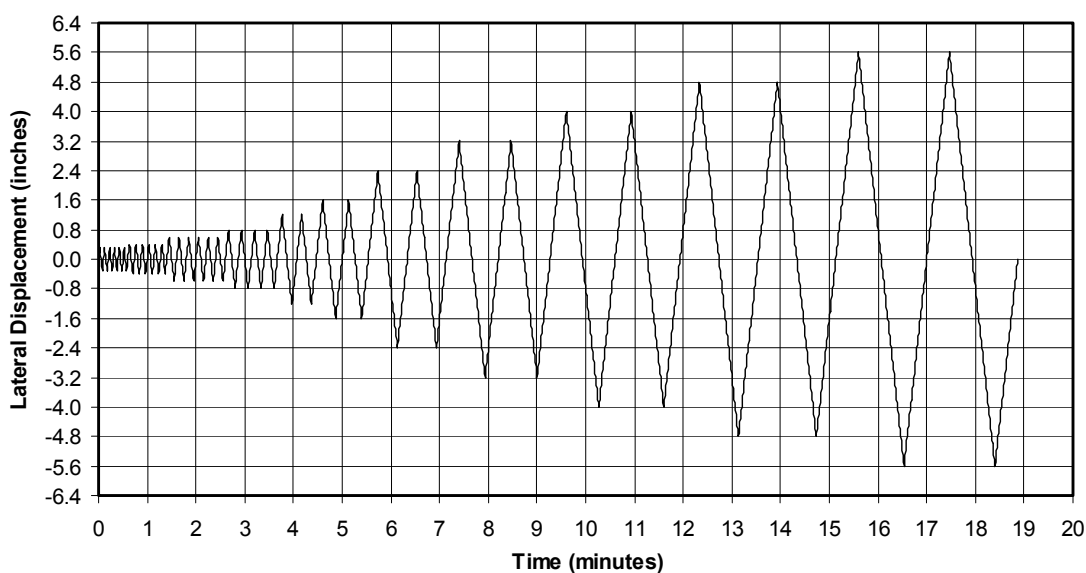


Figure 15. Modified SAC-2 time history at 12 in. per minute stroke rate and 0.4 inch FME (δ_y).

Acronyms

AISC	American Institute of Steel Construction
APA	American Plywood Association
ASD	allowable strength design
ASTM	American Society for Testing and Materials
BSC	Building Sciences Corporation
CERL	Construction Engineering Research Laboratory
CUREE	Consortium of Universities for Research in Earthquake Engineering
DL	dead load
FEMA	Federal Emergency Management Agency
HD	holddown capacity (vertical)
IBC	International Building Code
LRFD	Load and resistance factor design
LVDT	linear variable differential transformers
NDS	National Design Specification
NEHRP	National Earthquake Hazards Reduction Program
OSB	oriented strand board
PSP	Plywood Shear Panel (specimen designation prefix)
SAC	acronym designating a joint partnership of the <u>S</u> tructural Engineers Association of California; <u>A</u> ppplied Technology Council; and <u>C</u> onsortium of Research Universities for Earthquake Engineering
SH	stroke horizontal (i.e., lateral displacement)
SPD	sequential phased displacement
SPF	spruce pine fir
TR	threaded rod

TS	tube, structural
TSF	total shear force
TVF	total actuator vertical force

CERL Distribution

Chief of Engineers

ATTN: CEHEC-IM-LH (2)

Engineer Research and Development Center (Libraries)

ATTN: ERDC, Vicksburg, MS

ATTN: Cold Regions Research, Hanover, NH

ATTN: Topographic Engineering Center, Alexandria, VA

Defense Tech Info Center 22304

ATTN: DTIC-O

6

2/01

REPORT DOCUMENTATION PAGE

Form Approved
OMB No. 0704-0188

Public reporting burden for this collection of information is estimated to average 1 hour per response, including the time for reviewing instructions, searching existing data sources, gathering and maintaining the data needed, and completing and reviewing this collection of information. Send comments regarding this burden estimate or any other aspect of this collection of information, including suggestions for reducing this burden to Department of Defense, Washington Headquarters Services, Directorate for Information Operations and Reports (0704-0188), 1215 Jefferson Davis Highway, Suite 1204, Arlington, VA 22202-4302. Respondents should be aware that notwithstanding any other provision of law, no person shall be subject to any penalty for failing to comply with a collection of information if it does not display a currently valid OMB control number. PLEASE DO NOT RETURN YOUR FORM TO THE ABOVE ADDRESS.

1. REPORT DATE April 2001			2. REPORT TYPE Final		3. DATES COVERED (From - To)	
4. TITLE AND SUBTITLE Alternative Shear Panel Configurations for Light Wood Construction: Development, Seismic Performance, and Design Guidance					5a. CONTRACT NUMBER	
					5b. GRANT NUMBER	
					5c. PROGRAM ELEMENT NUMBER	
6. AUTHOR(S) James Wilcoski, Chad Fischer, Tim Allison, and Kelly Jo Malach					5d. PROJECT NUMBER	
					5e. TASK NUMBER	
					5f. WORK UNIT NUMBER GQ9	
7. PERFORMING ORGANIZATION NAME(S) AND ADDRESS(ES) U.S. Army Construction Engineering Research Laboratory (CERL) P.O. Box 9005 Champaign, IL 61826-9005					8. PERFORMING ORGANIZATION REPORT NUMBER ERDC/CERL TR-02-12	
9. SPONSORING / MONITORING AGENCY NAME(S) AND ADDRESS(ES) Office of Building Systems, ATTN: EE-41 Department of Energy 10000 Independence Avenue SW Washington, DC 20585					10. SPONSOR/MONITOR'S ACRONYM(S) DOE-PATH	
					11. SPONSOR/MONITOR'S REPORT NUMBER(S)	
12. DISTRIBUTION / AVAILABILITY STATEMENT Approved for public release; distribution is unlimited.						
13. SUPPLEMENTARY NOTES Copies are available from the National Technical Information Service, 5285 Port Royal Road, Springfield, VA 22161.						
14. ABSTRACT Shear panels are used in light wood construction to resist lateral loads resulting from earthquakes or strong winds. These panels are typically made of wooden sheathing nailed to building frame members, but this standard panel design interferes with the installation of sheet insulation. A non-insulated shear panel conducts heat between the building interior and exterior, wasting considerable amounts of energy. Several alternative shear panel designs were developed to avoid this insulation-mounting problem, and sample panels were tested according to standard cyclic test protocols. One of the alternative designs consisted of diagonal steel straps nailed directly to the structural framing. Several others consisted of sheathing nailed to 2 x 4 framing, then set into a larger 2 x 6 structural frame in such a way that no sheathing protruded beyond the edge of the 2 x 6 members. Also, samples of industry-standard shear panels were constructed and tested in order to establish a performance baseline. Analytical models were developed to size test panels and predict panel behavior. A procedure was developed for establishing design capacities based on both test data and established baseline panel design capacity. The behavior of each panel configuration is documented, and recommended design capacities are presented.						
15. SUBJECT TERMS wood frame building, wood construction, seismic performance, single family housing, lateral load resistance, multi-family housing						
16. SECURITY CLASSIFICATION OF:			17. LIMITATION OF ABSTRACT	18. NUMBER OF PAGES	19a. NAME OF RESPONSIBLE PERSON Jim Wilcoski	
a. REPORT Unclassified	b. ABSTRACT Unclassified	c. THIS PAGE Unclassified			SAR	136

